Available online at www.sciencedirect.com

ScienceDirect

Procedia Engineering 00 (2017) 000–000

Procedia Engineering

www.elsevier.com/locate/procedia

Sustainable Civil Engineering Structures and Construction Materials, SCESCM 2016

Compare the results between model laboratory-test for rigid pavement and EverStressFE software analysis

Christian Gerald Daniel[a,*], Firdaus Chairuddin[b]

[a]*Atmajaya Makassar University , Tanjung Alang Street No. 23, Makassar, Indonesia*
[b]*Civil Engineering From Hasanuddin University , Tamalanrea Street, Makassar, Indonesia*

Abstract

EverStressFE is a 3D finite element modeling software that can be used to analyze the multilayer –model pavement (up to 4 layers possible); which requires elastic modulus and Poisson ratio of each layer as input value. The purpose of this paper then is to develop a comparison between EversStress-FE based analysis and laboratory test result, and determine the accuracy of the software. In this study, displacement and microstrain behaviours are compared. The vertical strain governing at both top and bottom fiber of concrete layer from laboratory test are 38 and 44 respectively, compared to EverStressFE result ($\varepsilon \leq 5.65$) (in microstrain). Displacement at the center is 3.4mm and 0.3mm according to laboratory test and EverStressFE respectively. The outcome shows that results of EverStressFE is approximately 10 times smaller than laboratory test result, in terms of displacement and microstrain, meaning that the software is not accurate to validate the laboratory test.

Peer-review under responsibility of the organizing committee of SCESCM 2016.

Keywords: Elastic modulus; Poisson ratio; rigid pavement; microstrain; displacement; EverStressFE.

1. Introduction

Typically there are several mechanical behavior of a pavement that are often analyzed: stress, strain, and displacement, which gives different characteristic on each different type of pavement (asphalt, concrete, or small element pavement). Currently there are different approaches to analyze pavement behavior under loading; single layer method, dual layer method, and multi-layer method using Finite Element analysis (FEM). This paper is trying

* Corresponding author. Tel.: +31 6 50 62 63 17.
E-mail address: Christian.geralddaniel@gmail.com

Peer-review under responsibility of the organizing committee of SCESCM 2016.

to analyze mechanical behavior of concrete (rigid) pavement using EverStressFE software, which according to William G. Davids (2009) - professor in University of Maine USA, is a FEM software-based that can be used to analyze strain and displacement behavior of a pavement using multi-layer analysis. The aim of this paper is to develop a comparison between EverStressFE analysis result and laboratory test result, furthermore to determine if this software can give a satisfying and accurate result.

2. Literature review

2.1. Multilayer theory

The first one who tested pavement response under point load is Boussinesq, in 1885 (Hardiyatmo, 2010). He made an equation to determine stress, strain, and displacement, making correlation with Poisson ratio and Elastic Modulus (Tu, W., 2007). Boussinesq's equation was suitable for single layer response.

$$\varepsilon_r = \frac{(1+v)}{2E} q \left[1-2v - \frac{2(1-v)z}{\left(a^2+z^2\right)^{0.5}} + \frac{z^3}{\left(a^2+z^2\right)^{1.5}} \right] \quad (1)$$

$$\varepsilon_z = \frac{(1+v)}{E} q \left[1-2v + \frac{2vz}{\left(a^2+z^2\right)^{0.5}} - \frac{z^3}{\left(a^2+z^2\right)^{1.5}} \right] \quad (2)$$

Burmister (1943) had developed Boussinesq's theory, generating a theory to solve stress distribution in two or more layers with different Elastic modulus and Poisson ratio (Hardiyatmo, 2010).

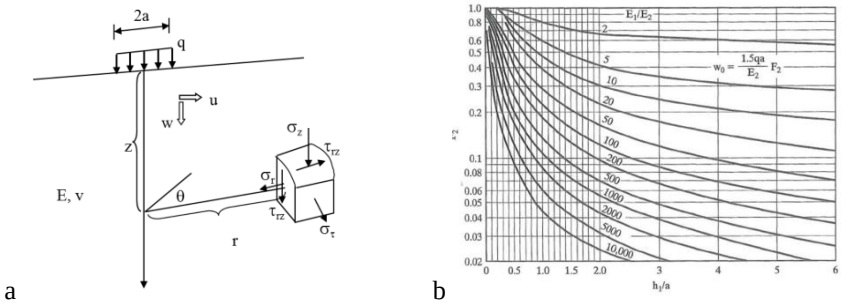

Fig. 1. (a) Boussinesq's theory; (b) Graphic invented by Burmister for displacement calculation at 2 layers system

2.2. EverstressFE review (Davids, 2009)

EverStressFE version 1.0 (available for download at www.civil.umaine.edu/everstressfe) is a user-friendly three-dimensional (3D) finite-element based software for the analysis of pavement structure subjected to various wheel/axle load combinations. EverStressFE is useful for both researchers and designers who want to perform complex mechanics-based analyses of pavement systems.

Traditional analysis software such as EverStress, BISAR, or KENLAYER are based on available analytical solutions, and therefore may not realistically account for complex loads, mixed boundary conditions, inter-layer slip and debonding, and 3D response. General-purpose finite element packages can overcome these limitations; nonetheless, it is slightly difficult to learn and use the approach, and simulation times can be long for 3D analysis.

EverStressFE solves the problem faced by the previous approaches, by its efficient 3D finite element solver and coupled with a highly graphical and user-friendly interface.

Some of the main features of EverStressFE are summarized below

- Intuitive and user-friendly graphical user interface.
- Ability to model systems with 1-4 layers.
- Modeling of multiple-wheel systems
- Batch analysis capabilities.
- Visualization of results.

3. Research methods

Methods that are used in the tests are laboratory experiment and analysis using software EverStressFE. The steps are:

3.1. Unconfined compressive strength tests.

The purpose is to determine the value of elastic modulus and Poisson Ratio of each element; which both of them are input parameters in EverStressFE software analysis. The procedures are: Prepare the test instruments (such as set Universal Testing Machine (UTM), Data Logger, Computer, LVDT cables, Strain Gauge, and bearing plate); connect the data logger and computer that has been installed with software Visual Log; Connect the LVDT cables to data logger; Start the test, as the loads done mechanically by the UTM.

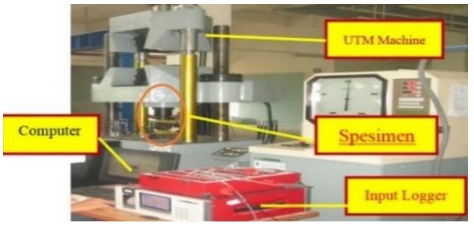

Fig. 2. UCS Test Apparatus

3.2. Load test multilayer.

The load test is done to find the values of deformation, stress, strain, and the capacity of maximum load that can be endured by each specimens. The procedures are: Install the 1x1 m box at the portal ; Attach the strain gauge at the specimens ; Put the specimens to the box ; Install the sets of hydraulic pump to portal, then set the load cell ; Do the test, with the loading using hydraulic pump that operated manually. (Note: the maximum load given by the pump is 50 ton).

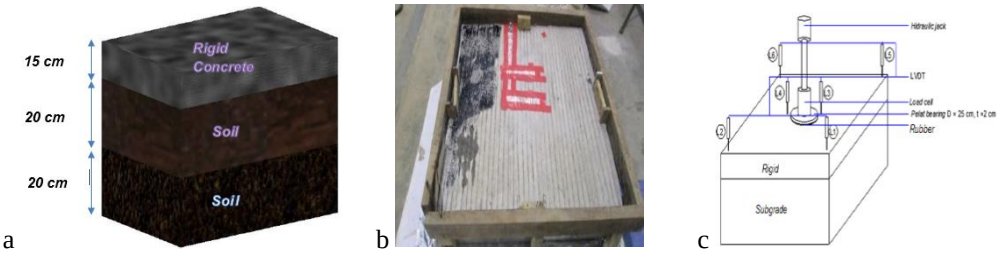

Fig. 3. (a) Sketch of the specimen; (b) Specimen of rigid pavement; (c) Sketch of specimen on test apparatus

3.3. Processing the test results

Some graphics, as the result of load test are produced by using software Microsoft Excel 2013, after copying the test results from software Visual Log.

3.4. Compare the result of load test using software EverstressFE

The graphics done by Microsoft Excel will be compared with the analysis of software EverStressFE. The work steps of EverStressFE software are shown below:

Input the dimension value of each layer, and each value of elastic modulus and Poisson Ratio. ; Input the load value; (according to the area of contact which is obtained from the area of bearing plate used (507 cm2), the maximum load is 35.0 kN); For Tab Meshing, a change was not done; After that on tab Solver, press Solve. ; Some graphics will be shown on tab Results; Graphics that are shown will be captured then compared with the result of data-processing load test.

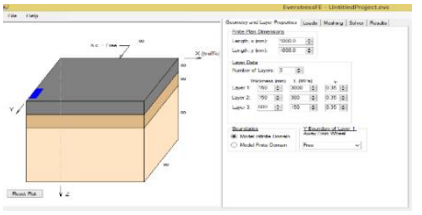

Fig. 4. EverStressFE User Interface

3.5. Limitation of test

- The test done only measure vertical response, no lateral or longitudinal responses are measured.
- The test results is not depth-dependent.
- Strains are only measured in concrete layer.

4. Results and discussion

4.1. Unconfined compressive strength tests.

The value of Elastic modulus 11.91 MPa, and Poisson Ratio 0.0465 for soil sample.

The value of Elastic modulus obtained is 23799.237 MPa, and Poisson Ratio 0.22 for concrete sample.

4.2. Load test

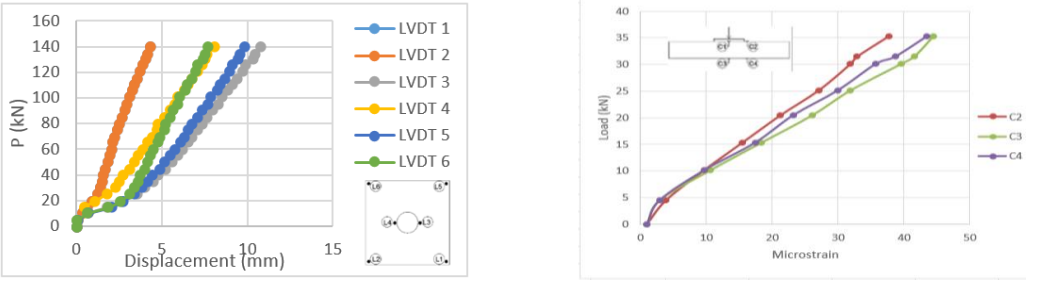

a b

Fig. 5. (a) Correlation between loads and displacement; (b) Correlation between load and strain for concrete slab

From the graphic it can be concluded that the displacement at P= 35 kN (maximum load in EverStressFE) is 3.4 mm at the centre (average of LVDT 3 and 4).
Furthermore, the strains (ε_z) are 38 and 44 at top and bottom fibre, respectively. Note that C1 parameter is error that should not be considered in the result. Meanwhile, calculation using Boussinesq Theory yields (ε_z) = 4.9 and 4; (ε_x) and (ε_y) are 9.9 and -3.3, at top and bottom fibre, respectively. (All in microstrain)

4.3. EverStressFE Analysis.

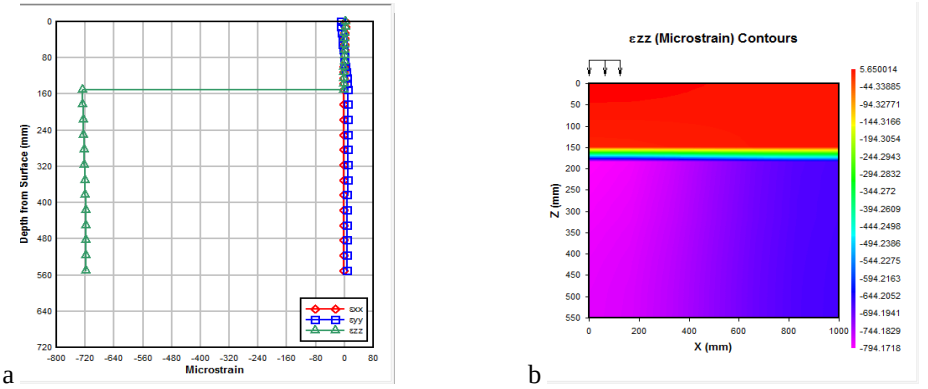

Fig. 6. (a) 2D Graphs of correlation between depth and strain; (b) Contour for micro strain

Depicted from the graph, the microstrain at surface are ε_x, ε_y and $\varepsilon_z \leq 5.65$, as well as at depth = 150mm.

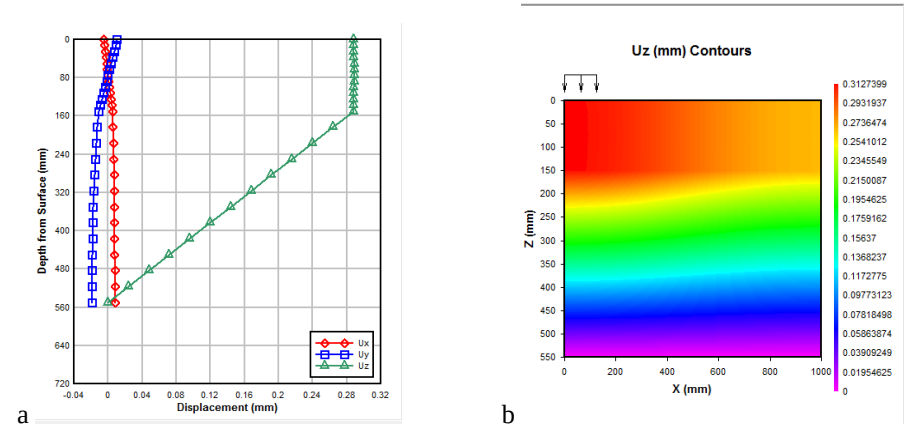

Fig. 7. (a) 2D Graphs of correlation between depth and deflection/displacement; (b) Contour for vertical displacement

The vertical displacement at the surface is 0.3mm.

5. Conclusion

- The vertical strain governing at both top and bottom fibre of concrete layer are 38 and 44 respectively (in microstrain) from laboratory test, which are approximately 10 times larger than EverStressFE result (5.65 for top and bottom fibre).
- Displacement occurring at the center is 3.4mm according to laboratory test, which is also 10 times larger than EverStressFE result (0.3mm).

- The results of analysis using EverStressFE are approximately 10 times smaller than laboratory test result, in terms of vertical displacement and strain, which possibly means that the software is not accurate to be used. However, more tests with wider comparison parameter has to be attempted in the future to support this conclusion.

References

[1] Bezababih, A.G. et al., Comparative Study of Flexible and Rigid Pavements for Different Soil and Traffic Conditions, Journal of the Indian Roads Congress, July-September 2009
[2] Colorado Ready Mixed Concrete Association, 2005. Specific's Guide for Previous Concrete Pavement Design.
[3] Chairuddin, F. et al. 2013. Experimental Study on Permeable Asphalt Pavement Used Domato Stone (Quartzite Dolomite) as Course Agregate for Surface Layer of Road Pavement. Advanced Materials Research (Volume 935), pp.255-258.
[4] Daniel, C.G. et al. (2014, September). The Comparison of Deflection and Strain Values Between EverstressFE Software Analysis and Multilayer Laboratory Test Results [electronic version]. IOSR Journal of Engineering.
[5] El Shaer M.H., Technical Report Stresses and Strains in Flexible Pavement Using Computer Program, Cairo University Post-Graduate Highway Engineering, Egypt.
[6] M. Miradi, A.A.A. Moleenar, M.F.C. van de Ven, (2009), Performance modeling of porous asphalt concrete using artificial intelligence, Road Materials and Pavement Design, ICAM 2009, pp.263-280
[7] M. Y. Darestani, et al., experimental study on structural response of rigid pavements under moving truck load, ARRB Conference – Research into Practice, Canberra Australia, 2006
[8] Nur Ali, M. Wihardi Tjaronge, Lawalenna Samang and Muhammad Isran Ramli, Juni 2011. "Experimental Study on Effects of Flood Puddle to Durability of Asphaltic Concrete Containing Refined Butonic Asphalt". The 9th Eastern Asia for Transportation Studies Coference, Jeju, South of Korea.
[9] EverStressFE1.0 Software for 3D Finite-Element Analysis of Flexible Pavement Structures: Summary of Features and Capabilities. 2009

Available online at www.sciencedirect.com

ScienceDirect

Procedia Engineering 00 (2017) 000–000

Procedia Engineering

www.elsevier.com/locate/procedia

Sustainable Civil Engineering Structures and Construction Materials, SCESCM 2016

An analysis and empirical correlation of dynamic and resilient modulus test results for asphaltic concrete mixtures

Yasir Ali[a]*, Muhammad Irfan[b], and Sarfraz Ahmed[b]

[a]*Department of Civil Engineering and Built Enviroment, Queensland Univeristy of Technology, Kelvin Grove, Brisbane-4001, Australia*
[b]*Department of Geotechnical and Transportation Engineering, Military College of Engineering, National University of Sciences & Technology (NUST), Risalpur-24080, Pakistan*

Abstract

This paper investigates the impact of different loading pattern on the performance of asphalt concrete (AC) mixtures. Four wearing course mixes including Asphalt Institute, Superpave and Pakistan's National Highway Authority (NHA) gradations were evaluated. Dynamic modulus |E*| test was conducted at two temperatures (25 and 40°C) and six frequencies (0.1 to 25 Hz) whereas resilient modulus test was performed at two temperatures (25 and 40 °C) and 1 Hz frequency with two load pulse durations (100 and 300 ms). The results revealed an increase in temperature from 25 to 40°C, translated into 45% and 78% drop in |E*| and resilient modulus values on average, respectively for the tested gradations. The resilient modulus test results indicated that the size of the specimen statistically affected the measured resilient modulus value as the values obtained for 100 mm diameter specimens were higher than 150 mm diameter specimens at all testing temperatures. Also, resilient modulus values found at 1 Hz (100 ms load duration) were comparable with the dynamic modulus values at the loading frequency of 5 Hz at test temperature of 25°C. The correlation approach presented in this study could be utilized to predict the dynamic modulus from measured resilient modulus values of AC mixtures.

Peer-review under responsibility of the organizing committee of SCESCM 2016.

Keywords: Asphalt mixtures; loading pattern; Temperature; Frequency; Statistical analysis; Mechanistic-Empirical design.

* Corresponding author. Tel.: +32-465415453; fax: +32-29119166.
E-mail address: engr.yasirali@gmail.com

Peer-review under responsibility of the organizing committee of SCESCM 2016.

1. Introduction

With the advent of M-EPDG the importance of resilient modulus is diminished and dynamic modulus test is solely used as performance test to characterize AC mixtures [1]. But still resilient modulus is accepted in AASHTO 1993 pavement design procedures and used by many highways agencies across the world.

The resilient modulus (Mr) test can be performed on field as well as laboratory prepared cores. The cylindrical specimen is subjected to loading in diametral plane which tends to develop the tensile stress perpendicular to loading direction. The measurement of resilient modulus using indirect tension test incorporates haversine pulse loading of 0.1 s trailed by rest period of 0.9 s. However, to simulate the moving truck speed, loading pulse of 0.03 s followed by 0.97 s rest period can be used. This test measures horizontal and vertical deformation (strains) at center of specimen.

The dynamic modulus measures the viscoelastic behavior of AC mixtures under compressive sinusoidal loading at varying test temperatures and loading frequencies which caters both viscous and elastic response of the mix. However, the resilient modulus is property of bounded and unbounded AC materials characterizing the elastic behavior under haversine loading. On comparison, these two test methods differ by the loading pattern as dynamic modulus indulges the continuous sinusoidal loading with no rest period whereas resilient modulus incorporates the waveform haversine loading with given rest period, hence elastic rebound would occur during the test. The resilient modulus have shown steadfast and beneficial results of mixture properties for field extracted cores. On contrary to that, the AASHTO mechanistic-empirical design guide has made huge impact as it encompasses both empirical and mechanistic approach to design and analysis and uses dynamic modulus as basic input parameter for material characterization, hence, various studies are underway to characterize mixtures using dynamic modulus [2].

These two methods have been used most widely and can be used as surrogate to each other. Therefore, this study aimed to focus on the performance evaluation and developing a correlation of material behavior under different loading conditions of dynamic and resilient modulus tests for local as well as global mixtures. The objectives of this paper is twofold: 1) To develop the correlation relationship to estimate the dynamic modulus using resilient modulus under same loading conditions and test parameters. 2) To investigate the influence of specimen size on resilient modulus. The selection of material and testing procedure is elaborated in ensuing paragraphs.

2. Materials and testing

This study used for wearing mixes of nominal maximum aggregate size 19 mm and 12.5 mm and the asphalt binder of penetration grade 60/70. The gradations include: Pakistan's National highway authority (NHA)'s Class A and B [3], superpave mix [4] and asphalt institute manual series (MS)-2 mix [5]. The percent passing for each gradation is presented in Table 1. The volumetrics were determined in accordance with Marshall standard procedures and tabulated in Table 2.

Table 1 Gradation for Asphalt Mixtures

Sieves (mm)		37.5	25.4	19	12.5	9	6.4	4.75	2.36	1.18	0.6	0.3	0.015	0.075
Layers	Gradations	Passing (%)												
Wearing Course	NHA-A	100	100	95	76	63	52	42.5	29	20	13	8.5	6	5
	NHA-B	100	100	100	82	70	59	50	30	20	15	10	7	5
	Superpave	100	100	100	94	87	74	65	37	21	14	9	7	5
	MS-2	100	100	100	95	82	69	59	43	30	20	13	8.5	6

Table 2 Volumetric Parameters and Optimum Binder Content of Asphalt Mixtures

Layer Type	Mix Type	Optimum Asphalt Content	Air Voids (%)	VMA (%)	VFA (%)	Stability (Kg)	Flow (mm)
Wearing Course	NHA-A	4.0	4.0	12.15	66.08	1362	12.04
	NHA-B	4.1	4.0	12.95	65.16	1291	12.65
	Superpave	5.0	4.0	14.70	69.18	1424	13.55
	MS-2	4.8	4.0	14.52	67.73	1544	13.12

The specimens for performance testing were fabricated using superpave gyratory compactor. The mixtures were left in oven prior to compaction for short term aging for two hours at 135 °C. For |E*| testing, cylindrical specimens of 100 mm diameter were taken from compacted six inches diameter specimens in accordance with AASHTO TP62-07 [6] whereas for Mr testing, 100 mm and 150 mm diameter specimens were taken with approximate height of 2 inches. The air voids were controlled at 4% ± 0.5.

Dynamic modulus test was carried using asphalt mixture performance tester (AMPT) which generally consists of environmental chamber, confining pressure system to apply pressure upto 210 kPa. Triplicate specimens were tested for each of two temperatures (25, and 40 °C) and six different frequencies (0.1 to 25 Hz). The resilient modulus test was carried out using universal testing machine (UTM) consisting of chamber for conditioning of test specimen and temperature control. This test was performed at two temperatures (25 and 40 °C) for triplicate specimen of each mix.

3. Results

3.1. Dynamic modulus

The ratio of peak-to-peak stress to peak-to-peak recoverable strain under sinusoidal loading is represented by dynamic modulus (|E*|). The compressive sinusoidal load was applied to simulate the dynamic movement of vehicles. Triplicate specimens were tested for each mix at two temperatures (25 and 40°C) and six frequencies (0.1 to 25 Hz). The phase angle (φ) is defined as an angle to which axial strain lags behind the compressive stress. The results suggested that initially phase angle increases with increase in temperature and decreases with increase in frequency. However, this seems to be deemed fit until temperature reaches 37.8 °C, as the phase angle tends to behave oppositely and tends to decrease with increase in temperature and decreases with decrease in frequency.

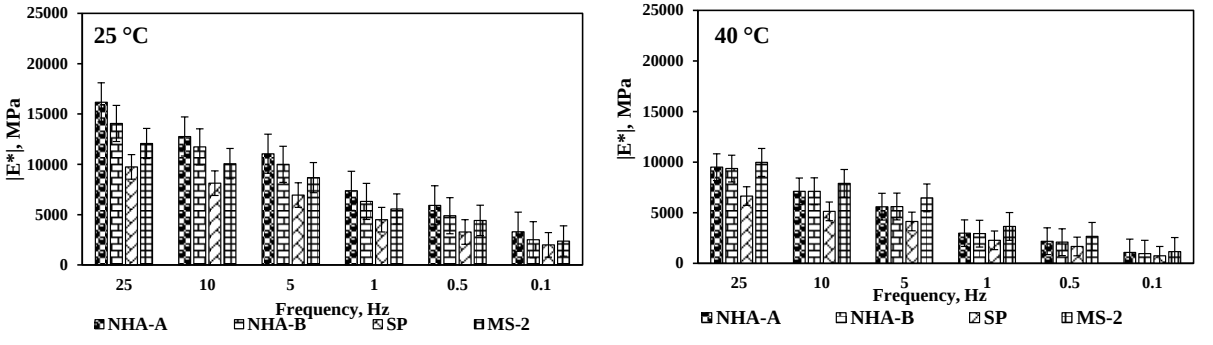

Fig. 1 Dynamic modulus test results.

Figure 1 presents the dynamic modulus test results. It can be inferred that at constant frequency, the increase in temperature causes |E*| to decrease significantly as it can be seen by lower dynamic modulus values at higher temperatures and at constant temperature, the increase in loading frequency resulted increase in dynamic modulus values, which is consistent with past researches reported by various researches [7-9]. An increase in temperature (from 25 to 40°C), translated into 45% drop in |E*| values on average. As the loading frequency is increased, 80% of variation in |E*| values on average was attributed to the sweep of frequency (from 25 to 0.1 Hz).

3.2. Resilient modulus

The comparison of Mr obtained for two specimen sizes is illustrated in Figure 2. It can be inferred that resilient moduli obtained for 100 mm specimens found higher than those obtained for the specimen sized 150 mm. The difference between two specimen sizes become more prominent once temperature is increased from 25°C to 40°C. The ratios of 100 mm specimens to that of 150 mm specimens on average for four mixtures (NHA-A, NHA-B, SP, MS-2) were found to be 1.23, 1.18, 1.40, and 1.40, respectively, for 25°C temperature and 1.46, 1.24, 1.17 and 1.97, respectively, for 40°C temperature.

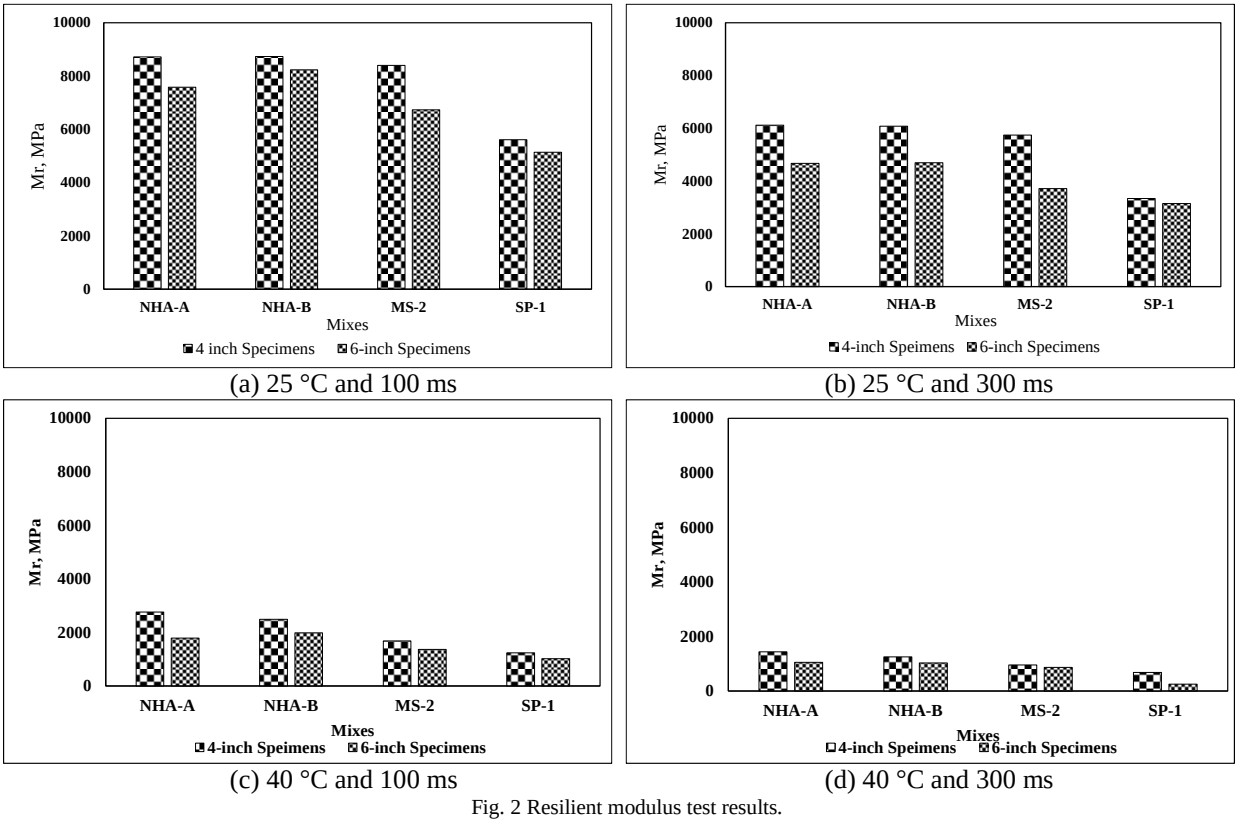

(a) 25 °C and 100 ms (b) 25 °C and 300 ms

(c) 40 °C and 100 ms (d) 40 °C and 300 ms

Fig. 2 Resilient modulus test results.

3.3. Empirical correlation between resilient and dynamic modulus

Various research studies had illustrated the differences between dynamic modulus and resilient modulus [10-13]. Apart from this, researchers had attempted to develop the correlation between these two test methods using their study parameters [2, 9, 13, 14]. Birgission et al. [2] performed various tests and analysis procedures to predict dynamic modulus from indirect tensile strength tests. Ping and Xiao [9] conducted a comparison study on dynamic modulus and resilient modulus and found that dynamic modulus performed at 4 Hz has strong correlation with resilient modulus performed at frequency of 1 Hz (0.1 ms).

There are some basic difference in both dynamic and resilient modulus test. These differences are the loading pattern (tension or haversine versus compressive or sinusoidal), loading duration (no rest period versus rest period) and material property (Viscoelastic versus elastic), and these differences are in agreement with previous studies [9, 11]. The dynamic modulus is evaluated at various frequencies and hence, it is necessary to locate the frequency that most closely simulate the actual traffic loading. This would be helpful in design of pavement using various approaches.

A comparison between resilient modulus (Mr) values with dynamic modulus |E*| values was carried out to ascertain the frequency at which dynamic modulus values tie with the resilient modulus values at 25°C. A strong correlation was found between the dynamic modulus values at 5 Hz load frequency with the resilient modulus values at 25°C temperature and 100 ms load pulse. A trend is observed that with increase in dynamic modulus resilient modulus is increased at a certain frequency (Figure 3). The figure indicates that resilient modulus values are very close to dynamic modulus values at loading frequency of 5 Hz. The coefficient of determination (R2) also suggests that about 85% of variation in |E*| is being captured by variation in Mr.

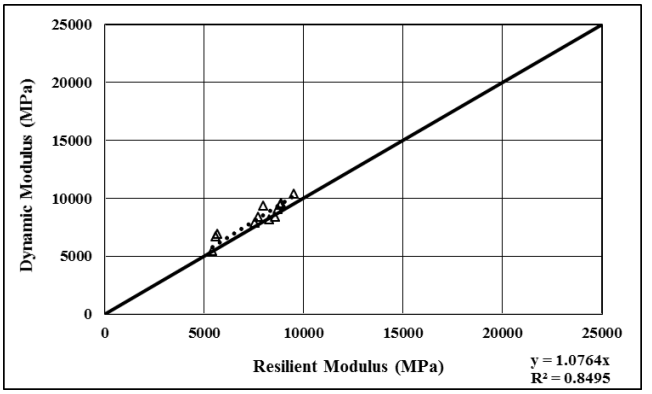

Fig. 3 Dynamic modulus vs Resilient modulus.

4. Conclusions

This paper presents the dynamic modulus testing of different asphalt concrete mixtures at two temperatures (25 and 40°C) and frequencies (0.1 to 25 Hz) and resilient modulus at two different temperatures (25 and 40 °C) and loading duration (100 ms and 300 ms). The dynamic modulus test results indicated that an increase in temperature yields lowering of dynamic modulus values significantly whereas an increase in frequency caused increase in |E*| values. For resilient modulus, temperature and loading duration have same effect analogous to temperature in |E*|. The statistical analysis revealed that specimen diameter is influencing factor in resilient modulus and 100 mm specimens have higher resilient modulus than 150 mm specimen diameter. Also, comparison of |E*| with Mr was carried out and results showed that |E*| is strongly correlated with Mr at 5 Hz for 25°C temperature.

Acknowledgements

This research was sponsored by National Highway Authority (NHA) through Highway Research and Training Center (HRTC) and was part of research project titled “Improvement of asphalt mix design technology for Pakistan” under collaboration agreement with National University of Sciences and Technology. The technical support and financial assistance provided by NHA, staff/ officials HRTC, and NUST is hereby acknowledged..

References

[1] National Cooperative Highway Research Program (NCHRP), Guide for Mechanistic-Empirical Design of New and Rehabilitated Pavement Structures. Final Report, NCHRP 1-37A. Transportation Research Board of the National Academies, Washington, D.C., 2004.

[2] Birgisson B., Roque R., Kim J., Pham L.V., The Use of Complex Modulus to Characterize the Performance of Asphalt Mixtures and Pavements in Florida, Final Report, BC-354-22, The Florida Department of Transportation, Florida, 2004.

[3] National Highway Authority (NHA). General Specifications. NHA Head Quarters, 27 Mauve Area, G-9/1, Islamabad. Pakistan, 1998.

[4] Federal Highway Administration (FHWA). Strategic Highway Research Programme, Washington D.C. USA. 1998.

[5] Asphalt Institute. Mix Design Methods for Asphalt Concrete and Other Hot-Mix Types. Manual Series No. 2, (MS-2). Lexington, KY. (1997).

[6] AASHTO, TP 62-07. Standard Test Method for Determining the Dynamic Modulus of Hot Mix Asphalt (HMA). American Association of State Highway and Transportation Officials, Washington D.C. USA. (2007).

[7] Clyne, T. R., X. Li, M. O. Marasteanu, and E. L. Skok. Dynamic and Resilient Modulus of MNDOT Asphalt Mixtures. Report MN/RC-2003-09. Minnesota Department of Transportation, Minneapolis, 2003.

[8] Pellinen, T. K., and M. W. Witczak. Stress Dependent Master Curve Construction for Dynamic Modulus. Journal of the Association of Asphalt Paving Technologists, Vol. 71, 281–309, 2002.

[9] Ping, W. V., and Xiao, Y. Empirical Correlation of Indirect Tension Resilient Modulus and Complex Modulus Test results for Asphalt Concrete Mixtures. Road Materials and Pavement design, 177-200. 2008.

[10] Witczak, M.W., A comparison of the Dynamic (Complex) Modulus Test (E*) and Indirect Diametral Test (Mr) for AC Mixtures, "White Paper" Report, NCHRP 1-37A Project, 1999.

[11] Drescher A., Newcomb D.E., Zhang W., Interpretation of Indirect Tension Test Based on Viscoelasticity, Transportation Research Record: Journal of the Transportation Research Board, No. 1590, Washington, D.C., 45-52. 1997.

[12] Zhang W., Drescher A., Newcomb D.E., Viscoelastic Analysis of Diametral Compression on Asphalt Concrete, Journal of Engineering Mechanics, Vol. 123, ASCE, 596-603, 1997.

[13] Kim Y.R., Seo Y., King M., Momen M., Dynamic Modulus Testing of Asphalt Concrete in Indirect Tension Mode, Transportation Research Record: Journal of the Transportation Research Board, No. 1891, Washington, D.C., 163-173. 2004.

[14] Loulizi A., Flintsch G.W., Al-Qadi I.L., Mokarem D., "Comparing Resilient Modulus and Dynamic Modulus of Hot-Mix Asphalt as Material Properties for Flexible Pavement Design", Transportation Research Record: Journal of the Transportation Research Board, No. 1970, Washington, D.C., 2006, p. 161-170.

Available online at www.sciencedirect.com

ScienceDirect

Procedia Engineering 00 (2017) 000–000

Procedia Engineering

www.elsevier.com/locate/procedia

Sustainable Civil Engineering Structures and Construction Materials, SCESCM 2016

Use of crumb rubber as an additive in asphalt concrete mixture

Paravita Sri Wulandari[a], Daniel Tjandra[a,*]

[a]*Petra Christian University, Siwalankerto 121 – 131, Surabaya, Indonesia*

Abstract

As the rapidly growing number of vehicles in Indonesia, the waste of tire rubber becomes a major environmental concern. The use of crumb rubber, which is the recycled tire rubber, as an additive in hot mix asphalt mixture is considered as a sustainable construction method. The purpose of this study was to investigate the effect of adding crumb rubber to asphalt mixture using wet process. The laboratory hot mix asphalt design tests were done by Marshall Method procedure. In this study, two different crumb rubber contents (1% and 2% by weight of asphalt mixture) and two different crumb rubber sizes (#40 and #80) were investigated. A comparative study was done among the unmodified and modified asphalt concrete mixtures considering the Marshall Stability value and the volumetric properties. The results showed that crumb rubber is recommended as an additive in asphalt mixture, as all the test results are within the standard requirements. The addition of crumb rubber tended to increase the strength and quality of asphalt mixture. However, it should be more concern about durability of asphalt mixture because of the lower asphalt content in crumb rubber modified asphalt mixture.

Peer-review under responsibility of the organizing committee of SCESCM 2016.

Keywords: asphalt concrete; crumb rubber; Marshall Stability; hot mix asphalt; wet process

1. Introduction

As the rapidly growing number of vehicles in Indonesia, the waste of tire rubber becomes a major environmental concern. The use of crumb rubber, which is the recycled tire rubber, as an additive in asphalt mixture is considered as a sustainable construction method. There have been many investigations on crumb rubber modified asphalt mixtures [1,2,3,4,5,6]. The addition of crumb rubber to the bitumen binder enhanced the physical properties of rubberised bitumen binder as indicated by reduction in penetration and ductility [1]. Laboratory test results show that crumb rubber modified asphalt mixture could improve the characteristics of asphalt mixtures [2, 3, 4].

* Corresponding author. Tel.: +6-231-298-3398; fax: +6-231-298-3392.
E-mail address: paravita@petra.ac.id

1877-7058
Peer-review under responsibility of the organizing committee of SCESCM 2016.

There are two basic process for adding crumb rubber in asphalt mixture, wet and dry process [5]. In wet process, crumb rubber is added to hot asphalt and allows the rubber and asphalt to react. The main process of wet process is swelling of the rubber. In dry process, crumb rubber is mixed with the hot aggregate prior to adding the bitumen. The addition of tire rubber in asphalt mixtures using dry process could improve the properties of resistance to permanent deformation at high temperature and cracking at low temperature [6]. The rubberized asphalt mixture with wet process could obtain the desired volumetric parameters as specified [3]. The purpose of this study was to investigate the effect of adding crumb rubber to asphalt mixture using wet process.

2. Research methodology

2.1 Materials

In this study, asphalt Pertamina with 60/70 penetration grade was selected. This study applied crumb rubber as additive in asphalt mixture. The sizes of crumb rubber used were no. 40 (0.42 mm) and no. 80 (0.177 mm). The coarse and fine aggregates used for this research was supplied from Pandaan (East Java Province, Indonesia).

2.2 Preparations of asphalt mixtures

Marshall Mix Design Method was applied throughout this study, for the unmodified and crumb rubber modified asphalt concrete mixture. This mix design method is commonly used to design the asphalt mixtures in Indonesia. In this study, several stages of laboratory examination were conducted. First stage was aggregate selection, including the determination of aggregate physical properties and the composite gradation for asphalt mixtures to meet the specification requirements. This specification was referring to General Specification 2010 (Revised 3) of the Department of Public Works of Indonesia [7]. Second stage was asphalt evaluation for both asphalt mixtures, unmodified asphalt concrete and crumb rubber modified asphalt mixtures, and also estimating of the asphalt optimum content for each asphalt mixtures. At the end, verification of the volumetric parameters was done. Three samples for each mixture were prepared.

Adding crumb rubber to asphalt mixtures was conducted based on wet process. The amounts of the crumb rubber were 1% and 2% by weight of asphalt mixture. Asphalt was heated at high temperature (about 150°C) before mixing with crumb rubber. The mixing temperature was kept constant in between 135-150°C. The mixing process was done manually until a homogenous mixture was reached. The crumb rubber asphalt mixture was then added to the hot aggregate. This study was done for two different crumb rubber sizes.

3. Results and discussion

3.1 Aggregates

Laboratory test results for general properties aggregate is shown in Table 1. Sieve analysis results of tested aggregates are shown in Figure 1 and Table 2. Table 2 also shows combined aggregate gradation for asphalt mixture. It was determined according to the specification requirement.

Table 1. Properties of coarse, medium and fine aggregates

Aggregate properties	Standard Test Method	Standard Requirements	Test Results
	Coarse and medium aggregates		
Bulk specific gravity	SNI 1969:2008	Min 2,5	2.772
Apparent specific gravity	SNI 1969:2008	-	2.854
Effective specific gravity	SNI 1969:2008	-	2.772
Water absorption	SNI 1969:2008	Max 3 %	1.695%
Los Angeles Abrasion	SNI 2417:2008	Max 40%	28.76%
Flakiness and elongation index	ASTM D - 4791	Max 10 %	9.29%
Adhesion of mineral aggregate to hot bitumen	SNI 2439:2011	Min 95	>95
	Fine Aggregates		
Bulk specific gravity	SNI 1969:2008	Min 2,5	2.754
Apparent specific gravity	SNI 1969:2008	-	2.844
Water absorption	SNI 1969:2008	Max 3 %	1.142

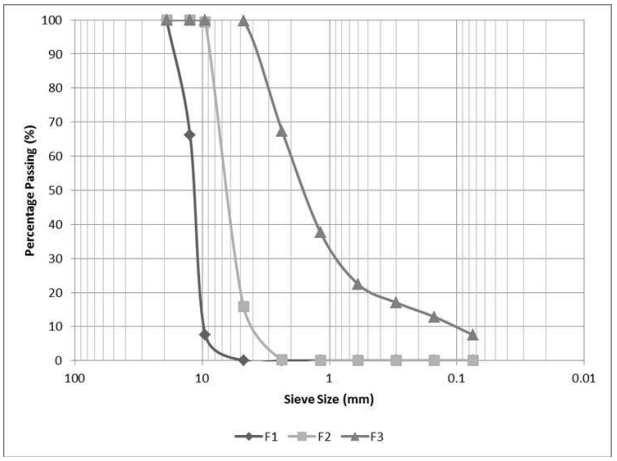

Fig 1. Sieve analysis results of tested aggregates

Table 2. Combined aggregate gradation for asphalt mixture

Sieve Size (mm)	Coarse Aggregate (F1) 10-15 mm		Medium Aggregate (F2) 5-10 mm		Fine Aggregate (F3) 0-5 mm		Filler Cement	Combined Aggregate	Specification
	% passing	20%	% passing	28%	% passing	50%	2%		
19.1	100.00	20.00	100.00	28.00	100.00	50.00	2	100.00	100
12.7	66.13	13.23	100.00	28.00	100.00	50.00	2	93.23	90-100
9.5	7.64	1.53	99.37	27.82	100.00	50.00	2	81.35	72-90
4.75	0.00	0.00	15.88	4.45	99.71	49.85	2	56.30	43-63
2.36	0.00	0.00	0.18	0.05	67.33	33.66	2	35.71	28-39.1
1.18	0.00	0.00	0.00	0.00	37.64	18.82	2	20.82	19-25.6
0.6	0.00	0.00	0.00	0.00	22.49	11.24	2	13.24	13-19.1
0.3	0.00	0.00	0.00	0.00	17.03	8.51	2	10.51	9-15.5
0.150	0.00	0.00	0.00	0.00	12.84	6.42	2	8.42	6-13
0.075	0.00	0.00	0.00	0.00	7.57	3.78	2	5.78	4-10

3.2 Physical properties of asphalts

Properties of asphalt and modified asphalt are shown in Table 3 and Table 4. It was observed that higher crumb rubber content had strongly effect on reducing penetration and ductility of asphalt, otherwise, the softening point had increased. All physical properties of asphalt were within standard requirements.

Lower penetration and higher softening point in crumb rubber modified asphalt indicated that crumb rubber made the asphalt more stiff, but also reduced the flexibility of modified asphalt. Lower ductility showed that asphalt had poor adhesive properties. A decrease in ductility value can be explained that modified asphalt was made by manual blending process and it has effects on the physical interactions of the bitumen and crumb rubber. [1] The blending process was a critical step to ensure a homogenous mixture. Homogeneity is crucial to defining asphalt mixture characteristics.

Table 3. Properties of asphalt with 60/70 penetration grade.

Asphalt Properties	Standard Test Method	Standard Requirements (Asphalt 60-70)	Test Results
Penetration at 25°C, dmm	SNI 06-2456-1991	60-70	64.3
Ductility at 25°C, cm	SNI 06-2432-1991	≥ 100	105
Softening Point, °C	SNI 06-2434-1991	≥ 48	52.2
Specific gravity	SNI 06-2441-1991	>1.0	1.03
Flash Point, °C	SNI 06-2433-1991	≥ 232	340

Table 4. Properties of crumb rubber modified asphalt

Asphalt Properties	Standard Test Method	Standard Requirements (Modified Asphalt)	Test Results (Crumb rubber size #40)		Test Results (Crumb rubber size #40)	
			1%	2%	1%	2%
Penetration at 25°C, dmm	SNI 06-2456-1991	Min. 40	41.33	44.00	43.80	41.50
Ductility at 25°C, cm	SNI 06-2432-1991	≥ 100	111	25	98	54
Softening Point, °C	SNI 06-2434-1991	≥ 54	54.06	57.96	57.35	65.35
Specific gravity	SNI 06-2441-1991	>1.0	1.033	1.033	1.033	1.033
Flash Point, °C	SNI 06-2433-1991	≥ 232	334	345	345	350

3.3 Optimum asphalt content

In order to determine the optimum asphalt content, asphalt content was varied at 5%, 5.5%, 6.0% and 6.5% by weight of asphalt mixture. Three samples were tested for each variation of asphalt content. Optimum asphalt content was determined based on the combined results of Marshall Test, corresponding to the requirement specification. Table 5 shows the optimum asphalt content for all asphalt mixtures. The crumb rubber does not have a significant effect on optimum asphalt content, but tended to decrease optimum asphalt content of asphalt mixture.

Table 5. Optimum Asphalt Content

Type of asphalt mixture	Unmodified asphalt mixtures	Crumb rubber modified asphalt mixtures (#40)		Crumb rubber modified asphalt mixtures (#80)	
		1%	2%	1%	2%
Optimum asphalt content (%)	6.0	5.5	5.3	5.5	5.5

3.4 Marshall Test Results

Marshall Test results for all asphalt concrete mixture are shown in Table 6. These Marshall and flow tests were conducted based on the determined optimum asphalt content for each asphalt concrete mixture. The use of crumb rubber as an additive material in asphalt mixture has satisfactory results, as all the parameters value are within the standard requirements.

Table 6. Comparison of Marshall Test results for all asphalt concrete mixtures

Type of asphalt mixture	Unmodified asphalt	Crumb rubber modified asphalt mixtures (#40)		Crumb rubber modified asphalt mixtures (#80)		Standard requirements (SNI 8198:2015)
		1%	2%	1%	2%	
Marshall Stability (kg)	1033.35	1210.10	1228.38	1393.53	1418.50	Min 800 (for unmodified asphalt concrete mixtures) Min 1000 (for modified asphalt concrete mixtures)
Flow (mm)	3.56	3.56	3.22	3.56	3.30	3-4.5
Marshall Quotient (kg/mm)	290.62	340.58	382.39	398.71	430.32	Min 250 (for unmodified asphalt concrete mixtures) Min 300 (for modified asphalt concrete mixtures)
VFB (%)	79.11	77.45	74.66	76.03	75.69	Min 65
VIM (%)	3.71	3.76	4.25	3.74	3.81	3-5 (for unmodified asphalt concrete mixtures) 3-5.5 (for modified asphalt concrete mixtures)
VMA (%)	17.78	16.63	16.74	15.60	15.66	Min 15

From the results of Marshall Test, it was observed that the higher crumb rubber content and finer crumb rubber cause an increase in Marshall Stability and Marshall Quotient. On the contrary, the addition of crumb rubber decreases flow parameter.

Marshall Quotient, which is ratio of stability to flow, indicates the strength and quality of asphalt mixture. The higher Marshall Quotient value shows the asphalt mixture has more stiffness and strength to cracking. Hence, the asphalt mixture has more resistance in permanent deformation. It is also shown, for higher crumb rubber content, flow tends to decrease. Lower flow value indicates the mixture has insufficient asphalt content and become more stiff. It is as shown on a decrease in optimum asphalt content (Table 5).

It was also shown the addition of crumb rubber decreases Voids Filled with Bitumen (VFB). VFB is the voids in the mineral aggregate filled with asphalt. The decrease in VFB indicates a decreasing effective asphalt film thickness, which results lower durability of asphalt mixtures.

Void in Mixture (VIM) tends to increase in higher crumb rubber content but decrease in finer crumb rubber. VIM shows the air void content. The higher air voids content decreases asphalt content in mixture. This result is as shown on a decrease in optimum asphalt content (Table 5).

The addition of crumb rubber decreases Void in Mineral Aggregate (VMA). It was also observed that the finer crumb rubber caused a decrease in VMA. The lower VMA indicates the less space is available for the asphalt film, however, a durable asphalt mixture requires an adequate asphalt film thickness.

4. Conclusions

Based on the results of laboratory investigation, conclusions of this research are described as the following,

1. Crumb rubber is recommended as an additive in asphalt mixture, as all the test results are within the standard requirements.
2. The addition of crumb rubber tends to increase the strength and quality of asphalt mixture. It is shown by an increase in stability and a decrease in flow.
3. Crumb rubber modified asphalt mixture needed less asphalt content. However, low asphalt content increases air void in mixture and thus mixture permeability increases. As permeability increases, asphalt mixture becomes less durable. Therefore, it should be more concern about durability of asphalt mixture because of the lower asphalt content in crumb rubber modified asphalt mixture.

References

[1] N.S. Mashaan, A.H.Ali, M.R., Karim, M. Abdelazis, Effects of crumb rubber concentration on the physical and rheological properties of rubberised bitumen binders, International Journal of the Physical Sciences. 6 (4), 2011, 684-690

[2] S. Rokade, Use of waste plastic and waste rubber tyres in flexible highway pavements, International Conference on Future Environment and Energy. IPCBEE Vol. 28, 2012, 105-108

[3] D. Zhang, X. Huang, Y. Zhao, S. Zhang, Rubberized asphalt mixture design using a theoretical model, Construction and Building Materials (67), 2014, 265-269

[4] D. L. Presti, Recycled tyre rubber modified bitumens for road asphalt mixture: a literature review, Construction and Building Materials (49), 2013, 863-881

[5] T. Butz, J. Muller, G, Riebesehl, Innovative methof for producing crumbed rubber modified asphalt, 5th Eurasphalt & Eurobitume Congress, Istanbul, 2012

[6] W. Cao, Study on properties of recycled tire rubber modified asphalt mixtures using dry process, Construction and Building Materials (21), 2007, 1011-1015.

[7] Directorate General of Spatial Planning and and Development, General Specification 2010 Revised 3, Jakarta, 2014

Available online at www.sciencedirect.com

ScienceDirect

Procedia Engineering 00 (2017) 000–000

Procedia Engineering

www.elsevier.com/locate/procedia

Sustainable Civil Engineering Structures and Construction Materials, SCESCM 2016

The effect of latex on permanent deformation of asphalt concrete wearing course

Henri Siswanto[a,*]

[a] *The Departement of Civil Engineering, The Faculty of Engineering, Universitas Negeri Malang, Malang 651444, Indonesia*

Abstract

Pavement rutting is primarily caused by the accumulation of permanent deformation in a portion or in all of the pavement layers. The accumulation of permanent deformation in surface layers is now considered to be the major caused for rutting. This requires solutions, one of which is to formulate an asphalt mix that has a high resistance to deformation, and one way to do this is to use latex as an additive. Thus, the purpose of this experimental study was to investigate the effect of latex in preventing deformation of the asphalt concrete wearing courses (ACWC). Four different latex to asphalt mixtures were investigated, namely 0%, 2%, 4% and 6% latex by weight of asphalt binder respectively. A wet process was used in the mixture blending. Specimens were tested in a wheel tracking machine at a temperature of 60ºC. The results indicated that latex decreased the rate of deformation in asphalt mixtures by increasing its dynamic stability.

Peer-review under responsibility of the organizing committee of SCESCM 2016.

Keywords: latex; permanent deformation; asphalt concrete wearing course.

1. Introduction

Permanent deformation in asphalt layers is one of the most significant types of asphalt pavements deterioration, and, depending on the level, it can be a considerable obstacle for traffic safety, driving comfort and overall life-cycle of pavement structure. Permanent deformation of the asphalt layer is caused by a combination of densification (volume change) and shear deformation (no volume change) from the repetitive application of traffic loads. Shear

* Corresponding author. Tel.: +62-853-352-400-60; fax: +62-341-582-087.
E-mail address: henri.siswanto.ft@um.ac.id

Peer-review under responsibility of the organizing committee of SCESCM 2016.

deformation of properly constructed (compacted) pavements is caused primarily by large shear stresses in the upper portions of asphalt layer(s) [1].

Although the rutting in flexible pavements can be the total sum of accumulated permanent deformations in one or more layers of the pavement structure, the accumulation of permanent deformation in the asphalt surfacing layer is now considered to be the major cause of rutting [2]. Conventional asphaltic concrete designed using the Marshall method has been shown to fail very rapidly due to rutting in high stress areas. To minimize this form of rutting, it is necessary to pay extra attention to material selection and mixture design and one solution is to formulate an asphalt mix that has a high resistance to deformation and one way to do this is to use latex as an additive.

Natural rubber latex at high temperatures increases the bitumen's viscosity (thickening) and at low temperatures it reduces thermal cracking associated with bitumen. At low temperatures bitumen freezes and becomes so stiff that it will crack under stress, natural rubber overcomes this by acting like an elastic band which hold the bitumen together and helps dissipate stresses as they develop. Natural rubber latex has also proven to be more cost effective than the use of natural rubber powder or recovered scrap tyres [3].

The application of natural rubber by mixing with asphalt materials in roadworks could improve the quality of road pavement, extend service life, and reduce maintenance cost [4]. Rutting is the dominant deterioration problem in Indonesia because of its hot climate. Indonesia is the second largest natural rubber producer globally behind Thailand [5]. The development of the utilization of latex on the main road construction needs to be done to solve the problem of rutting.

2. Method

2.1 Materials

The materials used in this study were a 60/70 penetration bitumen, aggregate and latex. The latex used in this research was natural rubber of 60% dry rubber content (DRC 60). It is available in Indonesian market. The aggregate gradation used can be seen in Figure 1. The Indonesian National Standards (SNI 1737–1989) were used and all test results had to meet SNI standards.

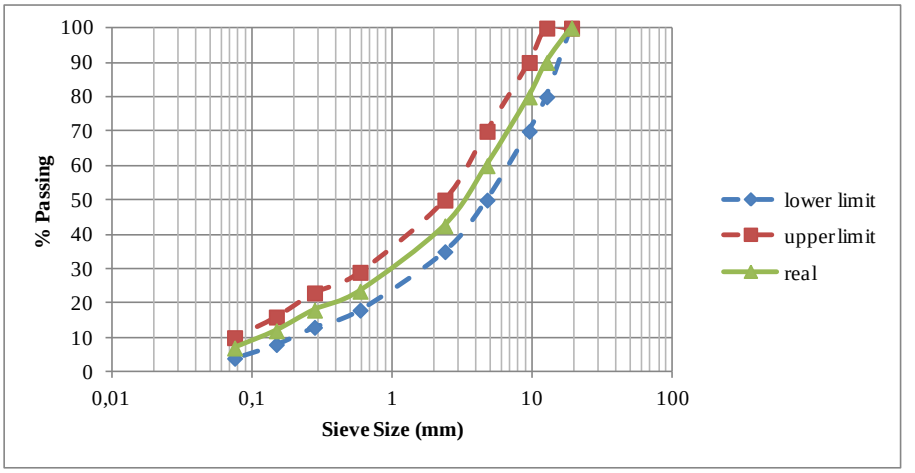

Fig. 1 The Grading Curves of Asphalt Concrete Wearing Course

2.2 Blending latex and bitumen method

According to Road Note 36 Specification for the Manufacture and Use of Rubberised Bituminous road materials and binders, the method of blending rubber with penetration grade bitumen will vary in detail depending on the form of rubber to be used [6]. In general, the finer the particle size is, the more rapid the blending is. For binders harder

than 300 pen., the binder should be heated to a temperature of 140-170ºC depending on bitumen hardness in a boiler the capacity of which will allow for at least a 50 percent increase in binder volume. The boiler should be fitted with a propeller-type stirrer or other means of agitation which will ensure that any material added to the binder will be drawn down into it. Latex should be added slowly in small quantities and allowed to remain on the surface for about 20 seconds before stirring it. The intensity of foaming should be gauged and the remainder of the latex added at such a rate to ensure that the intensity of foaming is not to great for the capacity of the boilier used. After addition of the latex, the binder should be allowed to cool below 130ºC unless it is to be used immediately. Stirring should be continued for a minimum period of 20 minutes after the addition of the rubber.

2.3 Testing of the specimens

The procedure used to obtain the optimum binder contents were in accordance with the Marshall procedure. The binder contents investigated varied from 5.0% to 7.0% of total mixture weight, in increments of 0.5 percent. Three specimens were prepared for each binder content. For mixing pruposes, binder was heated to the temperature that produced a kinematics viscosity of 170±20 centistokes, for compaction the required viscosity was 280±30 centistkes.

Compaction was carried out by applying 75 blows to each face of the specimens, in accordance with the criterion for heavy traffic. The specimens were weighed in air and in water to determine the bulk specific gravity of the compacted mixes. At each binder content the following mix properties were determined; the specific gravity of the compacted mix, the void in the mineral aggregate (VMA), the voids in the mix (VIM) and the voids filled with the binder (VFB).

The average Marshall stability and flow value was determined for each binder content. The parameters obtained and then plotted against binder content were; stability, flow, unit weight, VIM, VFB and VMA. Optimum Binder Content (OBC) was determined from their graphs. The results of the Marshall tests are summarized in Table 1,which shows that the OBC is achieved at a binder content of 6.5%.

Table 1. Summary of the Design Results of the Marshall Method Compared to Indonesian Specifications

Design Parameters	Unit	Value	Indonesian Specifications	
			Min	Max
Marshall stability	kg	1011	800	-
Flow	mm	3.39	3	-
VIM	%	4.74	3.5	5.5
VMA	%	17.74	15	-
VFB	%	75.66	65	-
Marshall Quotient	kg/mm	330	250	-
OBC	%	6.5	-	-

Six specimens containing latex and two without latex, all at optimum binder content were prepared for the wheel tracking test. The specimens, 30x30x5 cm in size, were prepared according to the specified procedure. The same mixing procedure as for the Marshall test was employed and the specimens were compacted in a roller compaction mechine to a density approximately equal to that of Marshall specimens compacted with 75 blows. The compaction was carried out at contact pressure of 5.6 kg/cm^2 with 75 passes.

Before the wheel tracking test was begun, the specimens were immersed in the water bath of the wheel tracking apparatus for about 30-40 minutes at 60°C. The test was performed at a wheel contact presure of 6.5±0.15 kg/cm^2 that corresponded to a dual wheel, single axle load of 8.16 tons on a 5.25x20 tire at a pressure of 480 kN/m^2. Each specimen was subjected to approximately 2640 passes of the wheel at a rate of 44 passes per minute.

3. Results and discussion

The mix made without latex (0% latex) had an optimum binder content of 6.5%, all mixtures prepared had this optimum bitumen content. Data on the wheel tracking test are presented in Fig 2 and Table 2. Fig. 2 shows that deformation at the end of test, i.e. after 2640 passes of the loading wheel, was reduced with increasing latex content. Deformation decreased from a value of 9.73 mm (mix with 0% latex) to 7.86 mm, 6.84 mm, and 6.20 mm by adding 2%, 4% and 6% latex respectively, corresponding to precentage decreases of 19.70%, 29.70% and 36.28%. The data collected indicated that adding latex significantly increased resistance to deformation. Other parameters used to evaluate performance in the wheel tracking test were Dinamic Stability (DS) and Rate of Deformation (RD). Data in Table 2 shows that DS increased by 13.1%, 38.61% and 53.48% by adding 2%, 4% and 6% latex respectively and RD decreased by 11.52%, 27.92% and 34.9%. This experimental study conducted in temperature of 60ºC and thus the addition of latex to asphalt mixes improves resistance to deformation at high temperatures. The higher latex content in the mix, the lower deformation of the ACWC.

Some studies on adding latex to asphalt mixes also found that it enhanced the physical and the mechanical properties of aphalt mixtures [7,8,9,10,11,12,13]. Using a dynamic creep test indicated that the addition of latex and carbon black to asphalt mix was able to sustain a higher load [7]. A study by [8] found that base on the condition survey and Tensile Strength Ratio (TSR) testing revealed that the latex polymer (UP-5000) was comparable to hydrated lime in preventing moisture induced distress in hot mix asphalt pavements in Oregon.

Table 2. Dynamic stability and Rate of Deformation at Various Latex Content

Time		Deformation (mm)											
(minute)	Cycles	0% Latex			2% Latex			4% Latex			6% Latex		
		I	II	Average	I	II	Average	I	II	Average	I	II	Average
0	0	0,00	0	0,00	0,00	0,00	0,00	0,00	0,00	0,00	0,00	0,00	0,00
0,5	11	0,48	0,53	0,51	0,45	0,49	0,47	0,49	0,43	0,46	0,38	0,35	0,37
1	22	0,88	0,94	0,91	0,82	0,91	0,87	0,75	0,67	0,71	0,6	0,55	0,58
2	44	1,33	1,43	1,38	1,23	1,36	1,30	1,17	1,03	1,10	0,94	0,86	0,90
3	66	1,71	1,83	1,77	1,60	1,77	1,69	1,46	1,3	1,38	1,18	1,08	1,13
4	88	2,00	2,14	2,07	1,86	2,05	1,96	1,78	1,58	1,68	1,39	1,27	1,33
5	110	2,28	2,44	2,36	2,15	2,37	2,26	1,95	1,73	1,84	1,62	1,48	1,55
10	220	3,67	3,93	3,80	2,98	3,29	3,14	2,97	2,63	2,80	2,35	2,15	2,25
15	330	4,89	5,23	5,06	3,69	4,08	3,89	3,68	3,26	3,47	3,1	2,84	2,97
20	440	5,74	6,14	5,94	4,40	4,87	4,64	4,42	3,92	4,17	3,69	3,37	3,53
25	550	6,58	7,02	6,80	5,13	5,67	5,40	5,09	4,51	4,80	4,31	3,95	4,13
30	660	7,03	7,51	7,27	5,54	6,12	5,83	5,49	4,85	5,17	4,69	4,30	4,50
35	770	7,71	8,23	7,97	6,00	6,64	6,32	5,91	5,23	5,57	5,13	4,69	4,91
40	880	8,16	8,72	8,44	6,40	7,08	6,74	6,24	5,52	5,88	5,51	5,05	5,28
45	990	8,58	9,16	8,87	6,73	7,43	7,08	6,6	5,84	6,22	5,89	5,39	5,64
50	1100	8,88	9,48	9,18	7,03	7,77	7,40	6,82	6,04	6,43	6,13	5,61	5,87
55	1210	9,21	9,83	9,52	7,28	8,04	7,66	7,08	6,26	6,67	6,36	5,82	6,09
60	1320	9,41	10,05	9,73	7,45	8,23	7,84	7,26	6,42	6,84	6,47	5,93	6,20
Dynamic Stability (passes/mm)				767			868			1065			1179
Rate of Deformation (mm/min)				0,057			0,051			0,041			0,037

An experimental study by [9] found that 6% by weight of natural rubber in asphalt was the most effective ratio to develop low penetration, high softening point, high penetration index, high torsional recovery, and high toughness - tenacity. The roads with this mix had high strength and resistance, while increased of viscosity did not cause problems in aggregation of asphalt-concrete.

This research also showed increase in the mechanical properties of the ACWC by adding latex, i.e. the addition of latex to the mix increased resistance to deformation of the ACWC.

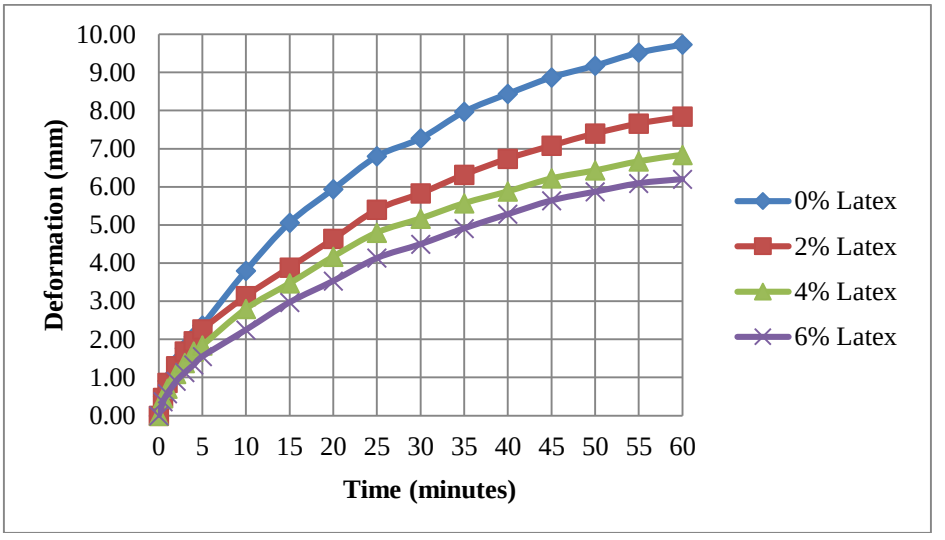

Fig.2 Deformation - Time Relationships

4. Conclusions

The results indicated that; 1) latex decreased the rate of deformation in asphalt mixtures by increasing its dynamic stability, 2) the higher latex content in the mix, the lower deformation of the ACWC, and 3) adding latex significantly increased resistance to deformation of the ACWC.

References

[1] M. W. Witczak. NCHRP Report 580: Specification Criteria for Simple Performance Tests for Rutting: Volume I: Dynamic Modulus (E*); Volume II: Flow Number and Flow Time. Transportation Research Board, Washington, DC, 2007.
[2] R. Garba. Permanent Deformation Properties of Asphalt Concrete Mixtures. Thesis the Departement of Road and Railway Engineering Norwegian University of Science and Technology. 2002.
[3] C.S. Ruggles. The Efficient Use of Environmentally-Friendly Natural Rubber Latex in Road Construction - Past, Present and the Future. Seminar "Rubber in Transport", Breda, The Netherlands, 2004.
[4] N. Tuntiworawit, D. Lavansiri and C. Phromson. The modification of asphalt with natural rubber latex. Proceedings of the Eastern Asia Society for Transportation Studies, Vol. 5. 2005. pp. 679-694.
[5] Reuters. Assesment of Indonesia's Rubber Industry Research and Market. http://www.reuters.com/article/research-and-markets. Assesed 14th April 2016.
[6] Transport Road Research Laboratory. Road Note 36 Specification for the Manufacture and Use of Rubberised Bituminous road materials and binders. 2nd Edition. Published by HMSO. 1968.
[7] E.O. Ekwulo and E.A. Igwe. Effect Of Loading Frequency On Dynamic Modulus Of Rubber Latex-Modified Asphalt Concrete. International Journ al of Current Research. Vol. 3, Issue, 10, 2011. pp.026-030.
[8] M. Lynde and E. Brooks. Evaluation Of Latex Polymers To Resist Stripping In Asphalt Pavements In Oregon. Final report SPR 554. Federal Highway Administrations Washington. D.C. 2005
[9] N. Vichitcholchai, J. Panmai and N. Na-Ranong. Modification of Asphalt Cement by Natural Rubber for Pavement Construction. Rubber Thai Journal 1: 2012. pp 32-39.
[10] O. Alexandrova, K.E. Kaloush, J. Allen. Impact of asphalt rubber friction course overlays on tire wear emissions and air quality models for phoenix, arizona airshed. J Trans Res Board, No. 2011, Washington, D.C.; 2007. p. 98–106.
[11] R.G. Hicks, J.A. Epps. Life cycle costs for asphalt rubber paving materials. Proceedings of the Asphalt Rubber 2000 Conference, Vilamoura, Portugal; 2000, pp 1-26.
[12] K. E. Kaloush, Zborowski A, Sotil A. Performance evaluation of asphalt rubber mixtures in Alberta. Final Report. Tempe, Arizona: Arizona State University; 2003
[13] K. E. Kaloush K et al. Material characteristics of asphalt rubber mixtures. Proceedings Asphalt Rubber 2003 Conference, Brasilia, Brazil; 2003. pp. 129–45.

Available online at www.sciencedirect.com

ScienceDirect

Procedia Engineering 00 (2017) 000–000

Procedia Engineering

www.elsevier.com/locate/procedia

Sustainable Civil Engineering Structures and Construction Materials, SCESCM 2016

Characterizing cracking and permanent deformation; an attempt for predicting the end of the structural pavement life

Florentina P. Pramesti[a,*], A.A.A Molenaar[b], M.F.C. van de Ven[c]

[a] *Civil Engineering Dept, Faculty of Engineering, Universitas Sebelas Maret, Surakarta, Indonesia*
[b] *Road and Railway Engineering, Faculty of Civil Engineering and Geosciences, Delft University of Technology (Professor Emeritus)*
[c] *Road and Railway Engineering, Faculty of Civil Engineering and Geosciences, Delft University of Technology (Associate Professor Emeritus)*

Abstract

Durable, therefore sustainable, road needs to attain specific characteristics, among others, resistance to permanent deformation and cracking. Determining the development of both characteristics are important to be able to predict pavement life and performance. In this research, permanent deformation occurring in three pavement sections was measured by a transverse profilograph. The pavement sections were simple two layer structures consisting of a gravel asphalt concrete (GAC) layer on a sand subgrade. The length and the width of the section are 16 m and 4 m respectively. These three sections were tested by means of Lintrack, an Accelerated Pavement Test (APT) which allows large number of realistic wheel load applied in a limited period of time. The results of this measurements shows the development of permanent deformation, which is defined as 'rut depth', as function of the number of load repetitions. Using relation exists between the radius of curvature of a deflection profile and the tensile strain at the bottom of a slab, the creep/permanent strain as a result of permanent deformation was calculated. This paper is carried out to determine relations between the rut depth and the radius of curvature and between the rut depth and the creep/permanent strain. Also, cracking development was observed upon these three pavement section. The result shows that there is a rather good correlation between rut depth and permanent/creep strain which is independent of the layer thickness.

Peer-review under responsibility of the organizing committee of SCESCM 2016.

Keywords: Permanent deformation,cracking,pavement

* Corresponding author. Tel.: +622718205050; fax: +62271634524.
E-mail address: pungkypramesti@gmail.com, f.p.pramesti@ft.uns.ac.id

Peer-review under responsibility of the organizing committee of SCESCM 2016.

1. Introduction

In 1990 the Road and Railroad Research Laboratory (RRRL) of the Delft University of Technology (DUT) built an accelerated pavement testing system (APT) called Lintrack which allows large number of realistic wheel loads to be applied in a limited period of time. Four pavement sections consisting of a gravel asphalt concrete (GAC) top layer on a sand subgrade were tested by means of the Lintrack [1-4].

These pavements had 16 m long and 4 m wide. After testing of lane I, it was decided to perform another test with the same loading condition but on a thinner construction. Therefore, the asphalt thickness of the second test lane (II) was reduced by milling it in May 1995 from 150 to 80 mm and the same was done for the third lane (III) in June 1996. These milled off sections with a thickness of 80 mm asphalt were called 'VA' and 'VB' respectively. Only pavement section I, VA and VB will be discussed in this paper. Table 1. provides the details of the thickness and the loading conditions of the three sections [1].

Table 1. Details of the three Lintrack sections

Section's name	Asphalt thickness [mm]	Load characteristic	Total number of wheel load applied
I	150 (80+70)	super single F = 75 kN, p = 950 kPa	4×10^6
II became $\mathbf{V_A}$	150 became 80	super single F = 75 kN, p = 950 kPa	6.5×10^5
III became $\mathbf{V_B}$	150 became 80	super single F = 50 kN, p = 700 kPa	1.7122×10^6

F = wheel load, p = tire pressure

During these tests, several parameters were measured such as strain at the bottom of the asphalt layer, temperature, transverse profile measurements to determine the amount of permanent deformation and surface cracking. This information provides a great opportunity to relate the development of the rut depth and the permanent/creep strain and further to evaluate its effect to the development of the surface cracking.

The World Bank's HDM III model shows that there is a relationship between the rut depth and the amount of cracking [5, 6]. In that model the average rut depth depends on the amount of cracking in the following way;

Average rut depth = f (% cracked area * mean monthly precipitation)

Since the Lintrack sections were covered, they were protected against the influence of precipitation making MMP (mean monthly precipitation) = 0. This implies that the HDM III model could not be used for the Lintrack sections to determine whether cracking would influence permanent deformation or vice versa. It is, however, very well possible that permanent deformation affects the occurrence of cracking because if a significant rut depth develops, significant curvature of the pavement occurs, which possibly cannot be followed by the asphalt layer without cracking. So cracking could develop as a result of creep.

Based on the huge number of information provided by the Lintrack sections, this paper attempt to determine to what extent the observed longitudinal cracks were a result of permanent deformation and their effect on the end of pavement life. This research is part of research performed on matching laboratory and field asphalt fatigue performance [7].

Before the existence of any relationship between permanent deformation and the structural pavement life (cracking) will be discussed, attention is called for the fact that all permanent deformation in each of the Lintrack pavement sections was caused by permanent deformations in the sand subgrade. Deformations in the asphalt layer itself made, if present, only a very small contribution to the total deformation.

2. Cracking and permanent deformation observed

2.1. Observed cracking

During the Lintrack tests the progression of the crack pattern at the surface was recorded using two techniques. The first one was by taking photographs of the test lane (regularly) and the second by drawing the cracks on transparent plastic sheets (regularly). The surface area of the Lintrack sections that was loaded was 12.8 m long and

2.4 m wide and on this area the crack observations at the end of the loading/testing were made, as shown in Figure 1 a, b and c [1, 2, 4].

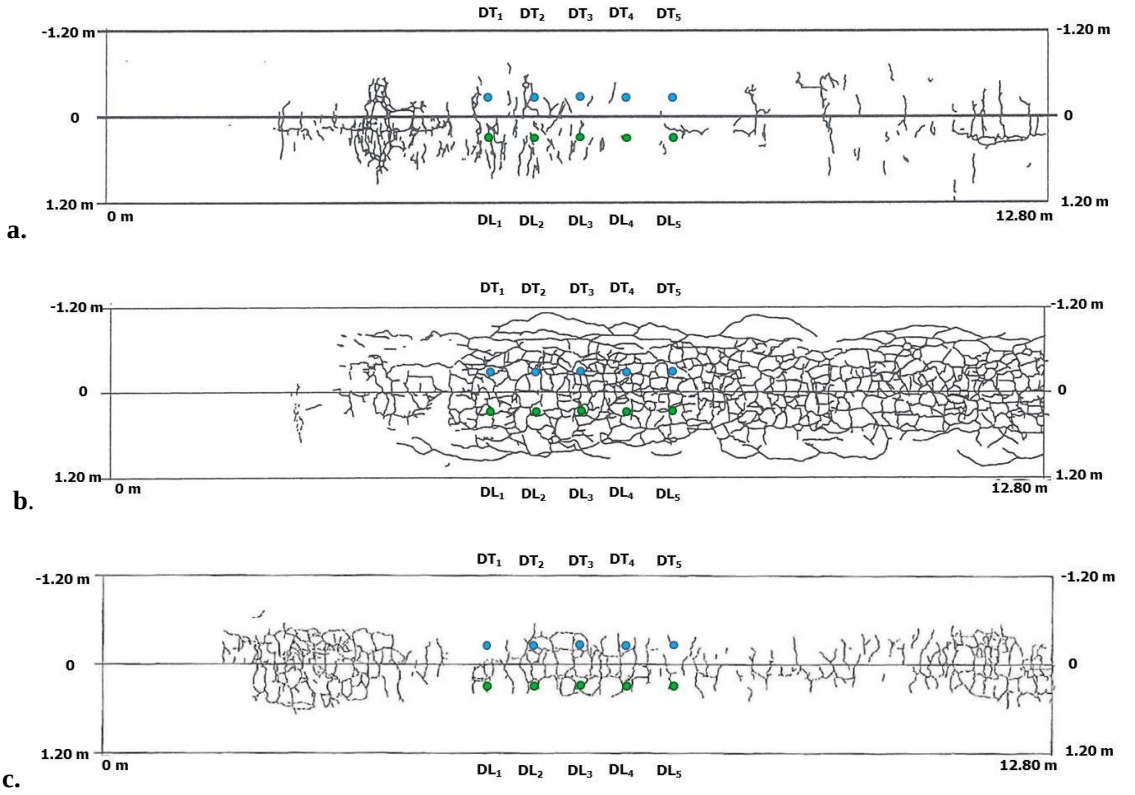

Fig.1. (**a**) Crack pattern of Lintrack section I after 4 Million cycles, wheel load 75 kN, 150 mm thickness. (**b**) section VA after 650 kilocycles, wheel load 75 kN, 80 mm thickness. (**c**) section VB after 1722 kilocycles, wheel load 50 kN, 80 mm thickness [1, 4]

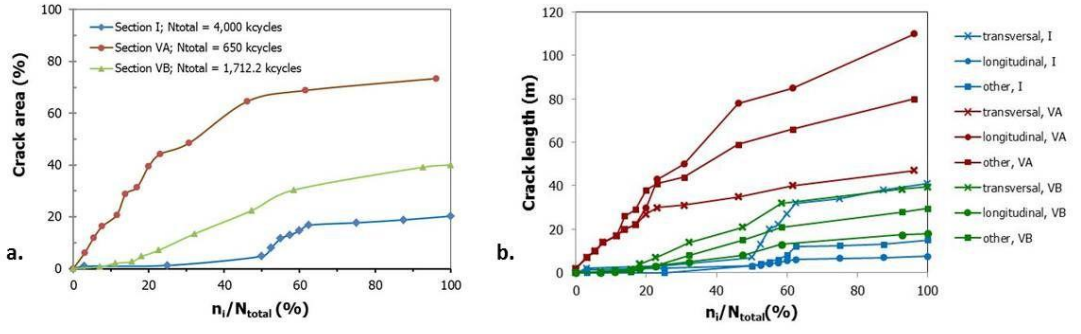

Fig. 2. (**a**) Development of the percentage cracked area on Lintrack sections I, VA, VB based on 100x100 grid size area (**b**) Development of crack length observed on Lintrack sections I, VA and VB (Pramesti [7] based on Groenendijk[1, 4] data)

The green and blue dots in Figure 1 describe the position of the five longitudinal and five transversal strain gauges respectively, which were placed close to the bottom of the asphalt layer. Figure 2 shows the development of the cracked area as a function of the number of load cycles applied which is shown as percentage of the total number of loads.

The amount of cracking was determined in the following way; an imaginary grid with cell sizes of 100 x 100 mm was laid over the travelled pavement surface. The percentage of the cells in which one or more cracks are visible is reported as the percentage cracked area. It should be kept in mind that the thinner VA and VB sections showed a denser crack pattern than the thicker section I and, therefore, showed a higher percentage cracked area at the end of the test than section I.

2.2. Observed permanent deformation

Permanent deformation occurring in the Lintrack sections was measured by a transverse profilograph comprising of an aluminium frame bridging the test lane and guiding the measuring wheel which travels across the pavement. Permanent deformation was defined as 'rut depth' and the results of the measurements are shown in Figure 3. The graph shows the development of permanent deformation as function of the number of load repetitions expressed as percentage of the total applied number of load repetitions. Section VA shows excessive permanent deformation development in the early stages of loading.

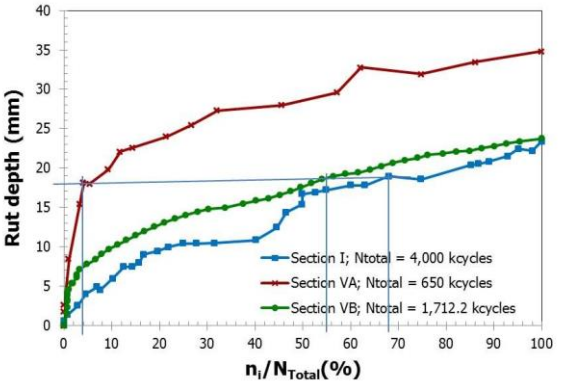

Fig. 3. Rutting of Lintrack sections I, VA and VB

According to the Dutch maintenance standard for motorways, maintenance action should be taken if the rutting depth reaches 18 mm. Based on this criterion, maintenance is supposed to be carried out at 4%, 55% and 68% of total loading for section VA, VB and I respectively. Figures 4.a. to 4.c. show the development of rut depth profiles on sections I, VA and VB.

3. Permanent strain and radius of curvature of the rut depth profile

From the theory of slabs it is known that a simple relation exists between the radius of curvature of a deflection profile and the tensile strain at the bottom of the slab [8].

$$M_{1x} = Eh^3 \frac{\left(\frac{1}{R_x} + \mu \frac{1}{R_y}\right)}{12\left(1-\mu^2\right)} \quad \text{and} \quad M_{1y} = Eh^3 \frac{\left(\frac{1}{R_y} + \mu \frac{1}{R_x}\right)}{12\left(1-\mu^2\right)} \tag{1}$$

where:

M_{1x} = bending moment in the x direction,
M_{1y} = bending moment in the y direction,
R_x = radius of curvature in the x direction,
R_y = radius of curvature in the y direction,
E = elastic modulus of the slab,
h = thickness of the slab,
μ = Poisson's ratio.

The stresses can be calculated as:

$$\sigma_x = 6\frac{M_{1x}}{h^2} \quad \text{and} \quad \sigma_y = 6\frac{M_{1y}}{h^2} \tag{2}$$

If we are dealing with a circular load in the centre of a large slab,

$$R_x = R_y \quad \text{and} \quad \sigma_x = \sigma_y \tag{3}$$

Since:

$$\varepsilon_x = \frac{(\sigma_x - \mu\sigma_y)}{E} = \frac{(1-\mu)\sigma_x}{E} \tag{4}$$

we can develop a relation between the curvature and the tensile strain by substituting σ_x with Equation (2), we obtain:

$$\varepsilon_x = \frac{6(1-\mu)M_{1x}}{Eh^2} \tag{5}$$

Furthermore Equation (6) is developed by substituting M_{1x} in Equation (5) with Equation (1), where (ε_x) is the horizontal strain at the bottom, h is the thickness of the slab and (R_x) is the radius of curvature [8].

$$\varepsilon_x = \frac{h}{2R_x} \tag{6}$$

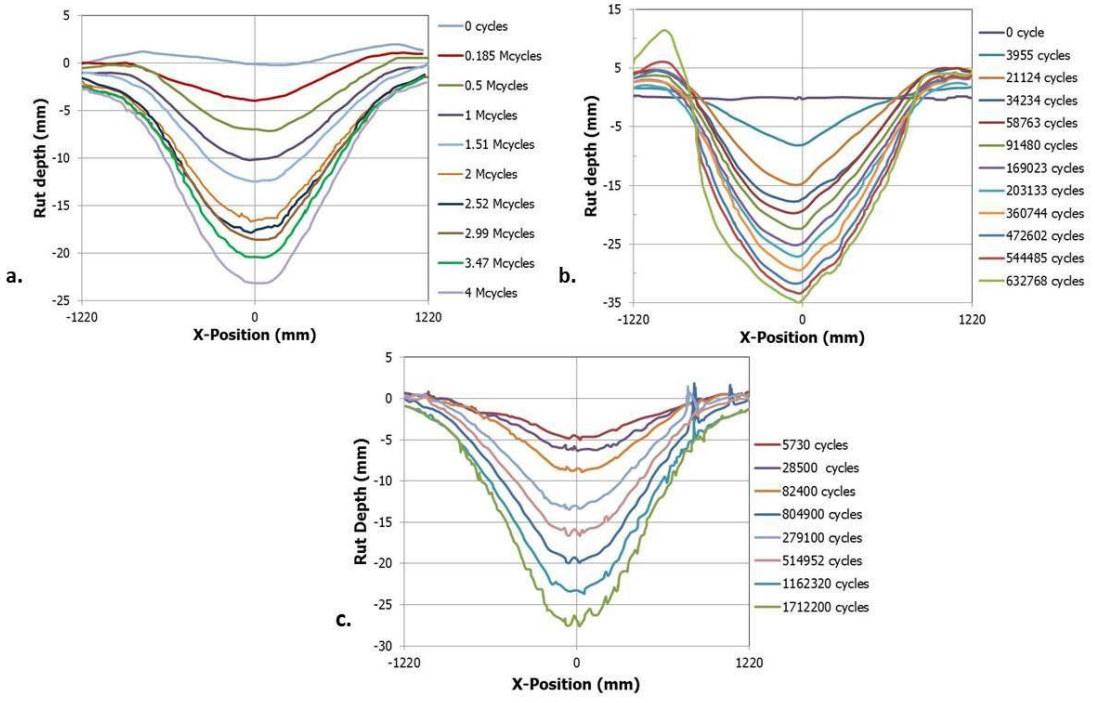

Fig. 4. Rut depth profile of each Lintrack section at several loading cycles [1, 4].
(**a**) Section I. (**b**) Section VA. (**c**) Section VB

In this study this relationship was used to calculate the creep/permanent strain as a result of permanent deformation. When a rut depth profile is modelled as an arc, with the length of the chord defining the base of the arc being W and the height measured at the midpoint of the arc's base is H, then the radius of this arc can be estimated using Equation (7).

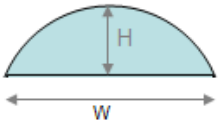

$$\text{Radius} = \frac{H}{2} + \frac{W^2}{8H} \tag{7}$$

When applying this principle on the curvature as a result of rut depth formation, then the challenge is to define H. This is because there is uncertainty of how big the arc should be. However some trials on the curvatures show that using H as 10.75% of the total rut depth will give the maximum strain [7]. Therefore, this 10.75% is used to make a consistent calculation in determining R.

Because of the irregular shape of the rut depth profiles, the W at a certain H could not be easily determined. Then, each rut depth profile was described using a polynomial function. They are shown in Figure 5 as dashed lines. These 'new' lines improved significantly the determination of the width of the arc (W) at a certain H value.

Based on the crack pattern shown in Figure 1.b, section VA is the only section that shows a significant amount of longitudinal cracking. The longitudinal cracking appears in the outer side of the wheel path. Figure 4.b. shows that at the outer sides of the wheel path also deformation in the shape of ridges developed (in the area from the -1220 to -800 and from 800 to 1220). Then, for this section, two deformations will be analysed which are the rut depth between -800 to 800 and the high ridge between -1220 to -800.

By using these new rut depth profiles, W was estimated. Hence the radii and the permanent strain could then be determined using Equation 7 and 6 consecutively.

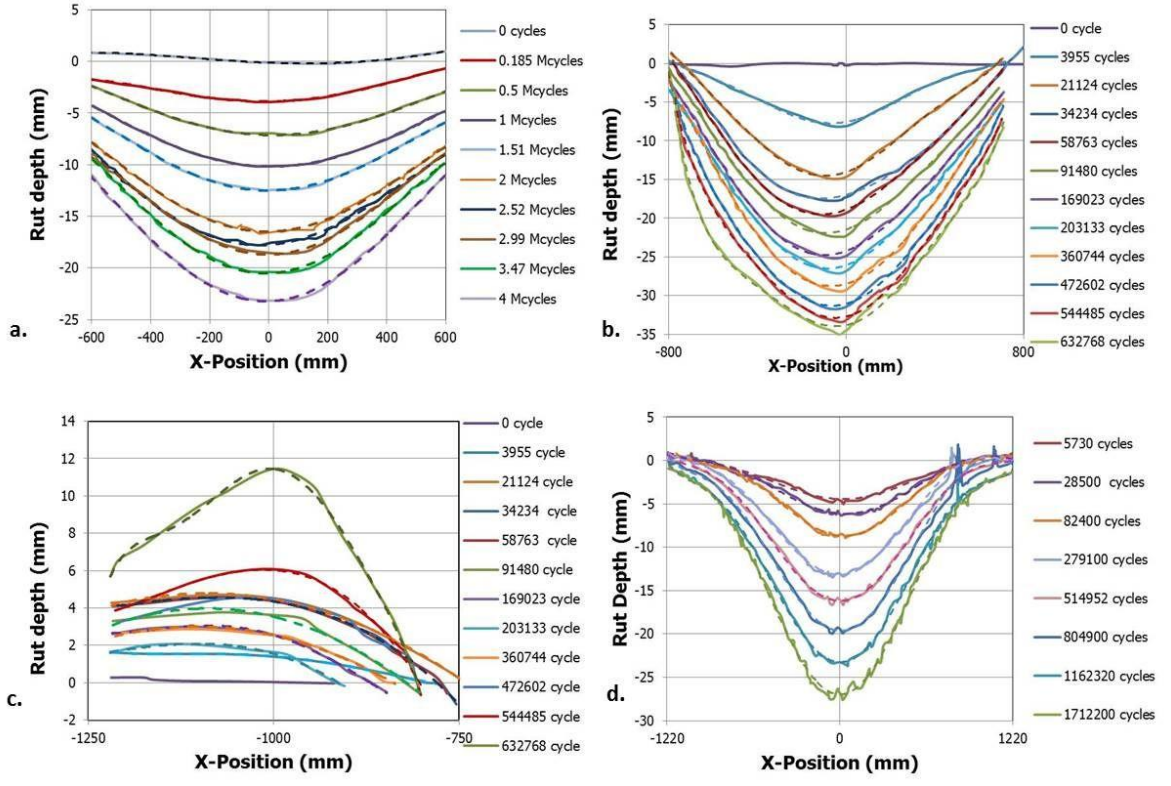

Fig. 5. Polynomial function of the rut profile (dashed line) at several loading cycles (**a)** section I. (**b)** section VA at the X-position from -800 mm to 800 mm. (**c)** Section VA at the X-position from -1220 mm to -800 mm. (**d)** Section VB

4. Relationship between the rut depth and the radius of curvature and between the rut depth and the permanent strain

The relation between the rut depth and radius and between rut depth and permanent strain as determined from the data obtained on the three sections are shown in Figure 6 and 7.

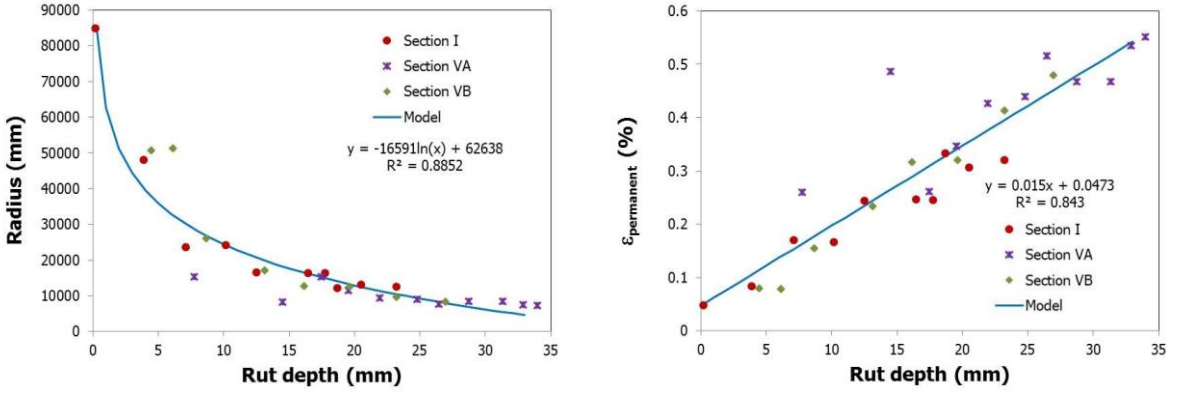

Fig. 6. Relation between (a) rut depth and radius of curvature and (b) rut depth and permanent/creep strain

Figure 6.a shows a nonlinear relation between the rut depth and the radius. However, the three sections show a similar pattern which can be represented by means of a logarithmic trend line. Meanwhile the relation between rut depth and permanent strain presented in Figure 6.b shows a linear relation between the rut depth and the permanent strain. Figure 6.b is an interesting one because it shows that there is a rather good correlation between rut depth and permanent strain which is independent of the layer thickness. This relationship, however, might be dependent on the amount of lateral wander.

5. Rut depth, permanent strain and cracking

The relationship that was developed between the number of load repetitions and the permanent strain of section I, VA and VB are shown as the blue line in Figure 7, 8, and 9 respectively (also the orange line in Figure 8 shows the development of the permanent strain of the ridge side of section VA). It is recalled that the permanent strain is acting at the bottom of the asphalt layer in the transversal direction and could, therefore, give rise to longitudinal cracking in the centre of the wheel path. Figures (a) and (b) show the development of the crack length and cracked area subsequently with respect to the number of load repetitions.

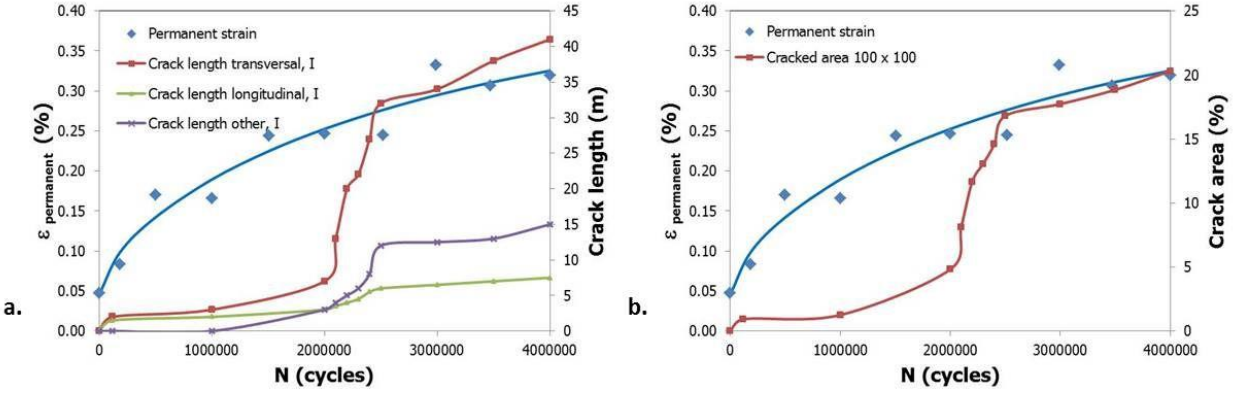

Fig. 7. Development of the permanent strain and crack length (**a**) and cracked area (**b**) of Section I

Figures 7 (a) and 7 (b) show that the crack development was rather slow until $2x10^6$ load repetitions and that the crack lengths increased significantly after $2x10^6$ cycles. At that number of load repetitions, the permanent strain value is around 0.25% and the rut depth around 17 mm (see also Figure 5.a.).

The blue line in Figure 8.a shows immediate and rapid increase of the permanent strain during the first 100,000 load repetitions while it developed at a much slower pace after 100,000 load repetitions. On the other hand the orange line, which represents the development of the permanent strain at the top of the ridge, shows that the permanent strain was rather constant at around 0.25% for a rather long period but increased dramatically after 500 kcycles. Figure 8 (a) and (b) show that cracking started immediately.

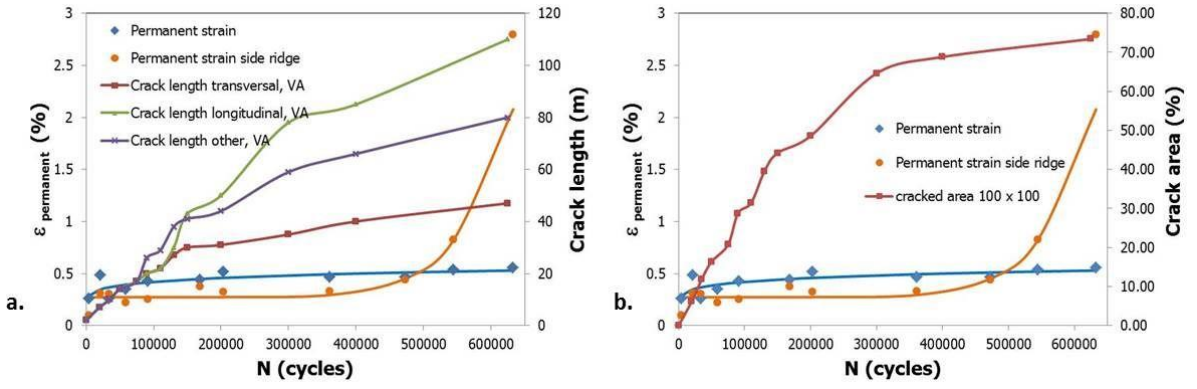

Fig. 8. Development of the permanent strain and crack length (**a**) and cracked area (**b**) of Section VA

Section VA is the section that shows quite a number of longitudinal cracks. This type of cracking was not only present in, or near, the centre of the wheel path, as was also the case in section I and VB, but many of these longitudinal cracks were also present at the edges of the rut profiles in section VA. These cracks were less present in Section VB and quite rare in Section I. From Figure 8 it can be concluded that after 75000 load repetitions, when the permanent strain had reached a value of 0.4%, the permanent strain is not increasing rapidly anymore. It seems as if the 0.4% strain is about the maximum the pavement can take. At that moment the rut depth is 22 mm and the cracked area is 20%.

The orange line in Figure 8 seems to indicate that a permanent strain of 0.4% is about the maximum the pavement can take because a very rapid increase in strain is observed after this strain level has been reached (at 450,000 load repetitions). Taking into consideration the size of the cracked area at that moment (see Figure 8.b) the pavement can be considered to be completely failed.

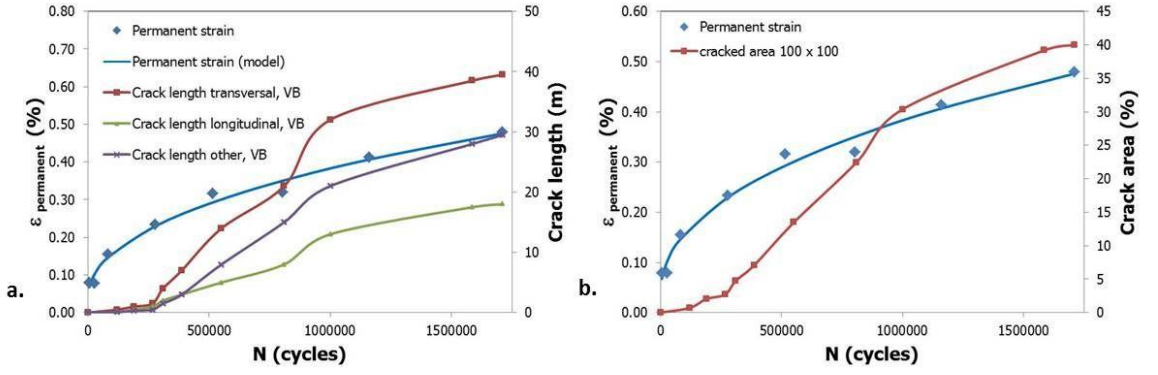

Fig. 9. Development of the permanent strain and crack length (**a**) and crack area (**b**) of Section VB

Figure 9(a) and (b) show that the cracks started to develop at around 278,000 cycles. At that point, the permanent strain is around 0.23% and the rut depth 13 mm. The 0.4% strain level is reached after approximately 1.1 million

load repetitions and at that moment the cracked area amounts 32%. The rut depth at that moment was 22 mm.

6. Summary of findings with respect to the relationship between rut depth and cracking

The most important findings with respect to the relation between permanent deformation and cracking are summarized in Table 2.

Table 2. Summary of findings with respect to the relationship between rut depth and cracking.

Section	I	VA	VB
Nr of load repetitions at which cracking starts to increase	2,000,000		267,200
Permanent strain when cracking starts to increase	0.25%		0.23%
Rut depth when cracking starts to increase	16.6 mm		12.1 mm
Nr of load repetitions at which permanent strain equals 0.4%		75,000	1,000,000
Rut depth at a permanent strain of 0.4%		22 mm	22 mm
Cracked area when permanent strain equals 0.4%		20%	32%

From the results shown in Table 2 it appears that at a rut depth of around 15 mm, crack development starts to accelerate and that at a rut depth of 20 mm the sections can consider to be failed. It should be noticed that these findings are based on the performance of the Lintrack sections where permanent deformation was a result of deformation of the subgrade and NOT because of the asphalt layer. It is, however, noteworthy that these findings closely agree with the definitions of failure as used in the pavement evaluation and overlay design system as developed by the Transport and Road Research Laboratory in the UK which are shown in Table 3 [9].

Table 3. Classification of pavement condition according to Croney [9]

Classification	Visible evidence
Sound	No cracking. Rutting beneath 2-m straightedge less than 10 mm.
Critical	(a) No cracking. Rutting between 10 and 20 mm.
	(b) Cracking confined to a single crack in the wheel-track, with rutting less than 20 mm.
Failed	Cracking extending over the area of the wheel-track and/or rutting greater than 20 mm.

The results show that permanent deformation and structural performance were closely related in case of the Lintrack pavements. These findings also explain the cracking of the Lintrack sections is also caused by permanent deformation.

7. Conclusion

In this paper the surface cracking and permanent development of three accelerated pavement test sections (Lintrack 1990) was discussed. Parameters that were thought to be of importance for determining the pavement life were studied, being cracking (including crack length and cracked area) as well as permanent deformation.
This study showed that part of the observed longitudinal cracking in the Lintrack sections is quite strongly related to rutting. This statement is based on the following findings:

- Progressive development of cracking seemed to occur when the rut depth was around 15 mm or larger.
- The rut depth profile analyses showed that there is a rather good correlation between rut depth and permanent/creep strain which is independent of the layer thickness.
- It is clear that correlating the calculated pavement life to the cracked area is not recommended since quite some visible cracking, especially in VA and VB, must have been caused by rutting and some cracking must have been top down cracking initiated by compaction during construction. That permanent deformation did have an influence on the cracking performance was nicely shown when analysing the behaviour of Section

VA. There it appeared that the ridge that developed next to the rut depth clearly corresponded with the longitudinal cracking observed in that area

Acknowledgements

The authors would like to thank the the Road and Railroad Research Laboratory (RRRL) of the Delft University of Technology (DUT) where the project was executed. The financial support from the Ministry of Higher Education in the form of scholarship for the first author is highly appreciated. The scholarship was made this research possible. Furthermore, the continuation of the research is funded by Hibah Doktor Muda of Universitas Sebelas Maret Surakarta 2016 granted to the first author.

References

[1] J. Groenendijk, "Accelerated Testing and surface cracking of asphaltic concrete pavements," PhD, Delft University of Technology, Delft The Netherlands, 1998.

[2] P. D. Bhairo, "Comparison of the predicted and Observed Pavement Life of LINTRACK Test Lane Va," Delft University of Technology, Delft, The Netherlands, 1997.

[3] H. Sabha, "Estimation of Crack Growth Parameters and Fatigue Characteristics of Asphalt Mixes Using Simple Test," Delft University of Technology, Delft, The Netherlands, 1995.

[4] J. Groenendijk and C.H. Vogelzang, "Pavement Performance Under LINTRACK Accelerated Loading, Extending measurement report and interpretation report section Vb," Delft University of Technology, Delft, The Netherlands, 1998.

[5] W.D.O. Paterson, *Road Deterioration and Maintenance Effects*. Baltimore, U.S.A.: John Hopkins University Press, 1987.

[6] T. Watanatada, C. G. Harral, W. D. O. Paterson, A. M. Dhareshwar, A. Bhandari, and K. Tsunokawa, *The Highway Design and Maintenance Standards Model: Description of the HDM-III model* vol. 1: Johns Hopkins University Press, 1987.

[7] F. P. Pramesti, *Laboratory and Field Asphalt Fatigue Performance, Matching Theory with Practice*: TU Delft, Delft University of Technology, 2015.

[8] A.A.A. Molenaar, "Structural Evaluation and Strengthening of Flexible Pavements Using Deflection Measurements and Visual Condition Surveys, Lecture Note CT 4860 Structural Design of Pavement , Part VI," Delft University of Technology, Delft the Netherlands, 2009.

[9] D. Croney, *The Design and Performance of Road Pavements. Transport and Road Research Laboratory*. London: Her Majesty's Stationery Office, 1977.

Available online at www.sciencedirect.com

ScienceDirect

Procedia Engineering00 (2017) 000–000

Procedia Engineering

www.elsevier.com/locate/procedia

Sustainable Civil Engineering Structures and Construction Materials, SCESCM 2016

Evaluation of proposed backcalculation procedure in Indonesia overlay design guide

Bagus Hario Setiadji[a,*], Supriyono[a]

[a] *Department of Civil Engineering, Diponegoro University, Jl. Prof. Soedarto, SH., Tembalang, Semarang, Indonesia 50275*

Abstract

Indonesia Directorate General of Highways' overlay design guide Pd T-1-2002-B was developed by adopting the design procedure from 1993 AASHTO Design Guide. One evaluation in the guide was an evaluation of subgrade condition, in terms of elastic moduli, using backcalculation procedure from field deflection data. One main drawback of the backcalculation procedure in the guide is the use of adjustment factor (*C*) to make the calculated moduli conform to the measured ones. In addition, the guide also did not provide the evaluation of remained capacity of surface layer that could be the important key for deciding the overall condition of the existing pavement. In this paper, a backcalculation procedure in the guide for determining remaining capacity of surface layer was proposed. For the sake of comparison, another backcalculation procedure based on best-fit trial-and-error approach was employed, and the results of both algorithm procedures were validated using measured pavement properties pavement properties from Long-Term Pavement Performance (LTPP) database. The results of the study indicated that proposed procedure failed to produce the expected results. Besides, the high deviation between calculated moduli (from both backcalculation procedure) and measured ones leads to a recommendation of developing a better backcalculation procedure in the future.

Peer-review under responsibility of the organizing committee of SCESCM 2016.

Keywords: overlay design guide; backcalculation procedure; layer moduli.

* Corresponding author. Tel.: +62-812-2559-9605
E-mail address: bhsetiadji@undip.ac.id

Peer-review under responsibility ofthe organizing committee of SCESCM 2016.

1. Introduction

In rehabilitation program, ones are initially advised to review the remained capacity of both subgrade and surface layer as a basis of consideration whether it is necessity to provide additional structural layer in order to ensure that the road could last up to end of its service life.

In Indonesia, the procedure to evaluate the remained capacity of the pavement structure, as a part of overlay thickness determination, has been proposed in overlay design guide Pd T-1-2002-B [1] (namely as 2002 Design Guide, for the rest of the paper), as support document for selecting pavement structure layers in 2013 Design Manual [2]. This procedure is actually an adoption of 1993 AASHTO Guide for Design of Pavement Structure with minor revision.

In the design guide, there is a procedure to determine the remained capacity of the subgrade by backcalculating deflections collected from the field. Setiadji et al. [3] stated that there was a problem found in the backcalculation results produced by the design guide, that is, the backcalculation subgrade resilient modulus should be multiplied by an adjustment factor *C* of no more than 0.33 to enable this modulus used in the design. The use of adjustment factor *C* did not have any strong scientific justification. In addition, the use of constant *C* was only for fine-grained soils, and there was no justification on the use of the constant on granular subgrade [4]. Setiadji et al. [3] also found that in most cases, the adjustment factor C could exceed much beyond the values recommended, that is, 0.33. Due to this, Setiadji et al. [3] recommended another backcalculation procedure to replace the one used in 2002 Design Guide.

Beside the manner of subgrade resilient modulus, it is interesting to know that 2002 Design Guide did not provide any procedure to evaluate remained capacity of the surface layer (E_1), as important layer that has the largest capability to withstand against traffic load. The guide only provides effective modulus (E_p) to represent remained capacity of all layers above subgrade. Therefore, this study aimed to propose a backcalculation procedure in 2002 Design Guide to evaluate the capacity of remained surface layer. Furthermore, to examine the accurateness of the modulus obtained, a validation of the calculated modulus against the measured ones was also presented.

2. Research methodology

This research consisted of two main parts: (i) estimation of pavement layer moduli using backcalculation procedures or programs; and (ii) comparison between the calculated moduli and validation them against the measured ones.

2.1. Pavement structure used in this study

In this study, the structural layers were arranged so that it can ease to be employed in backcalculation procedures in predicting layer moduli. The arrangement of the pavement layers was showed in Fig. 1.

Fig. 1(a) shows the typical pavement structure in practice. Two alternatives of arrangement of the pavement layers could be pavement structure in Fig. 1(b) or Fig. 1(c). The first alternative (Fig. 1(b)) is made to ease determining subgrade resilient modulus (M_r), while the above layers are representing by composite modulus, called as effective modulus (E_p). The second one is as following the concept of equivalent thickness [5] to enable predicting elastic modulus of surface layer (E_1), while the capacity of the rest is represented by equivalent modulus (E_e). In this paper, the subgrade resilient modulus (M_r) and elastic modulus of surface layer (E_1) in Fig. 1(b) and 1(c) approaches respectively are the expected results, while the another modulus in both figures could be neglected.

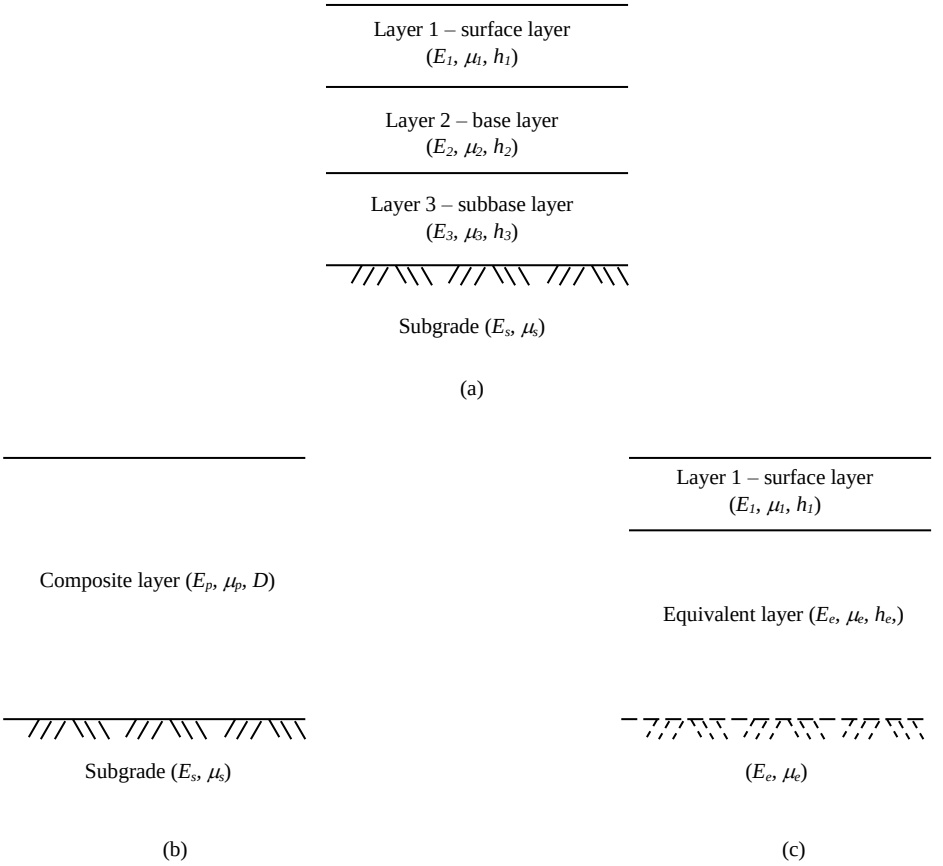

Fig 1. Pavement structural layers used in this study: (a) real structure in practice; (b) structural layers to determine E_s; (c) structural layers to determine E_1

2.2. Backcalculation analysis used in this study

There were two backcalculation procedurse used in this study, i.e. backcalculation procedure in 2002 Design Guide that adopted from the similar procedure in 1993 AASHTO Design Guide, and a best-fit-trial-and-error backcalculation algorithm. The latter was the backcalculation procedure used as a comparison against the one in the guide.

The backcalculation procedure as a part of structural evaluation of existing pavement in 2002 Design Guide consists of several equations [1] as follows.

$$M_r = \frac{0.24P}{d_r r} \tag{1}$$

$$d_0 = 1.5pa\left\{\frac{1}{M_r\sqrt{1+\left(\frac{D}{a}\sqrt[3]{\frac{E_p}{M_r}}\right)}} + \frac{\left(1-\frac{1}{\sqrt{1+\left(\frac{D}{a}\right)^2}}\right)}{E_p}\right\} \tag{2}$$

$$r > 0.7\ a_e \tag{3}$$

$$a_e = \sqrt{a^2 + \left\{D\left(\frac{E_p}{M_r}\right)^{1/3}\right\}^2} \tag{4}$$

In which:

d_0 = deflection measured at the center of the load plate, in.
p = load plate pressure, psi.
a = load plate radius, in.
D = total thickness of pavement layers above the subgrade, in.
M_r = subgrade resilient modulus, psi
E_p = effective modulus of all pavement layers above subgrade, psi.

The values of M_r and E_p are determined using equations (1) and (2). Both values are valid if and only if the statement in equation (3) is true.

The aforementioned procedure initially was used to evaluate the capacity of subgrade supports, in terms of resilient modulus (M_r). In this paper, this procedure was extended to enable determining the elastic modulus of surface layer (E_1, see Fig. 1(c)) by using several adjustments, i.e. selection of appropriate deflection and sensor offset, and also replacement of total thickness D with surface layer thickness h_1.

The second backcalculation algorithm used in this study is one of best-fit-trial-and-error backcalculation programs, namely EVERCALC. This program was developed by Washington State Department of Transportation. This program uses a nonlinear least square optimization technique with CHEVRONX as the forward calculation program. Levenberg-Marquardt algorithm was implemented in EVERCALC as general minimization method and this makes the program could converge quickly with only small iteration [6]. EVERCALC is an iterative optimization backcalculation method with an objective function to minimize an error function. To achieve its objective function, a seed modulus that could produce tolerable error is necessary to be firstly determined.

This program allows users to simulate up to 5 pavement layers and the use of up to 10 sensors (depending on the type of falling-weight deflectometer/FWD used) in predicting the layer moduli. In this study, different sensor arrangements were used: seven-sensor and two-sensor arrangements, for determining E_s and E_1 respectively. The use of sensor arrangements was to show the capability of the program in handling different sensor combinations in order to obtain the most accurate results.

2.3. Data used in this study

All data used in this study was obtained from long-term pavement performance (LTPP) database, that is, a database that stores a huge pavement performance data as a part of major research areas of the Strategic Highway Research Program (SHRP) [7]. The data collected was from thousands road segments located in United States and Canada. The use of LTPP data in this study due to the following reasons: comprehensive and easy to find. Besides, backcalculation algorithm is basically a mechanistic approach, therefore, the use of data from anywhere is possible.

The types of data obtained from this database were as follows: soil classification, deflections (d), layer thickness (h), and subgrade resilient modulus (M_r), surface layer elastic modulus (E_1). The first three data was employed to estimate layer moduli, while the rest was considered as the measured moduli and to be used to validate the calculated ones.

Because not all aforementioned data can be found in every road segment, the number of road segment with complete data that can be selected is limited. Finally, four road segments were selected for this study. They are: road segment 0505 in Colorado state, road segments 1016 and 1802 in Mississippi state, and road segment 1001 in Utah state. In the rest of this paper, these segments were notated as locations A, B, C and D.

3. Results and analysis

The first step of conducting this study was to prepare the backcalculation program, EVERCALC. The program was set to run with default load plate radius = 5.91 in., and seed moduli E_1 = 1000 ksi (or E_p = 500 ksi) (with the range of the moduli of 100 – 5000 ksi), and E_s = 45 ksi (with the range of the moduli of 1 – 100 ksi). Seven sensors were selected with offset 0, 8, 12, 18, 24, 36 and 60 in. from the center of the load plate.

To analyze the sensitivity of the program in producing the moduli, five sets of hypothetical layer properties (as shown in the first column of Table 1) were created and deflections with error (d_m) were generated using the following formula [8]:

$$d_m = d_t + 0{,}02 d_t \frac{(r_1 - 0{,}5) r_2}{|r_1 - 0{,}5|} + 2 \frac{(r_3 - 0{,}5) r_4}{|r_3 - 0{,}5|} \quad (5)$$

in which: d_t = true deflection (μm); $r_1 – r_4$ = random number (from 0 to 1). The errors generated by equation (5) were limited in the range $\pm$ 2% of d_t in order to simulate the measurement error that generally produced by FWD [9].

The deflections with error generated by equation (5) then were backcalculated using procedure in 2002 Design Guide and EVERCALC to obtain the moduli E_p and E_s. The results of this analysis are depicted in Table 1 [3].

Table 1. Sensitivity Analysis of Both Methods Using Hypothetical Data

Layer Properties	Deviation of Elastic Moduli (%)			
	EVERCALC		2002 Design Guide	
	E_p	E_s	E_p	E_s
E_p = 200 ksi. E_s = 9 ksi. D = 12 in.. P = 15,985 lbs	2.08	0.73	4.42	12.17
E_p = 100 ksi. E_s = 9 ksi. D = 12 in.. P = 15,985 lbs.	1.15	0.56	7.54	8.08
E_p = 200 ksi. **E_s = 15 ksi**. D = 12 in.. P = 15,985 lbs.	2.62	0.65	7.99	8.71
E_p = 200 ksi. E_s = 9 ksi. D = 12 in.. **P = 11,241 lbs.**	3.31	0.45	3.75	12.39
E_p = 200 ksi. E_s = 9 ksi. **D = 20 in.**. P = 15,985 lbs.	2.43	1.31	2.02	14.18

From Table 1, it can be summarized that EVERCALC is less sensitive than backcalculation procedure in the guide in estimating the moduli. This is an important indication to show that the backcalculation procedure should have a robust algorithm to ensure that it could produce accurate results.

Next, both of backcalculation procedures were used to predict subgrade resilient modulus (M_r or E_s). The results of the analysis are shown in Table 2.

Table 2. Comparison between EVERCALC and Design Manual in Determining E_s Values

Location of Data Collection (Type of Soil)	Average Measured Elastic Modulus E_s (ksi)	Average Calculated Elastic Modulus E_s (ksi)		Deviation between measured and calculated modulus (%)	
		EVERCALC	2002 Design Guide	EVERCALC	2002 Design Guide
A (A-6)	19.32	20.59	22.69	6.57	17.48
B (A-4)	13.02	15.92	17.10	22.28	31.39
C (A-2-4)	15.70	26.62	25.14	69.55	60.11
D (A-3)	9.30	11.55	11.70	24.17	25.76

Setiadji et al. [3] stated that as general, EVERCALC performed better in estimating subgrade resilient modulus than backcalculation procedure in 2002 Design Guide, as shown by the results in location A, B and D. Different result showed in location C, which is the additional data used in this paper. The high deviation between the calculated and measured modulus could be contributed by different time period when the deflection and measured modulus data were collected.

From Table 2, it could be summarized that the adjustment factor *C* required to make the backcalculated moduli similar with the measured ones is in the range of 0.62 – 0.85. The highest adjustment factor found in location with fine-grained soils (location A), while the locations with granular soils (locations B to D) need less adjustment factor. All adjustment factors exceeded the maximum allowable factor set by the guide, i.e. 0.33. This means that the adjustment factor is not relevant again in predicting the remained subgrade resilient modulus.

The second analysis of backcalculation results is depicted in Table 3. In this table, three backcalculation results were shown, that is, the surface layer modulus (E_1) produced by EVERCALC program (using 7- and 2-sensor) and the proposed backcalculation procedure in 2002 Design Guide, respectively.

Table 3. Comparison between EVERCALC and Design Manual in Determining E_1 Values

Location of Data Collection (Type of Soil)	Average Measured Elastic Modulus E_1 (ksi)	Average Calculated Elastic Modulus E_1 (ksi)			Deviation between measured and calculated modulus (%)		
		EVERCALC (7 sensor)	EVERCALC (2 sensor)	2002 Design Guide	EVERCALC (7 sensor)	EVERCALC (2 sensor)	2002 Design Guide
A (A-6)	361.50	222.40	275.27	217.40	-38.48	-23.85	-39.86
B (A-4)	1,219.93	1,681.25	1,217.38	1,278.58	37.81	-0.21	4.81
C (A-2-4)	1,693.36	23,836.41	3,365.71	19,535.00	1,307.64	98.76	933.32
D (A-3)	1,301.86	602.63	939.13	561.30	-53.71	-27.86	-59.30

The proposed backcalculation procedure in the guide was made by adjusting several parameters. The adjustment was especially conducted in equations (1) and (2), such as changing the total thickness *D* to surface layer thickness h_1, and selecting the deflection (*d*) that produced by sensor 4 or 5 (or sensor with distance 18 or 24 in. respectively from the load), instead of deflection produced by sensor 7 in original form. Besides, the statement in equation (3) also should be fulfilled.

EVERCALC program uses 7 sensors as default to predict the moduli, however, the use of 2 sensors gives flexibility to users in choosing the best pair of sensor that could produce the most accurate results [10].

Table 3 indicates that EVERCALC with two sensors performed better than other backcalculation results. The selection of the sensor combination was important in this stage. For this purpose, the combination of sensor no. 1 and 3 was selected due to this combination could produce more accurate result in previous research [10]. The use of 7 sensors in backcalculation analysis has a consequence that the possible error of the deflection data in the 7 sensors could lead to accumulation of errors in predicting the moduli.

As conclusion, the proposed backcalculation procedure in this study was failed to produce expected results. The modulus E_1 produced by this proposed procedure in location C, together with the one produce by EVERCALC with 7 sensors, were far beyond the typical values of E_1, in the range of 500 – 5000 ksi.

To see the distribution of the calculated moduli (E_s and E_1) against the measured ones, the results of both backcalculation procedures are plotted in Figs. 2 and 3. As shown in Fig. 3, almost all calculated modulus E_s over-estimate the measured ones and the calculated modulus from the two backcalculation procedures were similar distribution in location B and D.

In terms of E_1, there was a good distribution of the calculated modulus E_1 data in which some of them were under-estimate the measured modulus and the others were over-estimate the measured one. Among the backcalculation results, the ones produced by EVERCALC with 2 sensors were the best estimate of the measured modulus.

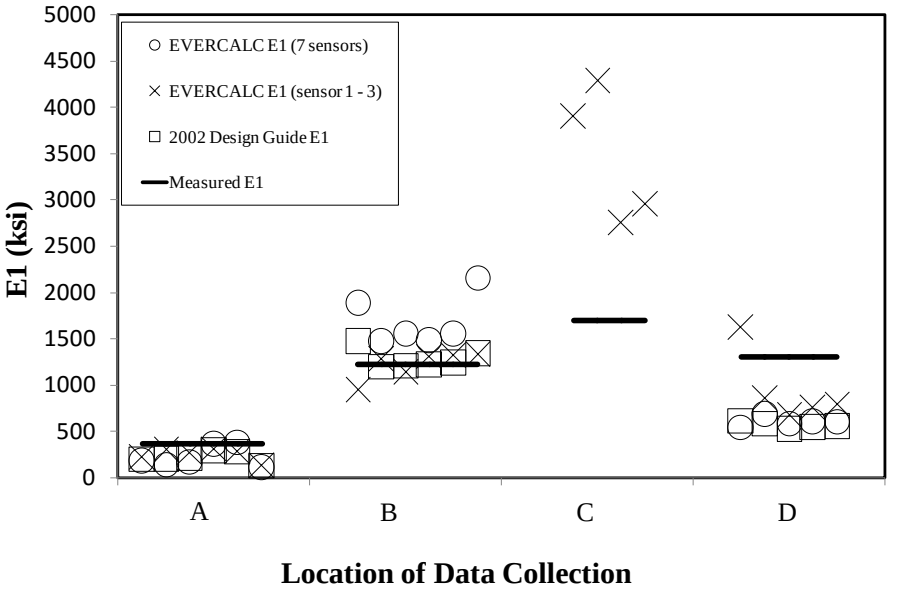

Fig 2. Distribution of Calculated E_1 towards Measured E_1

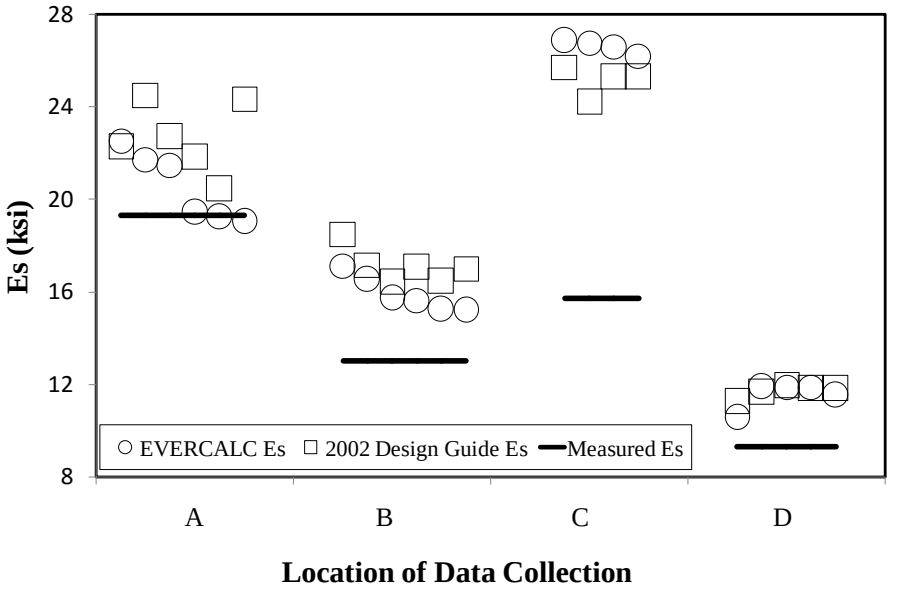

Fig 3. Distribution of Calculated E_s towards Measured E_s

Figs. 2 and 3 also reveal that although EVERCALC could predict the measured modulus better than that of backcalculation procedure in the guide, the high deviation produced actually is out of favor. A better backcalculation procedure, such as closed-form backcalculation algorithm, should be proposed in the near future in order to overcome this problem.

4. Conclusions

This paper presented the proposed backcalculation procedure in 2002 Design Guide to predict the layer moduli. For this purpose, some modification was made on the backcalculation equations. The results of the proposed procedure, in terms of subgrade and surface layer moduli, were then compared with that produced by another backcalculation program (EVERCALC, in this case) and validated against the measure ones.

The results of the analysis indicated that the proposed procedure failed to produce the expected results. This highlighted that the backcalculation procedure in 2002 Design Guide was not suitable to produce accurate calculated moduli. Besides, the deviation of the moduli resulted by EVERCALC leads to a recommendation of using better backcalculation procedure in the future.

References

[1] Directorate General of Highway. Flexible Pavement Design Guide. Pd T-01-2002-B. Ministry of Public Works Republic of Indonesia. 2002.
[2] Directorate General of Highway. Pavement Design Manual. No. 02/M/BM/2013. Ministry of Public Works Republic of Indonesia. 2013.
[3] Setiadji. B.H. Supriyono. Priyono. E.Y. Widyarini. G. Revision of Backcalculation Procedure in 2002 Design Guide. Submitted for Jurnal Transportasi. Parahyangan University. ISSN: 1441-2442.
[4] AASHTO. AASHTO Guide for Design of Pavement Structure, American Association of State Highway and Transportation Organization. 1993.
[5] Ullidtz, P. Pavement Analysis, Elsevier, 1987.
[6] Sivaneswaran. N. S.L. Kramer. J.P. Mahoney. Advanced Backcalculation using a Nonlinear Least Square Optimization Technique, Presented at the 70th Annual Meeting of the Transportation Research Board, Washington, D.C. 1991.
[7] Elkins. G.E. Schmalzer. P. Thompson. T. Simpson. A. Long-Term Pavement Performance Information Management System – Pavement Performance Database User Guide. FHWA Report No. FHWA-RD-03-088. Washington, DC, USA. 2003.
[8] Pronk. A.C. Implementation Problems and Reliability of Falling Weight Deflectometer (FWD) Measurements on Three Layer Systems. Proceedings of Association of Asphalt Paving Technologist. Williamsburg. VA. Vol. 57. 1998.
[9] Irwin. L.H. Yang. W.S. Stubstand, R.N. Deflection Reading Accuracy and Layer Thickness Accuracy in Backcalculation of Pavement Layer Moduli. Non-destructive Testing of Pavement and Backcalculatoon of Moduli. ASTM STP 1026. American Society for Testing and Materials. West Conshohocken. PA. (1989) 229-244.
[10] Fwa. T.F. Setiadji. B.H. Evaluation of Backcalculation Methods for Nondestructive Determination of Concrete Pavement Properties. Transportation Research Records. Vol. 1949. Journal of Transportation Research Boards. DOI: http://dx.doi.org/10.3141/1949-08. (2006). 83-97.

Available online at www.sciencedirect.com

ScienceDirect

Procedia Engineering 00 (2017) 000–000

Procedia Engineering

www.elsevier.com/locate/procedia

Sustainable Civil Engineering Structures and Construction Materials 2016, SCESCM 2016

Design and properties of renewable bioasphalt for flexible pavement

Djumari[a], Mujib Abdel Daim Yami[a], Muhamad Fachri Nasution[a], Ary Setyawan[a]*

[a] *Roadmate Research Group UNS, Jl. Ir. Sutami 36 A, Surakarta 57126, Indonesia*

Abstract

In the construction world, most flexible pavement constructions use synthetic asphalt made from crude oil and well-known as conventional asphalt. Therefore, to find more environmentally friendly construction people around the world are very interested in finding a bioasphalt. The bioasphalt is used because of several reasons, such as asphalt mixtures derived from plants and trees could replace petroleum-based mixtures. One of bioasphalt which can be used as an alternative material of conventional asphalt is resin (*damar*). The existence of damar in Indonesia is very huge, especially in Lampung, South Sumatera, Indonesia. In this study, the researchers used experimental research based on laboratory works. The percentages of natural resin used in the conventional asphalt 60/70 pen are 0%, 2.5%, 5%, 7.5% and 10% modification. The selected test, including Marshall stability test to get the optimum bitumen content, unconfined compressive test, indirect tensile test and permeability test. The research result shows that asphalt with resin is different with conventional asphalt 60/70 pen in terms of asphalt quality, because the asphalt modified with resin has higher penetration value and specific gravity than conventional asphalt. The result of the Marshall stability test, unconfined compressive test, indirect tensile test and permeability test is high if the asphalt modified with higher natural resin. On the other hand, the optimum bitumen content value relatively similar with the modification of natural resin.

Peer-review under responsibility of the organizing committee of SCESCM 2016.

Keywords: bioasphalt; flexible pavement; resin gum

* Corresponding author. Tel.: +62-815-485-585-90; fax: +62-271-634-524.
E-mail address: arysetyawan@staff.uns.ac.id

Peer-review under responsibility of the organizing committee of SCESCM 2016.

1. Introduction

Bioasphalt is an asphalt alternative made from non-petroleum based renewable resources. These sources include sugar, molasses and rice, corn and potato starches, natural tree and gum resins, natural latex rubber and vegetable oils, lignin, cellulose, palm oil waste, coconut waste, peanut oil waste, canola oil waste, dried sewerage effluent and so on. Bitumen can also be made from waste vacuum tower bottoms produced in the process of cleaning used motor oils, which are normally burned or dumped into landfills [1].

Resin is a natural or synthetic compound that begins in a highly viscous state and hardens with treatment. Typically, it is soluble in alcohol, but not in water. The compound is classified in a number of different ways, depending on its exact chemical composition and potential uses. It also has many applications, ranging from art to polymer production, and many consumers interact with products that contain it on a daily basis.

Natural resin comes from plants. A classic example is pine sap, which has the characteristic sharp odor of terpene compounds. A number of other plants produce resins, and they have been used by humans for thousands of years. Some plants exude a similar substance called gum or gum resin that does interact with water. Gum tends to be softer and more malleable. Plant resin can be clear to dark brown in color, and it varies in opacity and hardness. Some are also extremely volatile, since it contains unstable compounds [2].

Modifying the asphalt mix by adding additives to the bitumen or asphalt mix has proved to help improve the performance of asphalt pavement efficiencies. Among the modifiers of asphalt, fibers and polymers have gotten much attention for their expected excellent improvement effect. Various fiber and polymer modifiers, such as cellulose fiber, polyester fiber resin, epoxy resin, rock wool, fibrin and short asbestos and mineral fiber, have been widely used in different asphalt mixtures, including Stone Mastic Asphalt (SMA), Open Grade Friction Concrete (OGFC), Asphalt Concrete and Hot rolled asphalt [3].

Many former researches focused on the influence of fiber and polymer additives on the engineering properties of asphalt or asphalt mixture. Haoran et al made a study to investigate the possibility of utilizing a polyester resin for reinforcing flexible pavements. The application of a thin-layer coating with a polymer, unsaturated polyester resin (UPR) on the surface of a laboratory-prepared unmodified asphalt concrete mixture was studied as a tensile reinforcement method for such a material [4]. An attempt to use 100% resin has been conducted by adding same filler to improve bitumen properties, especially in increasing the bitumen ductility [5]. The research of using an animal waste product of swine manure has also been successfully to identify the chemical properties used for bioasphalt [6] Selected laboratory performance tests were conducted in this research and the results were compared with those of an unmodified asphalt concrete mixture and a series of modified asphalt mixtures. The resin modified was found to be effective in improving Marshall stability, tensile strength, compressive strength and permeability of asphalt concrete.

2. Research method

All tests had been carried at the Laboratory of Sebelas Maret University of Surakarta, Indonesia. This study has carried out by using experimental methods to evaluate the performance of Asphalt Concrete with Asphalt 60/70 pen and Asphalt 60/70 penetration resin modified binder and its suitability in road pavement precisely in hot mix asphalt.

2.1. Aggregate gradation for asphalt concrete and bitumen composition

The percentages of aggregates required for every sieve size were determined according to the Indonesian standards. Then the samples retained were calculated using the percent passing for every sample size. Table 1 summaries the upper and lower limit aggregate gradation according to Indonesian standards. The composition of 60/70 pen bitumen and the percentage of natural resin are described as Asphalt 60/70 pen (A), Asphalt 60/70 pen + Damar 2.5% (B), Asphalt 60/70 pen + Damar 5% (C) Asphalt 60/70 pen + Damar 7.5% (D) and Asphalt 60/70 pen + Damar 10% (E). The bitumen contents for these samples were ranged from 4.5 to 6.5 % of the total weight

according to ASTM 3515-96 [5]. It has been made the tests for bitumen to ensure that the selected bitumen properties are comply with the standard.

Table 1. The gradation of Asphalt Concrete

Sieve size		Upper Limit specification	Lower Limit specification
in	mm		
3/4"	19.1	100	100
1/2"	12.5	90	100
3/8"	9.5	72	90
#4	4.76	43	63
#8	2.38	28	39.1
#16	1.18	19	25.6
#30	0.59	13	19.1
#50	0.279	9	15.5
#100	0.149	6	13
#200	0.074	4	10
Pan		0	0

2.2. Sample production

The numbers of samples required are 3 samples for each percentage of bitumen and 15 samples for each type of bitumen compositions. Optimum bitumen content is needed to design the mix which gives the maximum stability and density, flow, median air voids in aggregate filled with bitumen and air voids in the mix. Determine the optimum binder content for the mix design by taking the average value of the following three bitumen contents found from the graphs will be obtained in Marshal test step. The amount of sample required for unconfined compressive test, indirect tensile test and permeability test are 3 samples of each type of bitumen produced at optimum bitumen content.

2.3. Marshall mixture design and testing

Marshall mix design is one of the oldest design methods used. Developed by Bruce Marshall for the Mississippi Highway Department in the late 30's, this method is still widely used by most states. The Marshall method criteria allow the engineer to choose an optimum asphalt content to be added to the specific aggregate blend to a mix where the desired properties of density, stability and flow are met. The Marshall method uses standard HMA samples that are 4 inches in diameter and 2 1/2 inches high. The preparation procedure is carefully specified, and involves heating, mixing, and compacting asphalt/aggregate mixtures. The Marshall Method for hot-mix asphalt concrete mix design is a rational approach to selecting and proportioning two materials, asphalt cement and mineral aggregates to obtain the specified properties in the finished asphalt concrete surfacing structure. The method is intended for laboratory design of asphalt hot-mix paving mixtures. Each type of asphalt mixture with a designated percentage of resin at optimum bitumen content were subjected to indirect tensile test, unconfined compressive test and permeability test.

3. Results and discussions

The aims of this research are to achieve the viability of using Asphalt 60/70 pen, resins (damar) modified bitumen as a binder for alternative industrial asphalt in flexible pavement design. All of the Asphalt Concrete mixture (AC) was prepared based on Marshall Mix design. The Asphalt concrete mixtures (AC) were between normal aggregate and Asphalt 60/70pen and damar modified Bitumen. The results of mixture properties of the five types of Asphalt concrete mixtures (AC) in terms of Marshall Stability Test (MS) to get optimum bitumen content,

Unconfined Compressive Strength Test (UCS) and Indirect Tensile Strength Test (ITS)and Permeability Test are presented and discussed.

3.1. The optimum bitumen content and marshall stability

Five types of blends were prepared for each type of asphalt cement mixture: Asphalt (A)60/70 pen, Asphalt (B), Asphalt (C) and Asphalt (E). Marshall Specimens were conducted according to (ASTM D 1559); specimens were prepared for each bitumen contents within the range given (4.5%, 5%, 5.5%, 6%,and 6.5%). The optimum bitumen content has been determined in this study based on the maximum Stability according to the Marshall Stability (MS) as illustrated in Fig. 1, the green line represents the Asphalt Pen 60/70, the purple line represents the ratio of damar 2,5%, the red line represents the ratio of damar 5%,the brown line represents the ratio of damar 7,5% and the blue line represents damar 10%. Table 2 shows the properties of OBC that obtained from the mix design. The results of Marshall mix design show that the values of optimum bitumen content are relatively similar for all asphalt concrete mixtures. However, the high percentage of resin resulted in higher Marshall stability, it indicates that resin modified bitumen could improve the stability of asphalt mixtures.

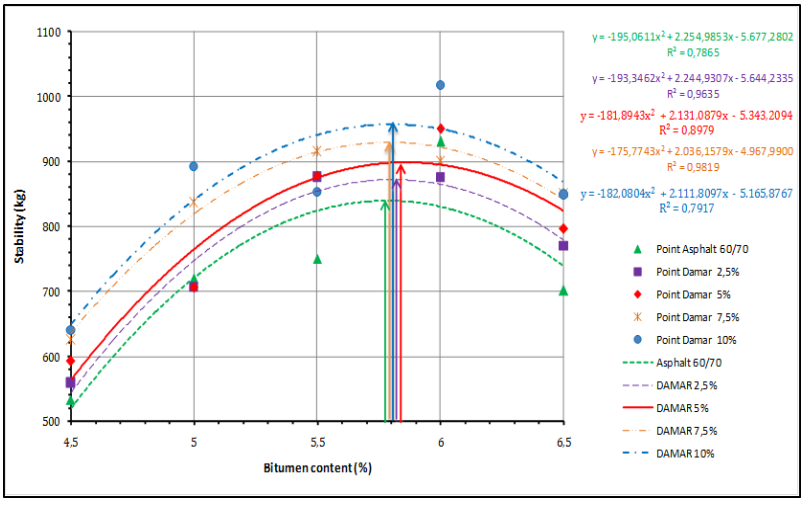

Fig. 1. The optimum bitumen content based on Marshall stability test

Table 2. Results of optimum bitumen content and Marshall stability

Explanation	Asphalt Type					Specification AASHTO
	A (0% Resin)	B (2.5% Resin)	C (5% Resin)	D (7.5% Resin)	E (10% Resin)	
Stability (kg)	839.86	872.20	898,79	928.69	957,44	800 kg
O.B.C %	5.78	5.81	5,86	5.79	5,80	(5 to 7) %

3.2. The indirect tensile performance

This test was conducted under conditions; it was determined by measuring the ultimate load to failure of a specimen that is subjected to a constant deformation rate of 50.8 mm/minute on its diametrical axis according to (ASTM D6931). It is the measure of pavement response in terms of tensile stresses based on average results of three samples for each type of asphalt mixtures, Figure 2 and Table 3 show the summarized results for the resilient modulus test for each type of asphalt cement mixture specimens at optimum bitumen content.

Table 3. Indirect Tensile Strength at optimum bitumen content

Asphalt Type		ITS (Kpa)
Asphalt Pen 60/70	(A)	447.63
Asphalt + resin 2.5 %	(B)	739.28
Asphalt + resin 5%	(C)	755.44
Asphalt + resin 7.5%	(D)	974.06
Asphalt + resin 10%	(E)	1070.96

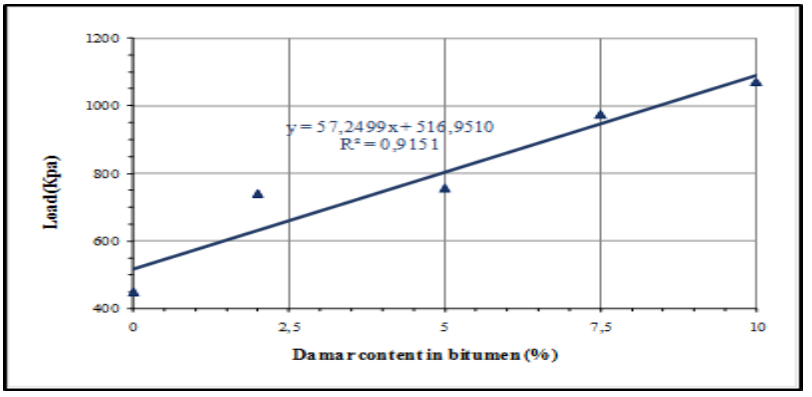

Fig. 2. The Indirect Tensile Strength against the percentage of resin

In the context of ITS result, A mixture with 60/70 pen bitumen got 447.63 KPA. When 2.5% damar added, the value of ITS is increase to 739.28 KPA. Then the result is getting higher again in line with the increase of damar content. Then based on ITS result, it can be seen that the greater the proportion of damar increased the ITS value. It is proven that asphalt with 10% modification got the highest score of ITS result that the other samples of resin. The overall correlation could be presented with the formula y=57.2499x+516.95 with R2 of 0.91.

3.3. The unconfined compressive strength performance

Unconfined Compressive Strength Test (UCS) is used to determine the resistance to permanent deformation of bituminous mixtures at the temperature of 25°C and loads. It is conducted by applying a static load to a specimen using OBC and then measuring the maximum load. This test is used to determine the permanent deformation of Asphalt Pen 60/70 and modified asphalt mixtures. It is noticed that the permanent deformation of the asphalt mixtures is correlated with the rutting potential. Figure 2 and Table 5 shows the summarized results of the Unconfined Compressive Strength Test (UCS) for each type of asphalt cement at optimum bitumen content.

Table 4. Unconfined Compressive Strength performance at obc

Asphalt Type		UCS (Kpa)
Asphalt Pen 60/70	(A)	4257.49
Asphalt + resin 2.5 %	(B)	5569.79
Asphalt + resin 5%	(C)	5902.01
Asphalt + resin 7.5%	(D)	7302.61
Asphalt + resin 10%	(E)	7857.16

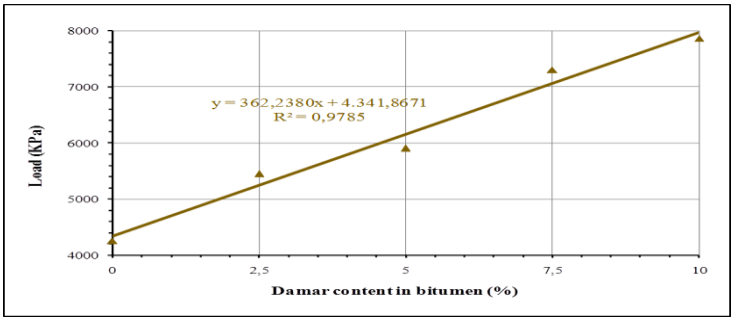

Fig. 3. The unconfined compressive strength against the percentage of resin

In the context of UCS test, the result of UCS for Asphalt 60/70 pen is lower than other combination. Then the increase of Damar to 2.5% will increase the UCS value to 5569.79 Kpa; the increase of damar 5% increased the UCS value to 5902.01 Kpa; the increase of damar 7.5% increased the UCS value to 7302.61 and increased of damar 10% increased the UCS value to 7857.16 Kpa. The result of UCS test was very strong with Damar modified bitumen between the ratio (5% up to 10%) and the formula is Y=362.23x+4341.88 with R^2 value of 0.98. The Optimum DamarContent from UCS test using the formula is 6.9726%.

3.4. The permeability performance

Permeability testing is important because one of the primary assumptions in the structural pavement design for conventional pavements is flexible (Asphalt Concrete) and the pavement must be impermeable. The basis for this design approach is to minimize the moisture infiltration and thus maintain the adequate support from the underlying unbound materials. Figure 4and Table 6 show the summarized results for the Test for each type of asphalt cement at optimum bitumen content. The calculations of coefficient permeability against the percentage of resin were calculated by the equation y=0.000026x+0.000697 with R^2 of 0.92. The higher content of resin in the asphalt concrete mixture result in lower permeability performance.

Table 5. The Results of Permeability Test at optimum bitumen content

Asphalt Type	Permeability (K) with Pressure Water 5 kg/cm²
Asphalt Pen 60/70 (A)	6.858E-04
Asphalt + resin 2.5 % (B)	6.186E-04
Asphalt + resin 5% (C)	5.890E-04
Asphalt + resin 7.5% (D)	5.406E-04
Asphalt + resin 10% (E)	4.003E-04

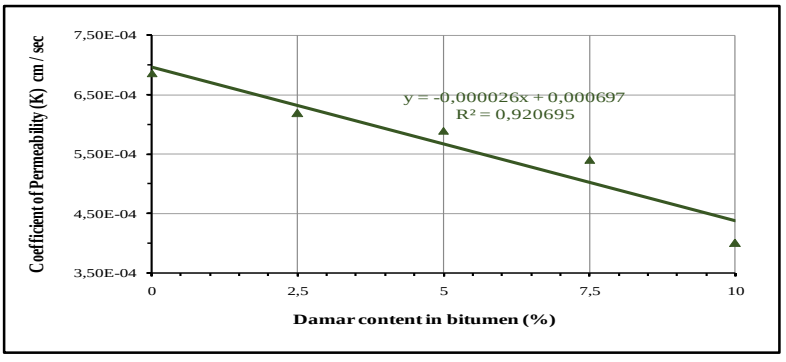

Figure 4. Results Permeability test for each type of asphalt cement mixtures at obc.

Experimental results conducted by Yami show that all resin-modified asphalt mixtures have higher flow, bulk density and VFA compared with control mixture [6]. It has been proved that increasing performance of bitumen properties modified with resin could potentially increase the projected mixture properties.

Conclusion

1. The results of Marshall mix design show that the values of optimum bitumen content are relatively similar for all asphalt concrete mixtures. However, the high percentage of resin resulted in higher Marshall stability, it indicates that resin modified bitumen could improve the stability of asphalt mixtures.
2. The indirect tensile strength is getting higher with the increase of damar content. It can be seen that the greater the proportion of damar increased the ITS value with the approach formula of $y=57.2499x+516.95$ with R^2 of 0.91.
3. The result of UCS test was very strong with Damar modified bitumen between the ratio 5% up to 10% and the formula is $y=362.23x+4341.88$ with R^2 value of 0.98. The optimum damar content from UCS test using the formula is 6.9726%.
4. The calculations of coefficient permeability against the percentage of resin were calculated by the equation $y=0.000026x+0.000697$ with R^2 of 0.92. The higher content of resin in the asphalt concrete mixture result in lower permeability performance, that indicates a better volumetric properties..

References

[1] EPA, 2006. *Data Quality Assessment* : A Reviewer's Guide, www.epa.gov/QUALITY/qs-docs/g9s-final.pdf. www.epa.gov/QUALITY/qs-docs/g9s-final.pdf . Data Quality Assessment : A Reviewer's Guide. EPA, 2006).

[2] Williams, Christopher, 2013. *Development of Rubber Modified Fractioned Bio Oil For Used As Non Crude Petroleum Binder For Flexible Pavement*. http://www.intrans.iastate.edu/people/staff/ details/?staffid=-716735796.

[3] Bueno, B.S, Silva W.R, Lima D.C, et al, 2003. *Engineering Properties of Fiber Reinforced Cold Asphalt Mixes*. Journal of Environmental Engineering.

[4] Zhu Haoran , Yang Jun, Cong Ling, Cui Juan and Wan Jun, 2000. *Influence of Polyester Fiber on the Performance of Asphalt*, Mixes.Southeast University.No. 2 Sipailou, Nanjing 2000, 96, P. R. China.

[5] Nasution, M.F., Setyawan, A. and Sumarsono, A., 2015. STUDI KARAKTERISTIK DASPAL DIBANDINGKAN DENGAN ASPAL PENETRATIONGRADE 60. *Matriks Teknik Sipil*, *3*(4).

[6] Fini, E.H., Kalberer, E.W., Shahbazi, A., Basti, M., You, Z., Ozer, H. and Aurangzeb, Q., 2011. Chemical characterization of biobinder from swine manure: Sustainable modifier for asphalt binder. *Journal of Materials in Civil Engineering*, *23*(11), pp.1506-1513.

Available online at www.sciencedirect.com

ScienceDirect

Procedia Engineering00 (2017) 000–000

Procedia Engineering

www.elsevier.com/locate/procedia

Sustainable Civil Engineering Structures and Construction Materials, SCESCM 2016

Marshall characteristics in asphalt concrete –Wearing corse (AC-WC) in various length and temperature submersion

Yetty Riris Rotua Saragi[a*], Partahi Lumbangaol[a], Ros Anita Sidabutar[a], Ben Saputra Siahaan[a]

[a]*University of HKBP Nommensen, Sutomo Street No.4A, Medan 20234, Indonesia*

Abstract

Early damaged of road pavement in Indonesia is commonly caused by weather and water submersion. The road pavement performances, i.e. road strength and durability are affected by the existing of water submersion and the load through the road. By using Marshall Test, the research aims to find out the effect of submersion to the Asphalt Concrete–Wearing Corse (AC-WC) characteristics, i.e. stability, flow, Marshall Quotient (MQ), Void in Mix (VIM) and Void in Mixed Aggregate (VMA) with 60/70 asphalt penetration and 6.1% asphalt content while submerged in water bath. The durationsof submersion are 1×24, 2×24, 4×24, 6×24 and 8×24 hours in various temperatures that are 32, 50, 60, 70 and 80^{o}C. The mixing asphalt consists of Corse Aggregate (CA), Medium Aggregate (MA) and Fine Aggregate (FA). Moreover, this experiment is done under Bina Marga specification. As the result, this research shows that the length and temperature of submersion influenced the Marshall Strength of asphalt AC-WC.The duration of Asphalt AC-WC submerged in water have affected its strength and durability shown by the decreasing of MarshallValue. Also, it occurs when the temperature of submersion was increased.

Peer-review under responsibility of the organizing committee of SCESCM 2016.

Keywords: AC – WC, length of submersion, submersion temperatures, Marshall parameter, road pavement

1. Introduction

A cause leading to the early failure of the pavement is a puddle on the road surface that attacks the bond between aggregate and asphalt. Hence, it will bring a load causing cracks when vehicles pass the road. Submerged road

* Corresponding author. Tel.: 08126368554
*E-mail address:*yettyririssaragi@yahoo.com

Peer-review under responsibility ofthe organizing committee of SCESCM 2016.

surface can be caused by poor water drainage system that cannot accommodate the high-intensity rainfall. This condition could be exacerbated when the road is submerged more than 24 hours (the limit standard of Marshal Strength) and is burdened by the overloaded vehicle exceeding the maximum permissible weight. Therefore, these reasons could affect the performance of asphalt pavements, especially its endurance or durability as the factor in Marshal Criteria.

As a surface layer, designing AC-WC (Asphalt Concrete-Wearing Corse) to be waterproof asphalts is the important aspect that needs to be considered in the highway construction. It is due to this asphalts will be the uppermost layer of pavement structures which contacts directly to loads and receive the distribution of passed vehicles' loads. The purpose of this study is to find out the effects of duration and temperature of water submersion in the AC-WC layer by Marshal Characteristics based on the specifications of Bina Marga.

2. Literature

The durability of pavements is one of crucial factors in the design process. Its durability characteristic is needed to ensure that the pavement layer retains the desired properties. The strength of durability in pavement will affect the pavement design, in which the planning and compacting processes of the mixture will provide the maximum impermeability and minimize the water and air intrusion in pavement.

Asphalt Concrete (AC) is the combination of aggregate that grades continuously, in which the filler and bitumen materials form the interlocking structures. AC is made by adding hot asphalt at the temperature of 275°F (135°C) to the combination of hot aggregate with temperature of 300°F (149°C). These two components are mixed and compacted with the minimum temperature of 225°F (107°C). The function of this AC-WC layer is to receive loads directly and protect the base course.

The AC Durability depends on its resistance to damage under traffic loads. This resistance can be reduced because of weather effects and mechanical damages of the aggregate. The durability defines as the ability of a material in asphalt pavements to be resistant towards the water, age and temperature.

According to Pangamanan (2015) who study the effect of temperature and duration of immersion in the stability and melting, the result shows that the temperature and duration of immersion affects the durability. The greater temperature and duration of immersion the mixture, the lower the level of durability of mixture is [2]. Moreover, a study on the mixing AC-WC with the variations of immersion's length and aging indicates that prolonged submersion and aging will decrease the level of durability mixture [3].

A study indetermining the Marshal characteristics and the rest of the Strength Index butonite mastic asphalt mix (BMA) has been done. The result reveals that although the mixture of asphalt concrete layer gives a higher yield than the BMA, the mixture of BMA still meets the Bina Marga specifications[5]. In addition, based on Tahir (2009), he studied the AC performance to the durability of concrete asphalt with the temperature of compaction variations and the duration of submersion. He obtained that the highest durability was in the solidification temperature of 120°C and 1- day-immersion [6]. Also, the study of the characteristics of AC-WC Marshal and durability from two different types of filler-Portland cement and stone dust- has been investigated by Putrowijoyo (2006). The results show that AC-WC filled by Portland cement had better Marshal and durability characteristics than the filler of stone dust [7].

3. Material and method

3.1. Material

In this study, the aggregate as the mixture of asphalt is in accordance with the general specifications of Bina Marga, Dep. PU 2010 (Table 1). The aggregate used (Table 2) is from the River Sibirubiru, Deli Tua, Deli Serdang district treated with stone crusher from PT.Karya Murni Perkasa, Medan.The filler that is used in this study is stone dust according to the SNI 03-6723-2002 standard. The addition of filler aims to fix the quality of the mixture and add the contribution of stone dust filler. From the test, it was obtained that the Specific Gravity (Gs) of stobe dust is 2.68 g/cc. Hence, the stone dust includes in sand types. From the test results, the grain sizes of stone dust are 2.32%

and sieve No.200 and No.4 respectively. The Value of Cu is 2.38 and Cc is 1.32. In addition, the material passing 75 microns in stone dust is 88.8%.

Table 1 Proportion of Mixed Aggregate

Number of Sieve	**Size of Sieve (mm)**	**CA**	**MA**	**FA**	**Weight Retained**	**% Retained**	**% Passing**	**SPEC**	**Proporsi (gram)**
No.3/4	19.1	-	-	-	-	-	100%	100	
No.1/2	12.5	2679	242.2	-	2921.2	9.74%	90.26%	90-100	116.848
No.3/8	9.5	3172	1569	40.44	4781.44	15.94%	74.32%	72-90	191.258
No.4	5.0	3185	1822	814	5821	19.40%	54.92%	54-69	232.84
No.8	2.3	364	3448	886	4698	15.66%	39.26%	39.1-53	187.92
No.30	0.6	324.6	345.4	2914	3584	11.95%	27.31%	23.1-30	143.36
No.50	0.291	86	755.6	1957.3	2798.9	9.33%	17.98%	15-22	111.956
No.100	0.15	20.6	349.8	1964	2334.4	7.78%	10.20%	9-15	93.376
No.200	0.075	1.6	862	982	1855.6	6.19%	4.02%	4-10	74.224
PAN		157.2	606	442.26	1205.46	4.02%	0%		48.18
Total		10000	10000	10000	30000	100 %			1200

Source: Results of Laboratory Tests on Highway UHN, Medan

Table 2 Testing Results Aggregate Density and Aggregate Absorption

Examination	**Coarse Aggregates (CA)**	**Fine Aggregates (FA)**
Bulk Density	2,688	2,247
Dry Surface Density	2,698	2,307
Apparent Density	2,716	2,391
Absorption (%)	0,363	2,670

Source: Results of Laboratory Tests of PT.Karya Murni Perkasa

3.2. Test marshall

To obtain the specimen needed, Job Mix Design (JMD) of AC-WC has been made in advance with the asphalt content of 5-7% with the addition of 0.5% in 25 samples (5 samples for each variation). Compaction is done by 2x50 times of the collision. The Marshal Test has used a cylindrical specimen with the height of 64 mm, the diameter of 102 mm and the mixing temperature of 130°C tested at 60°C ± 1°C with the constant loading rate of 51 mm/min until the collapse occurred. In this study, the Marshal Test for mix design used the hard asphalt with standard method of Marshal testing by maximum 25 mm (1 inch) aggregate size. The examination of the Marshal test at this stage was to determine the optimum bitumen content based on the Specifications of Bina Marga in 2010. Also, with the optimum bitumen content, 125 samples AC-WC by variations in temperature and soaking time (5 samples each variation) was created to determine the durability through Marshal Test.

3.3. Preparation of the test object in various length and temperature submersion

After obtaining the optimum bitumen content, a mixture of AC-WC for Marshal test has been made with variety of dipping time that were 1x24, 2x24, 4x24, 6x24 and 8x24 hour and soaking temperature that were 32, 50, 60, 70 and 80°C, which 3 samples for each variations are used. The variation of length and temperature of submersion was to determine the durability and damage caused by water.

As a result of the presence of water or the combination between water and mechanical forces given, the asphalt covering the aggregate surface will peel off. However, the strong levels of cohesion in asphalt will attach strongly on the surface of the aggregate, so that the peeling occurs as a result of the water influence or the combination water-mechanical force is very small or even not occurs at all. The adhesion and cohesion are the ability of asphalt particles to attach to each other and the ability to attach to and bind the asphalt aggregate.

3.4. Durability AC-WC

One of the characteristics of asphalt concrete mixtures is the durability. This characteristic is associated with the durability of a mixture from disintegration due to the effects of weather, water or traffic load. The durability or resistance in the surface layer is required to be able to restrain the tear caused by weather, water and temperature changes as well as by the friction of the vehicle wheels.

Water is a factor that can affect the declining of durability a mixing (asphalt). If the asphalt layer is always submerged by water, the durability of the mixture will reduce. Another factor that can also affect the durability of the mixture is compaction. The level of the mixture's durability is used as the parameter Residual Strength Index (RSI)- First Durability Index (FDI) and the Second Durability Index (SDI).

3.4.1 Residual strength index

The strength index was obtained through the testing of mechanical characteristics of specimen (stability and flow) divided into two groups. The first group was tested its Marshal stability after submersion in water at 60°C during the time T1 and the second group was tested after submersion at 60°C for the time T2 (Hunter, 1994). Based on the Marshal Stability value obtained in both submersions, Residual Strength Index (RSI) was determined by using equation (1). RSI value required by the specifications of Bina Marga in 2010 on AC-WC layer is the minimum of 90%. The value indicates that the asphalt layer is still considered to be quite resistant to the damage caused by water.

$$RSI = \frac{S_2}{S_1} \text{ x } 100\% \quad (1)$$

Where: S_1 = the average value of Marshall stability after soaking for T_1 (Kg)
S_2 = the average value of Marshall stability after soaking for T_2 (Kg)
RSI = Residual Strength Index (%)

3.4.2 First durability index

The first Durability Index can be calculated by using equation (2). The positive value of 'r' indicates a loss of strength, while a negative value of 'r' indicates a gained strength.

$$r = \sum_{i=0}^{n=1} \frac{S_i - S_{i+1}}{t_{i+1} - t_i} \tag{2}$$

Where : r = Decrease Stability Index (%)
S_{i+1} = Percentage of the residual strength at the time t_{i+1}
S_i = percentage residual strength at the time t_i
t_i , t_{i+1} = Period submersion (starting from the beginning of the test)

3.4.3 Second durability index

The Second Durability Index (SDI) can be calculated by using equation (3).

$$a = \frac{1}{2t_n} \sum_{i=0}^{n=1} (S_i - S_{i+1})[2t_n - (t_i + t_{i+1})] \tag{3}$$

Where t_n = total period submersion
a = Second Durability Index (SDI)

This Durability Index describes the lost power in a day. The positive value 'a' describes the loss of strength, while the negative value of 'a' was an added strength. Based on these definitions, the value is a <100. Therefore, it allows declaring that the percentage of the residual strength of the day (Sa) can be calculated using equation (4).

$$S_a = (100 - a) \tag{4}$$

The Second Value of Durability Index can also be expressed in terms of absolute value according to the equation (5).

$$A = \frac{a}{100} S_o \tag{5}$$

Where : A = the absolute value of lost power for one day (kg)
S_o = absolute value of the initial force (kg)

The absolute value of the residual strength of the day (SA) expressed according to the equation (6)

$$SA = S_o - A \tag{6}$$

4. Result and analysis

4.1 Optimum asphalt content

The Marshall Results on the AC-WC mixture with the asphalt content of 5-7% based on the specifications of Bina Marga in 2010 to produce the optimum bitumen content of 6.1%.

4.2 Test marshall result

With the asphalt content in accordance to the optimum bitumen content, Marshal Test is then performed with the

variety of durations and temperature of soaking (Figure 1). The minimum of Stability Values is 800 kg (the specifications of Bina Marga 2010).The longer submersion a sample is done, the lower the value of stability of the sample is obtained. Furthermore, if the soaking temperature is too hot soaking on a sample, its sample will melt and does not produce the stability value. The results of Marshal Test are shown in Table 3.

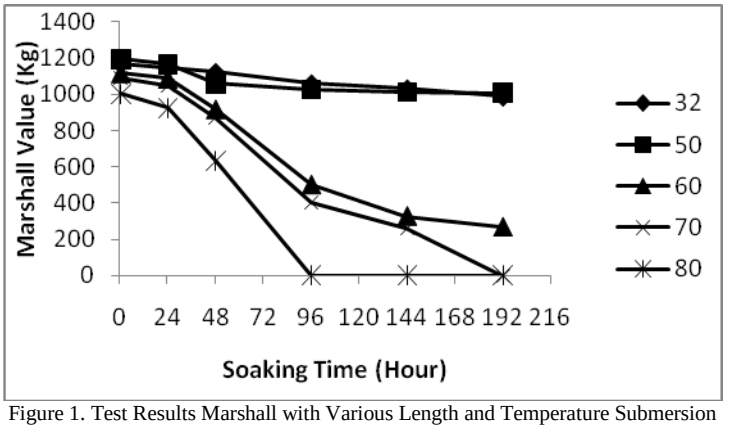

Figure 1. Test Results Marshall with Various Length and Temperature Submersion

Table 3. Result of Marshall Test in OAC with Various Length and Temperature Submersion

Parameter of Marshall	BM Spesification	Temp (°C)	Length of Submersion (hour)											
			0.5		24		48		96		144		192	
Stability (kg)	≥800	32	1170.0	√	1147.0	√	1123.0	√	1060.0	√	1032.0	√	988.0	√
		50	1195.0	√	1166.0	√	1027.0	√	1027.0	√	1012.0	√	1008.0	√
		60	1120.0	√	1090.0	√	504.0	×	504.0	×	330.0	×	270.0	×
		70	1090.0	√	1050.0	√	403.0	×	403.0	×	260.0	×	0.0	×
		80	1005.0	√	925.0	√	0.0	×	0.0	×	0.0	×	0.0	×
Flow (mm)	2 - 4	32	3.6	√	3.5	√	3.4	√	3.4	√	3.3	√	3.1	√
		50	3.5	√	3.5	√	3.4	√	3.2	√	3.1	√	3.1	√
		60	3.4	√	3.4	√	3.2	√	2.5	√	2.2	√	2.1	√
		70	3.5	√	3.5	√	3.3	√	2.5	√	2.1	√	0.0	√
		80	3.3	√	3.3	√	3.3	√	0.0	√	0.0	√	0.0	√
MQ (kg/mm)	≥250	32	340.0	√	328.0	√	330.0	√	309.0	√	310.0	√	317.0	√
		50	345.0	√	336.0	√	316.0	√	322.0	√	325.0	√	331.0	√
		60	331.0	√	327.0	√	214.0	×	206.0	×	150.0	×	129.0	×
		70	322.0	√	200.0	×	299.0	√	165.0	×	122.0	×	0.0	×
		80	290.0	√	282.0	√	272.0	√	0.0	×	0.0	×	0.0	×
VMA (%)	≥ 15	32	16.3	√	16.4	√	16.5	√	16.6	√	16.7	√	`16.7	√
		50	16.6	√	16.5	√	16.1	√	15.8	√	17.2	√	15.9	√
		60	16.4	√	16.4	√	16.5	√	17.2	√	15.8	√	16.7	√
		70	15.2	√	15.3	√	15.6	√	17.2	√	15.3	√	16.7	√
		80	15.0	√	15.1	√	15.3	√	15.8	√	15.3	√	16.3	√
VIM (%)	3 - 5	32	3.8	√	3.9	√	4.0	√	4.1	√	4.2	√	4.2	√
		50	4.1	√	4.0	√	3.6	√	3.2	√	4.8	√	3.3	√
		60	3.7	√	3.8	√	3.9	√	4.8	√	3.2	√	4.2	√
		70	2.5	×	2.6	×	3.0	√	4.8	√	2.6	×	4.2	√
		80	2.2	×	2.3	×	2.6	×	3.1	√	2.6	×	3.7	√
VFB (%)	≥ 65	32	76.8	√	76.2	√	75.8	√	75.5	√	75.0	√	74.7	√
		50	75.5	√	76.0	√	77.9	√	80.0	√	72.0	√	79.1	√
		60	77.0	√	76.6	√	76.1	√	72.2	√	79.8	√	75.0	√
		70	84.0	√	83.2	√	81.1	√	72.2	√	83.1	√	75.0	√
		80	85.5	√	84.6	√	83.3	√	80.2	√	83.0	√	77.2	√

Information : √ = meet spesification
× = not meet spesification

The VMA value will increase when the duration and temperature of submersion increase. This is due to the longer and the higher soaking temperature will produce the wider cavity becomes wider so that the density of the mixture is reduced. It results the binding of bitumen to aggregate is not optimal resulting the increasing of VMA value, and vice versa.

The flow value tends to decrease. This is caused by the density affecting closely the cavity. If the cavity is enlarged, the density will reduce. The increasing of the coarse aggregate percentage tends to increase the size of cavity because lots of gaps between fine aggregate and filler are available. Otherwise, if the percentage of coarse aggregate is less than normal conditions, the surface will be wider causing the decreasing of flow value. In addition, the greater the temperature and the longer the sample submerged in the water, the wider the cavity in sample and the easier the sample to melt or loss its power.

4.3 Durability

The Bina Marga 2010 specification requires that the value of RSI after soaking of 24 hours at 60°C is 90%. RSI results (Figure 2) shows that the longer the soaking time, the higher the soaking temperature that will decrease the RSI. Soaking temperature of 60°C for 24 hours gives 97.32% RSI value which still meets specifications. The RSI results also describes that the mixture of AC-WC is strongly influenced by the presence of water. The entire sample with soaking temperature variations still meet the specifications of 24-hour-soaking, while for further immersion, it does not.

The FDI value shown by the positive value of 'r' on the whole variations (Table 4) reveals that there is power loss in each variation. In addition, the result of IDP also describes that the mixture of AC-WC is strongly influenced by the presence of water. The SDI value indicated by the positive value of 'a' in all variety of length and temperature variations (Table 4.2) shows that the loss of power is occurred of each variation. Same as the others, the IDK results also showed that the mixture of AC-WC is strongly influenced by the presence of water. Overall, the result data shows that the greater the variation values of soaking duration and temperature, the greater the percentage strength losses of AC-WC layer. It also means that the longer AC-WC layer is submerged under water at high temperature, the greater the loss of power occurs.

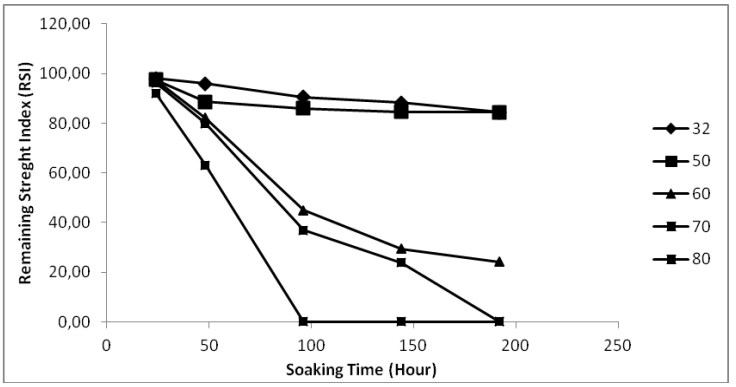

Figure 2. RSI Value with Various Length and Temperature Submersion

Table 4.2 Results of Durability Index

	First Durability Index (FDI)					
	Soaking	Soaking Time (Hour)				
	Temp (°C)	24	48	96	144	192
Slope,r (%)	32	0.08	0.17	0.36	0.67	1.36
	50	0.10	0.47	0.63	1.24	2.45
	60	0.11	0.75	1.63	2.82	5.42
	70	0.16	0.84	1.89	3.17	6.56
	80	0.34	1.54	3.20	5.08	10.15

Second Durability Index (SDI)						
	Soaking	Soaking Time (Hour)				
	Temp (°C)	24	48	96	144	192
The lost power of a day, a (%)	32	1.84	1.64	3.3.7	0.90	0.45
	50	2.27	7.10	1.73	0.47	0.04
	60	2.51	12.14	23.21	5.83	0.64
	70	3.44	13.21	26.78	4.92	2.86
	80	7.46	23.08	39.49	0.00	0.00
	Soaking	Soaking Time (Hour)				
The residual strength in one day, Sa (%)	Temp (°C)	24	48	96	144	192
	32	98.16	98.36	96.63	99.10	99.55
	50	97.73	92.90	98.27	99.53	99.96
	60	97.49	87.86	76.79	94.17	99.36
	70	96.56	86.79	73.22	95.08	97.14
	80	92.54	76.92	60.51	100.00	100.00
	Soaking	Soaking Time (Hour)				
The absolute value of lost power for one day, A (kg)	Temp (°C)	24	48	96	144	192
	32	21.55	19.20	39.38	10.50	5.28
	50	27.17	84.80	20.63	5.62	0.48
	60	28.11	136.00	260.00	65.25	7.20
	70	37.48	144.00	291.88	53.63	31.20
	80	74.96	232.00	396.99	0.00	0.00
	Soaking	Soaking Time (Hour)				
The absolute value of the residual strength of the day, SA (kg)	Temp (°C)	24	48	96	144	192
	32	1148.45	1150.80	1130.63	1159.50	1164.72
	50	1167.83	1085.20	1149.38	1164.38	1169.52
	60	1091.89	1034.00	910.00	1104.75	1162.80
	70	1052.52	1026.00	878.13	1116.38	1138.80
	80	930.04	938.00	773.13	1170.00	1170.00

5. Conclusion and Recommendation

5.1. Conclusion

From research conducted can be concluded as follows:

1. The longer the samples are submerged; the higher VMA value will be obtained. This is because the cavity becomes wider resulting the reducing of mixture density. The binding between bitumen and aggregate is not optimal leading to the increasing of VMA value, and vive versa.
2. The longer the samples areimmersed in water leads to the decreasing of flow value. It is caused by the connection between the density and the cavity is really close. When the cavity enlarges, the density reduces.
3. The greater the variations of length and temperature submersion, the greater the strength losses of AC-WC layer. It shows that the longer length of AC-WC submersion time and the greater temperature submersion, the greater the strength losses occurs.

5.2. Recommendations

1. Because the price of cement is expensive, we recommend that the use of cement in the concrete asphalt

mixing is not used even though cement has high holding capacity yield stability.

2. Aggregate scales should be checked in advance because its validity will greatly affect the process of creating and testing the specimen.
3. The compaction control should be concerned because the aggregate may rupture and cause interconnected aggregates because of the unperfected compaction.

References

[1] Anonim, (2010), Spesifikasi Umum 2010, Direktorat Jendral Bina Marga, Departemen Pekerjaan Umum, Jakarta, 2010

[2] Siahaan., B, Karakteristik Marshall AC-WC pada Variasi Suhu dan Lama Perendaman, Tugas Akhir, Program Studi Teknik Sipil, Fakultas Teknik, Universitas HKBP Nommensen, 2016

[3] Pangemanan.,V, Pengaruh Suhu dan Durasi Terendamnya Perkerasan Beraspal Panas Terhadap Stabilitas dan Kelelehan (Flow), Jurnal Sipil Statik, Vol.3 No.2, ISSN: 2337-6732, pp 85-90, 2015

[4] Setiawan., A, Pengaruh Penuaan dan Lama Perendaman Terhadap Durabilitas Campuran Asphalt Concrete Wearing Corse (AC-WC), Naskah Publikasi, Program Studi Teknik Sipil, Fakultas Teknik, Universitas Muhammadiyah Surakarta, Surakarta, 2014

[5] Fatmawati., L, Kharakteristik Marshall Dalam Asphal Campuran Panas AC WC Terhadap Variasi Temperatur Perendaman, Jurnal Wahana Teknik Sipil, Vol.18 No.2, pp 88-94, 2013

[6] Wahjoedi, Karakteristik Marshall dan Indeks Kekuatan Sisa (IKS) Pada Campuran Butonite Mastic Asphalt (BMA)", Jurnal Teknik Sipil dan Perencanaan, Vol. 11 No.2, pp 121-130, 2009

[7] Tahir., A, Kinerja Durabilitas Campuran Beton Aspal Ditinjau Dari Faktor Variasi Suhu Pemadatan Dan Lama Perendaman, Jurnal SMARTek, Vol.7 No.1, pp 45-61, 2009

[8] Putrowijoyo., R, Kajian Laboratorium Sifat Marshall Dan Durabilitas Asphalt Concrete Wearing Corse (AC-WC) Dengan Membandingkan Penggunaan Antara Semen Portland Dan Abu Batu Sebagai Filler", Tesis, Program Pasca Sarjana, Universitas Diponegoro, Semarang, 2006

Available online at www.sciencedirect.com

ScienceDirect

Procedia Engineering 00 (2017) 000–000

Procedia Engineering

www.elsevier.com/locate/procedia

Sustainable Civil Engineering Structures and Construction Materials 2016, SCESCM 2016

The application of porous concrete filled with soil and sands for low volume traffic road

Djoko Sarwono[a], Djumari[a], Rochim[a], Ary Setyawan[a,*]

[a]*Roadmate Research Group UNS, Jl. Ir. Sutami 36 A, Surakarta 5126, Indonesia*

Abstract

Pavements were usually planned as an impermeable layer to protect the sub grade from water intrusion which weakens the bearing capability of the sub grade. However, the more area to be protected from water ingress resulted in an abundant surface flow that cause reduction in green areas which impact on the reduction of water catchment areas. To anticipate this problem, the use of adequate strong pavement layer, but more environmentally friendly which allow the water to hang through the layer and absorbed into the sub grade that could cut the surface flow but keep up the potency of the layer is expected. The purpose of such layer is possible for low traffic volume road. The objective of this study is to design the adequate strength of porous concrete filled with soil and sand for low volume traffic road. The study was conducted using the experimental method, namely by reducing the proportion of fine aggregate in the mix design of conventional concrete. Crushed stone aggregate used is a uniform size of 1-2 cm. The proportion of fine aggregate used is 30% of the proportion of coarse aggregate. The voids of the each type of porous concrete were then filled with soil, natural sand and volcanic sand. The filled samples were then assessed for water permeability, speed of absorption and compressive strength. The test results with a variety filler of porous concrete, namely soil, natural sand and volcanic sand were obtained and analyzed. The highest vertical and horizontal permeability's achieved with natural sand filled samples by 0.38 cm/Sec and 0.364 cm/Sec, respectively. The rate of absorption achieves the highest value of 0.337 for porous concrete filled with natural sand. The high compressive strength value of 5.71 MPa belongs to the porous concrete filled with volcanic sand. However, it is recommended that the filled porous concrete is only suitable for low volume traffic road such as road shoulders, parking lots and pedestrian paths.

Peer-review under responsibility of the organizing committee of SCESCM 2016.

* Corresponding author. Tel.: +62-815-485-58590; fax: +62-271-634524.
E-mail address: arysetyawan@staff.uns.ac.id

Peer-review under responsibility of the organizing committee of SCESCM 2016.

Keywords: porous concrete, low volume traffic road, water permeability

1. Introduction

Porous concrete is a construction material that has unique characteristics. As the name implies, the porous concrete is concrete that has pores that can be penetrated by water. With the pores in concrete, it can be used to absorb runoff and simultaneously increase soil water reserves. With applied to the shoulder of the road, the water runoff from the road is expected to be absorbed into the soil, and can be reduced clearance of water discharge in the drainage channel [1].

Porous concrete pavement is very rarely used in the construction of infrastructure. But when viewed usefulness of porous concrete as concrete multifunction primarily to respond to the issue of green engineering, then the porous concrete can be considered worthy as one of lightweight construction materials that will play an important role in the future. Therefore, research is needed to improve the manufacture, composition and durability of porous concrete as construction materials that are environmentally friendly, especially for construction applications with relatively light loads [2].

Properties of porous concrete to consider is the permeability. Permeability is the ease of fluid to pass through the concrete, whereas an absorption is the entry of fluid into the concrete via capillary pipes contained in the concrete itself. Permeability is affected by the porosity of the concrete. Permeability is important to note because the porous concrete in addition serves to hold the load when used as a rigid pavement also serves to facilities so that rain water can seep under porous concrete pavement layer [3]. But in Indonesia weakness as the use of porous concrete pavement is the mud that causes the loss of ability to absorb water in the pores of concrete into the ground. It is necessary to test for permeability and pore concrete compressive strength with the use of volcanic sand, natural river sand and soil as a porous cavity filler in order to avoid the entry of sludge into the voids [4]. The compressive strength testing was conducted to determine whether the use of river sand, sand and soil effect on the compressive strength of concrete is porous.

In its application, the permeability of porous concrete on the field is different from the permeability in the laboratory, due to the combination of vertical and horizontal permeability. So the need to do a rate of absorption test for porous concrete pavement and compares the rate of absorption when the voids filled with the natural sand, soil and volcanic sand. So, the aims of this research are to determine the permeability and the rate of absorption of porous concrete, and to assess the influence of filling the voids on the compressive strength of porous concrete.

2. Research method

As in conventional concrete, the main constituent material of pervious concrete is Portland cement, aggregates, water and other added materials with specific composition. In porous concrete only uses coarse aggregate alone or with a little to no fine aggregate . Water/cement ratio factor must be kept in such a way that after hardened pores formed is not covered by a mixture of hardened cement paste. In addition to controls on w/c ratio is also intended that the grain aggregates can bind tightly to each other for permeability, rate of absorption and compressive strength corresponding to the characteristics of the cavity pervious concrete [5,6,7]. Filling the voids with soil, river sand and volcanic sand are expected to maintain the properties of the voids, rate of absorption as well as improve the compressive strength.

2.1 Aggregate gradation and sample preparation

The selected aggregate gradation is used as concrete aggregate as presented in Table 1, it could be seen that the coarse aggregate used disqualify as coarse aggregate for waterproof concrete according to SK SNI S - 36-1990-03 . Because gradation used for porous concrete is uniform gradation, it is expected to form voids that are interconnected so as to have a good permeability and rate of absorption. Table 1 shows the properties of coarse aggregate.

Table. 1 Aggregate gradation used for porous concrete

No	Sieve Diameter (mm)	Remaining Weight			Passing Weight Cumulative (%)	Standard according to ASTM C-33
		Gram	**%**	Cumulative **(%)**		
1	38,00	0	0	0	100	100
2	19,00	80	2,68	2,68	97,32	95 – 100
3	12,50	2020	67,67	70,35	29,65	-
4	9,50	685	22,95	93,30	6,70	22 – 55
5	4,75	185	6,20	99,50	0,50	0 – 10
6	2,36	15	0,50	100,00	0,00	0 – 0
7	1,18	0	0,00	100,00	0,00	-
8	0,85	0	0,00	100,00	0,00	-
9	0,30	0	0,00	100,00	0,00	-
10	0,15	0	0,00	100,00	0,00	-
11	0,00	0	0,00	100,00	0,00	-
Total		2985	100,00	865,83	-	-

Tabel 2. Coarse aggregate properties

Coarse aggregate properties	Test result	Standard
Bulk Spesific Gravity SSD	2,69	2,5 - 2,7
Absorbtion (%)	0,83%	-
Abrasion (%)	10%	< 50%

A number of sample were prepared for several tests as presented in Table 3.

Table 3. Number of various specimen, curing time and selected test

Type of Porous Concrete Specimen	Test	Curing Time (days)	Number of samples	Total sample
Without filler	Permeability	28	3	7
	Adsorption rate	7	1	
	Compressive strength	28	3	
Natural Sand	Permeability	28	3	7
	Adsorption rate	7	1	
	Compressive strength	28	3	
Volcanic Sand	Permeability	28	3	7
	Adsorption rate	7	1	
	Compressive strength	28	3	
Soil	Permeability	28	3	7
	Adsorption rate	7	1	
	Compressive strength	28	3	

2.2 Job mix design

The composition material for of oncrete mixture were carried out based on previous study on laboratory design for porous concrete [8] which comply the standard Public Works Department SK SNI T-15-1990-03 for the calculation of material requirements per 1 m^3 of K225 concrete. The composition of materials is presented in Table 4.

Table 4. Material composition for 1 m^3 of K225 concrete

No	Material	Composition/ m^3 concrete
1	Water	225kg
2	Portland Cement	448.83 kg
3	Sand	575.00 kg
4	Gravel	1116.17 kg
	Total Weight	2365 kg

The subsequent experiments were then carried out to adjust the porous concrete design by reducing the composition of fine aggregate (sand). Based on the standard of SK SNI S-36-1990-03 on waterproof concrete minimum provisions stipulated that the minimum content of fine aggregates in 1 m^3 of concrete is 450 kg/ m^3 for a nominal maximum grain size of 20 mm aggregate. The previous design of concrete found that the sand used for normal concrete is 575 kg/m^3, so it still qualifies as fine aggregate for watertight concrete. Finally, it was found that the mixture contains 30% fine aggregate and the use of 300 kg/m^3 cement contributed the most optimal porous concrete mixture design. Furthermore the trial of water/cement ratio found that the w/c ratio of 0.35 gave the highest compressive strength and flexural strength [8,9]. The material composition of porous concrete mix design is presented in Table 5.

Table 5. Material composition for 1 m^3 of porous concrete

No	Material	Composition/ m^3 concrete
1	Water	105kg
2	Portland Cement	300 kg
3	Sand	173.33 kg
4	Gravel	1666.67 kg
	Total Weight	2140.00 kg

3. Results and discussion

3.1. Concrete porosity

Porosity (Void In Mix) is the percentage of air voids in the mixture of porous concrete compare to the whole volume of concrete. As for the composition of the aggregate weight of each individual specimen can be seen in Tabel 6. The selected tests were conducted on a cylindrical specimen with a diameter of 4 cm and height of 6.5 cm. The calculation of porosity based on Void in Mixtures (VIM) method, the calculation and results is presented in Table 7. The average porosity of porous concrete is found to be 25.088%.

Tabel 6. The materials composition of porous concrete

% Sand	Weight (kg)			Total (kg)	Composition of Coarse Aggregater (%)	Composition of Fine Aggregater (%)	Composition of Portland Cement (%)
	Sand	Coarse aggregate	Cement				
30	0,273	2,635	0,474	3,381	77,921	8,061	14,019

Tabel 7. Concrete porosity calculation based on VIM method

Sand (%)	Number	Weight (gram)	Volume (cm^3)	Density (gr/ cm^3)	SGmix	Porosity (%)	Average Porosity (%)
30%	1	1065	526,709	2,022	2,718	25,600	25,088
	2	1094	526,709	2,077	2,718	23,574	
	3	1058	526,709	2,009	2,718	26,089	

3.2. Vertical and horizontal permeability test

Permeability testing in this study was conducted using two methods: vertical permeability and horizontal permeability, both methods using the principle of falling head permeability. The test specimen is used for testing the permeability of concrete with the diameter of 4 inches (10.16 cm) and a height of 6.5 cm. Variations of the test object are based on the type of filler, with three samples of each variety. The results of permeability measurement for the selected filled porous concrete are presented in Table 8.

Table 8. Horizontal and Vertical Permeability of the specimens

Type of Porous Concrete Specimen	Horizontal Permeability Coefficient kh (cm/sec)	Vertical Permeability Coefficient kh (cm/se)
Without filler	0,469	1,355
Natural Sand	0,364	0,15733
Volcanic Sand	0,348	0,38
Soil	0,307	0,204

3.3. The rate of absorption

Testing of the rate of absorption in this study was conducted using the principle of falling head permeability. The test object used for this test is a concrete plate with a size of 60cm x 60cm x 6,5cm for three samples of each variety. Variations of the test object are based on the type of filler with the similar sub grade condition.

Table 9. The rate of absorption

Type of Porous Concrete Specimen	The Rate of Absorption kh (cm/sec)	Vertical Permeability Coefficient kv (cm/sec)
Without filler	1,1467	1,355
Natural Sand	0,147	0,15733
Volcanic Sand	0,337	0,38
Soil	0,249	0,204

3.4. Compressive strength test

Compressive strength testing is carried out when the specimen has reached the age of 28 days using Compression Testing Machine to get the maximum load. From the test results showed in Table 10, it can be seen that the compressive strength of the filled porous concrete with soil , sand and volcanic sand contributed to an

increase in the compressive strength though not significantly. Increasing the maximum compressive strength is obtained by filling the cavity with volcanic sand.

Table 10. The Compressive Strenght of Filled specimens

Type of Porous Concrete Specimen	Average Compressive Strength (fc') (MPa)
Without filler	5,19
Natural Sand	5,28
Volcanic Sand	5,71
Soil	5,62

The test results on the porous concrete compressive strength test specimen cylinder with a diameter of 15cm and 30cm height at 28 days of curing are presented in Table 10. It could be identified the influence of the type of filler on the filled porous concrete compressive strength even though not significantly. The slight increase of porous concrete compressive strength value is obtained by filling the voids with volcanic sand. This is due to the volcanic sand has a good gradation so that result in reduced the porosity thereby increasing the compressive strength of porous concrete.

4. Conclusion

1. Filling the voids with soil, natural sand and volcanic sand lead to reduced permeability of porous concrete. Comparison of horizontal permeability of porous concrete filled with soil, natural sand and volcanic sand is 0.364 cm/sec; 0,348 cm/sec and 0.307 cm/sec, respectively. While the vertical permeability of porous concrete filled with soil, natural sand and volcanic sand is 0,157 cm/sec; 0.38 cm sec; 0.204 cm/sec, respectively. The hight permeability is achieved by filling the voids with river sand because the river sand has a larger grain size so that the voids are remain greater.
2. The rate of absorption in porous concrete achieved the faster rate by filling the voids with natural sand, which is 3,337 cm/sec, while for the one filled with soil is 0.147 cm/sec and volcanic sand is 0,249 cm/sec. So that in term of rate of absorption, the river sand is a priority.
3. Filling the voids of porous concrete, slightly increase the compressive strength of porous concrete. When the compressive strength is compared to the unfilled porous concrete of 5.19 MPa, the compressive strength of porous concrete filled with soil, natural sand and volcanic sand provide an additional value of 5.62MPa, 5,28MPa and 5,71Mpa, respectively. So it can be used as a porous concrete pavement for low traffic such as walkways, parks, road shoulders and parking lots.
4. The use of porous concrete pavement as environmentally friendly in addition to being able to pass the water, also reduces the cost of material requirements. For porous concrete using only 30% of the sand require compared to conventional concrete and require only 300 kg of cement per m^3 of concrete.

References

[1] Paul D. Tennis, Michael L. Leming, and David J. Akers. . 2004. Pervious Concrete Pavements. Portland Cement As- sociation
[2] Wanielista, M., M. Chopra, J. Spence, and C. Ballock. 2007. Hydraulic Performance Assessment of Pervious Concrete Pavements for Stormwater Management Credit. Final Report.Florida Department of Transportation, Talla- hassee.
[3] Chopra, ManojWanielista Marty, Craig Ballock, and Josh Spence. 2007. Construction and Maintenance Assess-ment of Pervious Concrete Pavements. Stormwater Management Academy. University of Central Florida Orlando, FL 32816.
[4] Rochim, R., Setyawan, A., & Sarwono, D. (2015). Pengaruh Pengisian Rongga Pada Perkerasan Beton Berpori Terhadap Permeabilitas, Kecepatan Resapan Dan Kuat Tekan. *Matriks Teknik Sipil*, *3*(1).
[5] National Ready Mixed Concrete Association 888-84nrmca.2004. ,Pervious Concrete. Concrete in practice. 888-84NRMCA
[6] ACI 522-010. (2010). Report On Pervious Concrete. American Concrete Institute Committee 522
[7] Amerikan Society for testing and materials.1918. Concrete And Material Agregates (Including Manual Of Agre- gates And Concrete Testing).ASTM. Philadelphia.

[8] Prabowo, D. A. (2014). Desain Beton Berpori Untuk Perkerasan Jalan Yang Ramah Lingkungan (Porous Concrete Pavement Design For Environmentally Friendly Pavement). *Matriks Teknik Sipil*, *1*(2).

Available online at www.sciencedirect.com

ScienceDirect

Procedia Engineering 00 (2017) 000–000

Procedia Engineering

www.elsevier.com/locate/procedia

Sustainable Civil Engineering Structures and Construction Materials 2016, SCESCM 2016

The evaluation of functional performance of national roadway using three types of pavement assessments methods

Suryoto[a], Dendy Paramaartha Siswoyo[b], Ary Setyawan[a,*]

[a] *Roadmate Research Group UNS, Jl. Ir. Sutami 36 A, Surakarta 57126, Indonesia*
[b] *Indonesian Highway Agency, Sragen Central Java, Indonesia*

Abstract

The road section of Palur-Sragen-Mantingan categorized as a national road and serve 43.00 km long arterial road, is the part of the middle lane that connects the important cities in Java Island. The damage that frequently occurs will certainly affect the safety and comfort of road users. Road surface condition assessment is one step to determine the type of program evaluation needs to be done. This study aims to determine the functional condition of the road by three methods and to assess the closeness of the relationship between these three methods. The descriptive study is carried out to conduct the comparability of the road condition assessment data resulted from three methods for analyzing the results of the assessment of road conditions between the years of 2011-2013. The assessment method of road conditions consists of the International Roughness Index, the Pavement Condition Index and the Surface Distress Index. The correlation between these methods were obtained from the Pearson correlation analysis based on *CurveExpert* program. The results showed that the linear regression analysis between the methods of IRI and PCI showed the value of PCI=0.966+10.919IRI, it means there is a positive correlation between the two methods and the r value is 0.976 indicates a very close correlation between the two methods. IRI and SDI method show the value of SDI=32.684+3.355IRI, it means a positive correlation between the two methods and the r value is 0.203 indicates a poor relation between the two methods. PCI and SDI method show the value of SDI=18.023+0.592PCI, it means there is a positive correlation between the two methods and the r value is 0.381 indicates a poor relation between the two methods. Limited from this research, the conclusion could be drawn that the different method of functional measurements could potentially result in the different pavement index, consequently the different decision for pavement and rehabilitation scheme.

Peer-review under responsibility of the organizing committee of SCESCM 2016.

Keywords: road assessment; functional performance; IRI; PCI; SDI.

* Corresponding author. Tel.: +62-815-485-585-90; fax: +62-271-634-524.
E-mail address: arysetyawan@staff.uns.ac.id

Peer-review under responsibility of the organizing committee of SCESCM 2016.

1. Introduction

Road damage that occurred in various regions is now a highly complex problem. The damage resulted in a longer travel time, congestion, traffic accidents and others. Accumulation of losses has an impact on the global economic development. Previous research has been done to relate the PCI and the service life of pavement [1] as well as the correlation between pavement distress and the rate of traffic emission [2].

The pavement damage could be caused by several conditions such as the age of the road serviceability has been passed, a puddle of water on the road surface, excessively traffic load (overload), improper planning, poor implementation o road monitoring. Besides the lack of maintenance costs, delays in financing, improper handling, and accelerating climate change and road damage.

The condition of the road needs to be carried out periodically both structural and non-structural conditions. Examination of the non-structural (functional) road conditions, have an objective to examine the roughness (texture), and skid resistance of the surface road. One of the stages in the evaluation of the road surface condition is to do an assessment of the existing condition of the road. The road condition value will be used as a reference to determine the type of maintenance or rehabilitation program that should be done, whether it is a reconstruction; periodic maintenance; or routine maintenance.

The selection of proper road maintenance is performed by assessing the condition of the road surface based on the type of damage, which is determined visually and using measuring devices NASRAA. There are several methods of approach that can be used in assessing the condition of roads, of which three of them are methods of IRI (International Roughness Index), PCI method (Pavement Condition Index) and the method of Highways (Surface Distress Index). Thus, this study is to develop the relationships between the flatness values (IRI) to the value of damage to the road surface (PCI) and the method of Highways (SDI).

The objective of this study is measuring the conditions of the national road segment Palur - Sragen - Mantingan and analyzing the correlation between the methods of the Pavement Condition Index, Surface Distress Index, and International Roughness Index.

2. Functional pavement condition assessment

Basically road conditions are divided into two performances, functional and structural performances. The functional assessment of road conditions are related into the driver comfort of riding, the methods of assessment are present serviceability index, pavement surface friction, pavement condition index, and wet-weather safety index. Meanwhile, the structural performances are associated with pavement structure to accommodate the fire traffic. Both performances indicate for long life pavement that define as no significant deterioration will develop in the foundations or the road base layers provided that correct surface maintenance is carried out. This definition implies that all pavement layers, except the road surface layer are considered as permanent pavement layers and common distress mechanisms should, in principle, be eliminated completely [3]. Ideally, both performance assessments should be carried out to ensure that long life pavement could be achieved for better road services. However, in Indonesia the common use to measure the pavement condition is functional assessment, even though some methods are sometimes carried out simultaneously.

2.1. Pavement Condition Index

An assessment of the pavement condition is the most important aspect in terms of determining the maintenance and rehabilitation schemes. To assess the condition of the pavement, first necessary to determine the distress type, distress quantity and distress severity level. Pavement Condition Index (PCI) is a scoring system based on the type of pavement conditions, the severity level of damage that occurred, and then can be used as a reference in maintenance effort [4].

2.2. International Roughness Index

International Roughness Index is the unit used to determine the condition of a road surface [4]. IRI is used as an indicator of the level of the ratio of surface roughness and quality of the road pavement [5]. One of the data used to determine the value of roughness of the road to use the NASRAA (National Association of Australian State Road Authorities) device to get the value of roughness of the road that will be presented by the International Roughness Index (IRI).

2.3. Highway method

According to the method adopted by The Highway Agency, there are only four elements used as support data to calculate the value of Surface Distress Index: Percentage of extensive cracking, the average crack width, the number of potholes/km and average of rutting [6,7].

2.4. The correlation of the three methods

Correlation analysis is a statistical method used to determine the degree of linear relationship between two variables. The more obvious linear relationship (straight line), the stronger or high degree of straight-line relationship between two variables [8,9]. The size of the degree of relationship this straight line is called the correlation coefficient. Regression analysis is a statistical method used to determine the possible forms of relationship between two independent variables (x) and dependent variable (y). The main objective determination of this method is to predict or estimate the value of one variable (y) in conjunction with the other variable (x).

3. Method

The research location is in the region of Central Java province, precisely in the region of Palur- Mantingan under the management of Local Commitment Officer (*PPK*) as presented in Fig. 1.

Fig. 1. Location of Research at Palur-Mantingan Segment of National Roadway

The method used in this research is descriptive research to perform the road condition assessment and the comparison of data generated from three methods for analyzing the correlations between the results. The data collected from the road assessment conditions between the years of 2011 to 2013.

Analysis to carry out an assessment of road conditions with the PCI method (Pavement Condition Index) namely; to determine the value of the condition of the surface layer of a road section which amount is influenced by the state of the pavement surface caused by the damage. Testing analysis of the road surface condition data using NAASRA Roughness-meter, data from IRI measuring devices NASRAA obtained by IRI roughness scale. Analysis methods of Highways to survey road conditions based on calculation of the value of SDI categories of use or damage with reference to the categories of damage for four elements used as support to calculate the value of SDI: percentage of extensive damage, the average crack width, the number of holes / km and an average depth of rutting.

Analysis of the data has been obtained from measurements on the existing road, whether it is the value of PCI, SDI and the value of IRI analyzed with the help of software *CurvesExpert*, that will then produce a model equation of correlation and regression between IRI with PCI, IRI with SDI and PCI with SDI. Heteroscedasticity test by using scater plot was then performed to detect the deviations from the terms of the classical assumptions on the regression model, in which the regression model must meet the absence of heteroscedasticity [10−12]. These three methods can then be obtained a linear equation and the relationship between the two variables.

4. Results and discussion

4.1. International Roughness Index performance

Initial data retrieval for road roughness values are taken every 100 meters distance to each point. IRI value on average at each road of Palur-Mantingan 2011-2013.

Table 1. The International Roughness Index Performances

No	Segment	Street Name	STA	Length (km)	Width (m)	IRI		
						2011	2012	2013
1	058	Palur-Bts Kota Sragen	5+800 – 25+900	20.100	14-7-14	3.82	4.02	5.56
2	058-11	Lingkar Utara Barat Sragen	0+00 – 3+673	3.673	7	8.90	5.02	5.45
3	058-12	S. Parman	3+673 – 6+500	2.827	7	8.55	4.25	4.53
4	058-13	Lingkar Utara Timur Sragen	6+500 – 10+600	4.100	7	4.48	4.92	5.38
5	059	Bts Kota Sragen-Mantingan	33+85 0 - 46+150	12.300	14-7, 14-7	3.82	4.08	5.38
						5.81	4.45	5.45

The IRI of Palur-Mantingan road section in 2011gave an average value of 5.81 m/km, indicates a fair road conditions, meanwhile in 2012 the value of IRI is 4.45 indicates a better road conditions, and then in 2013 the value of IRI 5.45 m/km indicates slightly decrease condition. Table 1 shows that IRI values indicate that the average roughness condition for Palur- Mantingan segment in 2011 was under moderate conditions, whereas the year 2012 was in good condition and in 2013 was under moderate conditions. These values could be used as a recommendation or assessment of road condition, so that the right treatment could be defined accordingly.

4.2. Pavement Condition Index performance

Based on data that have been collected from the existing road, subsequently, analyzed to obtain recapitulation of PCI value for Palur- Mantingan segment as presented in Table 2.

Table 2. The Pavement Condition Index Performances

No	Segment	Street Name	STA	Length (km)	Width (m)	PCI		
						2011	2012	2013
1	058	Palur-Bts Kota Sragen	5+800 – 25+900	20.100	14-7-14	44	47	46
2	058-11	Lingkar Utara Barat Sragen	0+00 – 3+673	3.673	7	51	63	55
3	058-12	S. Parman	3+673 – 6+500	2.827	7	60	50	60
4	058-13	Lingkar Utara Timur Sragen	6+500 – 10+600	4.100	7	49	52	51
5	059	Bts Kota Sragen-Mantingan	33+85 0 - 46+150	12.300	14-7, 14-7	45	51	55.70
						49.80	52.60	53.43

From the results in Table 2 that each road segment has a value of PCI in accordance with the respective road conditions. In the year of 2011 to 2013, the Palur-Bts.Kota Sragen segment with a PCI value of 44, 47 and 46, respectively, indicates that the segment has poor condition with only small change every year. In the same years, at the Sragen West North Rim segment with a PCI of 51,63,55 indicates a fluctuating condition from poor to fair condition depend on the maintenance activity. At S.Parman segment, over the three years showed the PCI about60,50,60, respectively, it indicates a fluctuating condition from fair to poor conditions. At the Sragen East North Rim to the road condition index over three years were 49, 52,41 indicate a poor condition. At Bts. Kota Sragen-Mantingan segment with an index of 45, 51 and 55.7 over the three years indicate an increase of road condition from poor to fair.

On average, Table 2 shows that the value of PCI at Palur-Mantingan segment in 2011 and 2012 under poor conditions, whereas the year 2013 increase to the fair condition.

4.3. Surface Distress Index performance

The calculation result based on Highways Method [8] using the calculation of SDI (Surface Distress Index) at every 100 meters of Palur-Mantingan segment, the pavement distress assessed are: percentage of extensive cracking, the average crack width, the number of holes / km and an average depth of rutting. The results are presented in Table 3.

Table 3. The Surface Distress Index Performances

No	Segment	Street Name	STA	Length (km)	Width (m)	SDI		
						2011	2012	2013
1	058	Palur-Bts Kota Sragen	5+800 – 25+900	20.100	14-7-14	65	45	40
2	058-11	Lingkar Utara Barat Sragen	0+00 – 3+673	3.673	7	55	30	25
3	058-12	S. Parman	3+673 – 6+500	2.827	7	75	80	20
4	058-13	Lingkar Utara Timur Sragen	6+500 – 10+600	4.100	7	65	40	50
5	059	Bts Kota Sragen-Mantingan	33+85 0 - 46+150	12.300	14-7, 14-7	75	40	45
						67	47	36

From the results in Table 3, it can be seen that each road has a value of SDI according to the road conditions respectively. The road distress has been fluctuating changed according to the pavement maintenance and rehabilitation activities. The performances of three years at Table 2 show that the value of the average of SDI at Palur- Mantingan segment in 2011 under moderate conditions, whereas in the year of 2012 the pavement performed good condition as well as in the year of the year 2013. It seems that the routine and periodic maintenance resulted in better pavement condition.

4.4. The correlation between International Roughness Index and Pavement Condition Index

Fig. 2 shows the linear regression fit line, dots spread randomly and a particular pattern is not clear performed. This means that the *heteroscedasticity* is not happening in regression models, so the regression model could be used to predict the value of IRI based on its independent variable input on PCI.

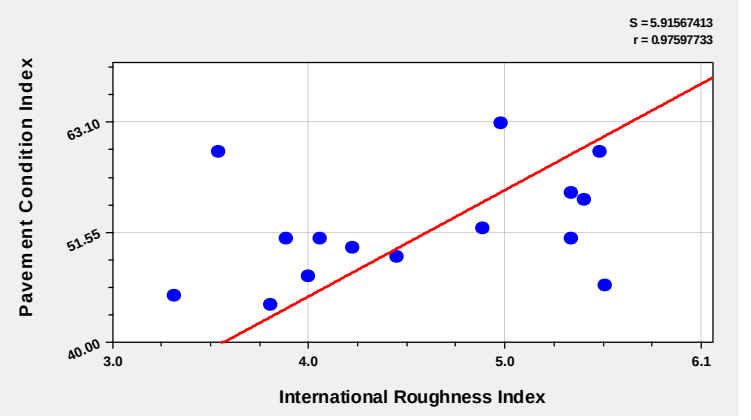

Fig. 2. The correlation between PCI and IRI

The correlation of the International Roughness Index and Pavement Condition Index shows a curve with y=a+bx where y=0.966+10.919x, where y is the value of PCI, constant value of a, the regression coefficient of b, and x is the value of IRI. Pearson correlation analysis of the curve indicates the value of r = 0.976 based on the correlation coefficient so the values have a strong correlation. While the value of the standard error number of regression model to predict the value of y is 5.915.

4.5. The correlation between SDI and IRI

Fig. 3 shows the linear regression line, the dots form a regular pattern of spread later narrowed. This means that the *heteroscedasticity* in regression models is not happening, so the regression model used to predict the value of Surface Distress Index based on its independent variable input of IRI.

The correlation between the International Roughness Index and Surface Distress Index is presented by the linear fit if by the curve of y=a+bx where y=32.684+3.355x, where y is the value of SDI, a = a constant value, b = regression coefficient, and x is the value of IRI. Pearson correlation analysis of the curve indicates the value of r = 0.203 based on the correlation coefficient table has a poor correlation. While the value of the standard error number of regression model to predict the value of y is 22.296.

4.6. The correlation between SDI and PCI

From 4 shows the linear regression line, the dots spread randomly and do not form a particular pattern is means that the *heteroscedasticity* is not happening in the regression model, so the regression model can be used to predict the value of PCI based its independent variable input of SDI.

The correlation of the Pavement Condition Index and Surface Distress Index is a linear curve fit shows the y=a+bx, where the value of y=18.023+0.592x, where y= the value of SDI, a = a constant value, b = regression coefficient, and x = the value of PCI. Pearson correlation analysis of the curve indicates the value of r = 0.381, based on the correlation coefficient table has a poor correlation. While the value of the standard error number of regression model to predict the value of y is 21.033.

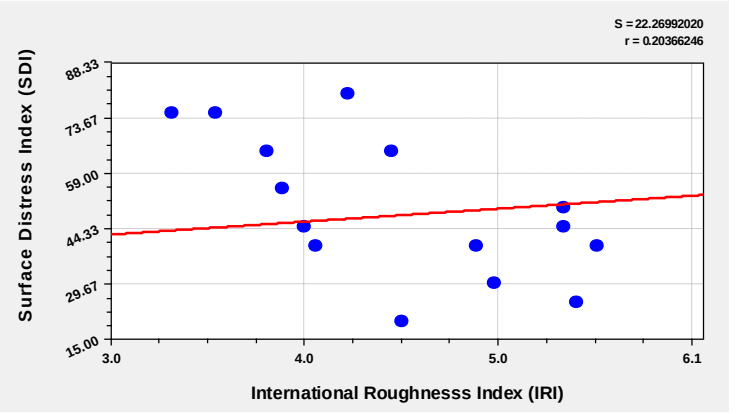

Fig. 3. The correlation Between SDI and PCI

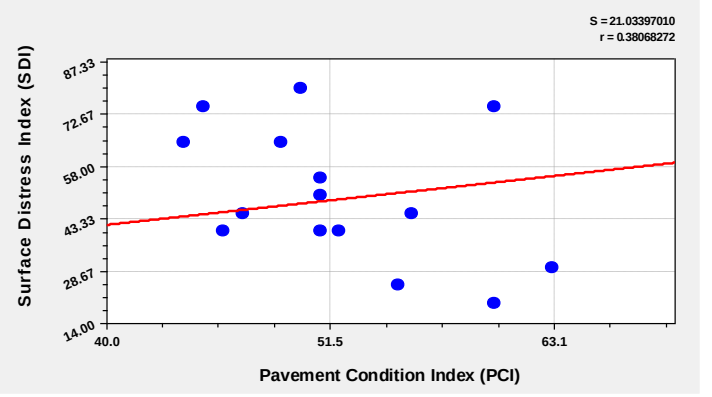

Fig. 4. The correlation of PCI and SDI

4. Conclusions

Based on the results of the analysis, conclusions could be drawn as follows :

- The results of IRI indicate that the average roughness condition for Palur- Mantingan segment in 2011 was under moderate conditions, whereas the year 2012 was in good condition and in 2013 was under moderate conditions. PCI at Palur-Mantingan segment in 2011 and 2012 under poor conditions, whereas the year 2013 increase to the fair condition. The average of SDI at Palur- Mantingan segment in 2011 under moderate conditions, whereas in the year of 2012 the pavement performed good condition as well as in the year of the year 2013. The results of the functional pavement condition survey indicate that the use of three methods resulted in different condition performances for the existing pavement surveyed.
- The linear fit for correlation between the methods show that the correlation between IRI and PCI methods showed r = 0.916 indicate a strong relationship. However, the linear fit for correlation between IRI and SDI demonstrate the value of r = 0.203 and the correlation between PCI and SDI demonstrate the value of r = 0.38, both r values indicate poor correlations.

References

[1] Setyawan, A., Nainggolan, J., & Budiarto, A. (2015). Predicting the Remaining Service Life of Road Using Pavement Condition Index. *Procedia Engineering,125*, 417-423.
[2] Setyawan, A., & Kusdiantoro, I. (2015). The Effect of Pavement Condition on Vehicle Speeds and Motor Vehicles Emissions. *Procedia Engineering, 125*, 424-430.
[3] Nantung, Tommy, et al. "Implementation initiatives of the mechanistic-empirical pavement design guides in Indiana." *Transportation Research Record: Journal of the Transportation Research Board* 1919 (2005): 142-151.
[4] Shahin, Mohamed Y. *Pavement management for airports, roads, and parking lots*. Vol. 501. New York: Springer, 2005.
[5] Utomo, SHT. (2001). Kajian Kondisi Perkerasan Jalan Arteri Di Kabupaten Sleman Menggunakan Cara Pavement Condition Index. *Media Teknik No. 2 Tahun XXIII Edisi Mei 2001. No. ISSN 0216-3012.*
[6] Christady, H., 2009, Pemeliharaan Jalan Raya, *Gadjah Mada University Press, Yogyakarta.*
[7] Djakfar L.dkk (2013), Evaluation of road roughness and road deterioation, *Jurnal Transportasi Vol. 13 No. 3 Desember 2013.*
[8] Bolla, M.E., 2012, Perbandingan Metode Bina Marga dan Metode PCI (*Pavement Condition Index*) dalam Penilaian Kondisi Perkerasan Jalan, *Universitas Nusa Cendana, Kupang, Tesis: Tidak Diterbitkan.*
[9] Kim, S. H. and Kim, N., 2006, Development of Performance Prediction Models in Flexible Pavement Using Regression Analysis Method, *Journal of Civil Engineering, KSCE, Vol. 10, p. 91-96.*
[10] Minarti, E., dkk (2014), Pengamatan Kerusakan Jalan dari Nilai Surface Distress Index (SDI) dan Nilai International Roughness Index. *(Studi Kasus: Jalan Nasional Ruas Calang-Teunom Km. 150 s/d Km. 157), Universitas Syiah Kuala, Aceh*
[11] Suwardo. Dkk (2004), Tingkat Kerataan Jalan Berdasarkan Alat *Rolling Straight Edge* Untuk Mengestimasi Kondisi Pelayanan Jalan (PSI dan RCI), Simposium VII FSTPT, *Universitas Katolik Parahyangan, 11 September 2004.*
[12] Hartono, 2009, SPSS 16.0 Analisis Data Statistika dan Penelitian, *Pustaka Pelajar, Yogyakarta.*

Available online at www.sciencedirect.com

ScienceDirect

Procedia Engineering 00 (2017) 000–000

Procedia Engineering

www.elsevier.com/locate/procedia

Sustainable Civil Engineering Structures and Construction Materials 2016, SCESCM 2016

Fairway traffic capacity in Indonesia

Edi Kadarsa*, Harun al-Rasyid S. Lubis, Ade Sjafruddin, Russ Bona Frazila

Department of Civil and Environmental Engineering, Bandung Institute of Technology, Bandung-40116, Indonesia

Abstract

Problems of congestion and road damage due to traffic density and excessive vehicle loads can be solved by shifting the traffic load of the highway to river transport. For regional areas in Indonesia, which are traversed by rivers with water levels and width navigable by various types of vessels, river transport can be the main alternative transportation of goods other than highways. South Sumatra is one of the provinces in Indonesia which has a network of rivers that can be traversed by large cargo vessels. Musi River with its tributaries network is the main fairway in South Sumatra where water levels of the river are affected by the environment, especially tides, seasons and sedimentations. This environmental influences have led to vessels being unable to sail safely and smoothly all the time. Therefore, it is deemed necessary to determine the fairway capacity as a riverway performance indicator that takes into account environmental influences, especially tides. Various research on capacity of inland waterways previously conducted have not specifically considered the effect of tides.

Peer-review under responsibility of the organizing committee of SCESCM 2016.

Keywords: fairway, capacity, jukung, barge, tides ;

1. Introduction

Problems of congestion and road damage can be reduced by shifting traffic load from highway to river transport. For areas traversed by wide and deep rivers, water transport can be a major alternative to transport goods in addition to road, considering the availability of rivers that can be directly passed by large vessels. Some countries in Asia, such as China, Vietnam and India, have utilized inland waterway transport (rivers and canals) and proved to have given a great contribution to the development of the economy of the respective country [1].

Rivers in Indonesia are mostly natural, i.e. affected by the environment, namely tides, sedimentations and seasons. The environmental influences cause the water levels to vary and have different velocities and directions,

* Corresponding author.Tel.: +0-000-000-0000 ; fax: +0-000-000-0000 .
E-mail address: aedikadarsah@gmail.com

Peer-review under responsibility of the organizing committee of SCESCM 2016.

their currents fluctuate all the time, causing changes in the type of sailing vessels. Fairway capacity is needed to determine the quantity of goods that can be transported by vessels through a segment of fairway at certain times, i.e. neap, transition or tide.

Research about the capacity of inland waterways have been conducted by previous researchers. Peterson (1955) [2], Fuji and Tanaka (1971) [3], Huang, Gan and Liu (2011) [4], Fisher, Treiber and Sohngen (2014) [5] conducted fairway capacity research with empirical and simulation approaches. These studies focused on the characteristics of river, the types of vessels, and the environment that are very different from those in Indonesia. The approach of simulation has been performed by Frima (2004) [6], Yeo, Roe and Soak (2007) [7], Guo Song, Wang and Tang (2010) [8], Qu and Meng (2012) [9] in the coastal channels where fairway capacity is affected by port service levels and strict regulations. Another simulation approach has been undertaken by Lin-ying (2011) [10] on river network based Gap Acceptance Theory. All the methods developed by previous researchers did not specifically consider tidal influences that happen every day.

The research objective is to determine a method to calculate the fairway capacity in Indonesia. This research was conducted on Musi River that represents the characteristics of the rivers used as fairway in Indonesia. Musi River has sufficient depth and width navigable by barges and jukungs as the main goods transport through rivers in Indonesia. Similar with other rivers, River Musi is influenced by tides, which has led to the difference in vessels traffic flows [11, 12].

2. Methodology

2.1. Basic theory of traffic flow

Within the basic framework of the traffic flow theory it is stated that macroscopic analysis is conducted on a group of vehicles, while microscopic analysis is carried out individually [13]. Determination of the capacity can be done by either macroscopic or microscopic analysis.

Table 1. Framework for Fundamental Characteristics of Traffic Flow

Traffic Characteristics	**Microscopic**	**Macroscopic**
Flow	Time Headways	Flow Rates
Speed	Individual Speeds	Average Speeds
Density	Distance Headways	Density Rates

(Source: [13])

Traffic flows of rivers in Indonesia are generally low and therefore it is difficult to use macroscopic approaches in determining the fairway capacity. Meanwhile, microscopic approach is made for vehicles that move individually, more suitable for determining the fairway capacity in Indonesia. The type of vessels sailing in Musi fairway varies depending on water levels. The diversity of the types of vessels that can sail there has caused the varied capacity of segments of the fairway. In order to avoid data collection and capacity calculation from being performed over and over again, it is necessary to set a standard vessel unit. The standard vessel unit is defined as the number of standard vessels that replace the other types of vessels in the traffic flow to suit conditions of certain fairways. The effect of the different types of vessels in the traffic flow is converted into standard vessel unit using influence factor (fv). In this research, an empty barge of 500 tons is set as the standard vessel based on the consideration that the vessel is the most widely used to freight transport on inland fairway in Indonesia. The barges were produced in the factory with such strict quality standards that both the shape and size are relatively similar. In addition, the standard vessel is set empty so that vessels carrying cargo with varying loads can be easily converted.

Research on vessel conversion coefficients was performed by Guo, Song, Wang and Tang (2010) [8] by comparing the fairway capacity sailed by a certain type of vessels, i.e. the type of standard vessels. The method has been adapted and used for fairway traffic so that the value of the influence factor can be determined.

2.2. Fairway capacity approach in this study

The interaction between two adjacent sailing vessels in the fairway is analogous with that of two adjacent vehicles moving on the road. On a congested lane which makes it impossible to overtake, vehicles are forced to follow the lead vehicle. In this condition, the following vehicle will set the distance to the lead vehicle in such a way that when the lead vehicle decelerates, there is still space for the following vehicle to come to a stop without collision.

The reaction time (T) of the driver of the following vehicle is started from the time the lead vehicle starts to decelerate until the following vehicle realizes the changing speed of the lead vehicle and subsequently decides to decelerate.

The position of the adjacent vehicles is represented by n for the lead vehicle and n + 1 for the following vehicle. According to Sutomo (1992) [14], the position of the vehicles after the lead vehicle has begun to decelerate can be explained by Figure 1 below :

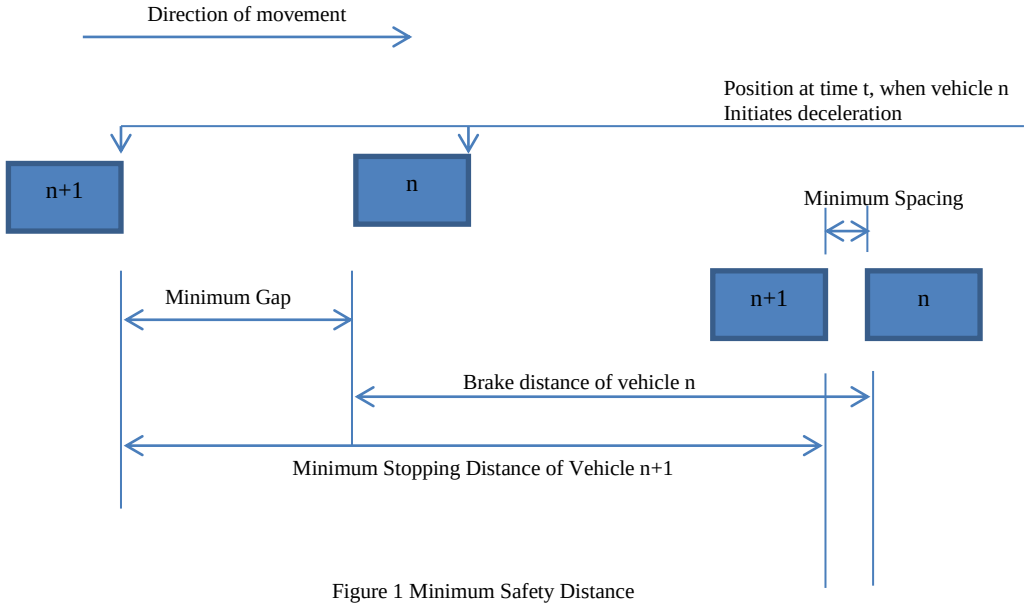

Figure 1 Minimum Safety Distance
(Source: [14])

$$\text{Brake Distance} = (V_n(t))^2 / 2.a_m \quad (1)$$

$$\text{Minimum Stopping Distance} = T.V_{n+1}(t) + (V_{n+1}(t))^2 / 2.a_m \quad (2)$$

Where:
$V_{n+1}(t)$ = speed of vehicle n+1 at time t
$V_n(t)$ = speed of vehicle n at time t
a_m = maximum deceleration.
T = reaction time

Theories about distance between two adjacent vehicles that are moving when the lead vehicle starts to decelerate until it stops can be used to determine the distance headway of the two adjacent vessels. In this research, the distance headway is determined by the following equation:

$$h = MSD + MSp + L \quad (3)$$

Where:
h = Distance Headway
MSD = Minimum Stopping Distance
MSp = Minimum Spacing
L = Length of Vehicle

The minimum stopping distance is the distance required by the following vessel to stop with maximum deceleration starting from the time the vessel's captain sees a disturbance in front, decelerates, until the vessel actually stops. The minimum spacing, on the other hand, is the distance between the front bumper of the following vessel and the rear bumper of the lead vessel after both vessels stopped.

In general, the relationship between speed and distance headway can be observed and studied using statistical analysis, namely Model Greenshield. In this model, the density is determined by Equation 4:

$$D = 1000/h \quad (4)$$

Where:
D= Density (ships/m)
h= Distance Headway (m)

Furthermore, the traffic flow is determined by Equation (5) and the flow (Q) is obtained through the curve relationship between traffic flow and speed (V). Capacity is the maximum flow obtained from the simulation of different speeds.

$$Q = V. D \quad (5)$$

Various types of vessels are converted into a standard vessel unit by multiplying a certain type of vessels with an influence factor. The influence factor of a type of vessel is obtained by comparing the capacity of the fairway traversed by the certain type of vessels with the standard type of vessels.

$$fpV = CV/CS \quad (6)$$

Where:
fpV = Influence factor of a type of vessel
CV = Fairway capacity sailed by a certain type of vessels on certain conditions.
CS = Fairway capacity sailed by a standard type of vessels on certain conditions.

2.3. Survey data

Fairway capacity is determined by the mathematical relationship between traffic flow, density and vessel speed (Equation 5). To determine the density some parameters are required, i.e. minimum stopping distance for a wide range of speeds, minimum spacing and length of the vessel as indicated by Equation 3 and 4.

There are two types of vessels determined in this study, i.e. barge and jukung with the following specifications:

Table 2. Vessel Specifications

Specification	**Types of vessel**	
	Barges	**Jukung**
Length	55 meter	20-24 meter
Width	10 – 12 meter	5 – 6 meter
Draft	2,4 – 2,7 meter	1,1 meter
Load Capacity	500 ton	60 – 80 ton

Specification	Types of vessel	
	Barges	**Jukung**
Machine Power	400 – 450 PK	300 – 350 PK
Maximum Speed	6 knot	12 knot

(Source: [16])

The maximum speeds of jukung and barge shown in Table 2 are the maximum speed of the vessel with fuel consumption still relatively low. When the vessels sail at a speed higher than the maximum speed as shown at Table 2, the machine power is going to be extremely larger, impacting the increase in fuel consumption.

Survey data for minimum stopping distance and minimum spacing were obtained through interviews with the vessels' captains, subsequently validated by the test vessels. Survey data show some jukungs moving up to a speed of 36 km/h (20 knot) and barges moving at up to a speed of 20 km/h (11 knot). In contrast to the barges which limit the speed up to 6 knots and only a little bit over 6 knot, there are several jukungs that sail over 12 knots. Therefore, to define minimum stopping distance of jukungs, the maximum speed that can be achieved, namely 20 knots will be used.

a **b**

Figure 2 (a) Jukung; (b) Barge

2.3.1. Minimum spacing

There are some factors affecting the minimum spacing in this research, namely river stream, position of two types of adjacent vessels and whether vessel is laden or empty. At high tide, there are water streams moving upstream. Conversely, during the neap, the water streaming upstream at high tide will be pulled back as downstream or towards the estuary. Therefore, in this research, the tidal effects are considered as follows:

- Tide conditions: vessels sailing downstream represent vessels sailing against the river stream, while the vessels sailing upstream represent vessels sailing in the direction of the stream.
- Transition conditions: calm river stream conditions
- Neap conditions: the opposite of tidal conditions.

There are two types of vessels in this study and the possible positions of the two stopping vessels are as follows:

- Jukung – Jukung
- Jukung – Barge
- Barge – Barge
- Barge - Barge

Interviews were conducted with barges' captains and jukungs' captains to collect the minimum spacing data. There are only a few number of barges and jukungs usually sailing in Musi fairway hence the number of the vessels

captains interviewed was not statistically counted; it depends on as many as found in the study area.

Length measuring instrument (100 meters) was used to give an overview to the vessels' captain about the distance between the two adjacent stopped vessels (minimum spacing) when the interview conducted. The length measuring instrument would be pulled until the vessel's captain said the instrument length was approximately equal to the minimum spacing of the two adjacent vessels.

Furthermore, the interview data were validated by the test vessels. The procedures performed on the test vessel are as follows:

- Vessels' captains were commanded to stop behind the vessel (jukungs or barges), parking without turning off the machine at a distance as close as possible but still safe from the risk of collision. Experiments were conducted using laden and empty vessels at 10 -12 a.m. in neap conditions for two different flow directions. Survey data collection for transition conditions was conducted at the Port of Palembang at 16:00 to 17:00 pm.
- Other surveyors measured the minimum spacing of the two adjacent vessels. The surveyors used motor boats and GPS to do the measurement.

2.3.2. Minimum stopping distance

Unlike the minimum spacing that is not influenced by the vessel speed, the stopping distances are affected by river stream, type of vessel, laden vessel or empty and vessel speed (ground speed); thus, it resulted in difficulties when the survey was conducted. It was difficult for the vessels' captains to imagine the vessel speed when decelerating to determine the stopping distance. Therefore, before conducting the survey, vessel speed categories were determined by the pilot survey in Musi Fairway, i.e.

- Jukung
  - Slow (4 – 6 knot)
  - Moderate (9 - 12 knot)
  - Fast (18 - 20 knot)
- Barges
  - Slow (2 – 3 knot)
  - Moderate (3 – 5 knot)
  - Fast (≥ 6 knot)

In general, the implementation of the interviews and validation using test vessels to determine the minimum stop distance is similar to the minimum spacing; the difference is only on measured vessel distances. Minimum spacing measures the distance of two vessels stopping, while minimum stopping distance measures the stopping distance after deceleration.

3 Modelling

Modeling is used to predict the minimum stopping distance for a wide range of speed and determine the traffic capacity of the fairway. The resulting models can be used to determine fairway capacity with the determined characteristics as follows: the characteristics of river, the type of vessels, and the environment must be similar with the Musi Fairway.

3.1. Spacing minimum

The results of the interview with the vessels' captains show that an empty vessel is more dangerous than a laden vessel when it stops because it is more easily carried away by river streams and wind. The difficulty the vessels' captains' face is to determine whether the lead vessel is laden or empty, causing the following vessel's captain in this

research to have assumed that the lead vessel was an empty vessel hence more dangerous. The minimum spacing of the data of two adjacent vessels featured as barge-barge and jukung-jukung are as follows:

Table 3 Vessel Minimum Spacing at Musi Fairway (in meters)

Type of Survey	Statistics	Positions and Conditions of Vessel											
		Jukung - Jukung						Barge - Barge					
		Empty			Laden			Empty			Laden		
		A1	A2	A3	A1	A2	A3	A1	A2	A3	A1	A2	A3
Interview	Maximum	6.00	4.00	6.00	5.00	3.00	5.00	43.00	50.00	50.00	40.00	35.00	40.00
	Minimum	2.00	0.50	2.00	1.50	0.50	1.00	25.00	30.00	30.00	20.00	20.00	25.00
	Mean	4.18	2.29	4.71	3.16	1.56	3.35	33.73	39.33	37.00	29.87	25.53	31.20
Test Vessel	Mean	4.50	1.00	4.00	4.00	1.00	3.50	31.00	N/A	34.00	25.00	N/A	29.00

Where:
A1: Tide Conditions A2: Transition Conditions A3: Neap Conditions

Minimum spacing data to barge-jukung and jukung-barge are not presented in this paper, because the method that used is only able to determine the fairway capacity that navigable by one type of vessel.

3.2. Minimum Stopping Distance Regression

Regression analysis was conducted to determine vessel stopping distances at various speeds for neap, transition and tide conditions. Figures 3 and 4 are examples of the results of the regression analysis conducted.

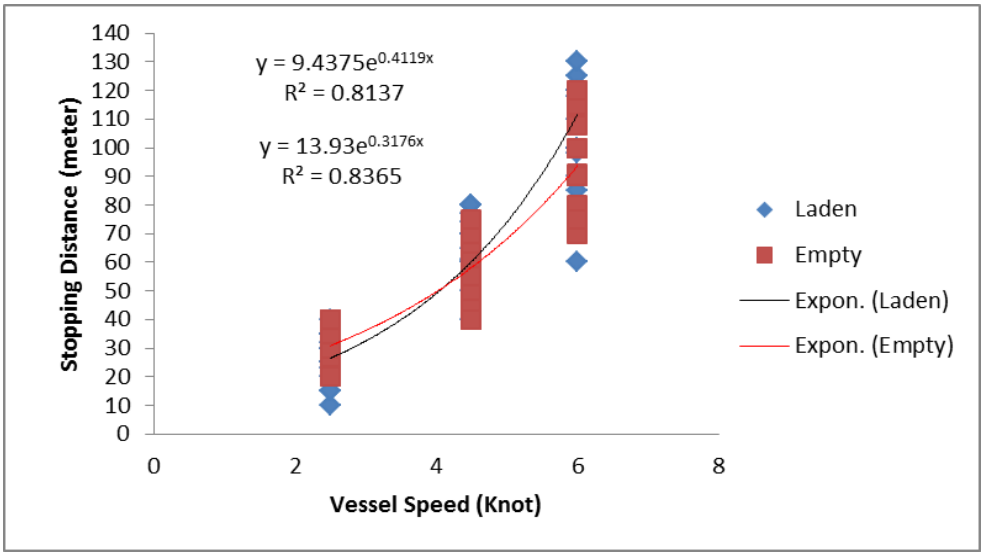

Figure 3 Regression Curve of Barge Stopping Distance on Tide Conditions

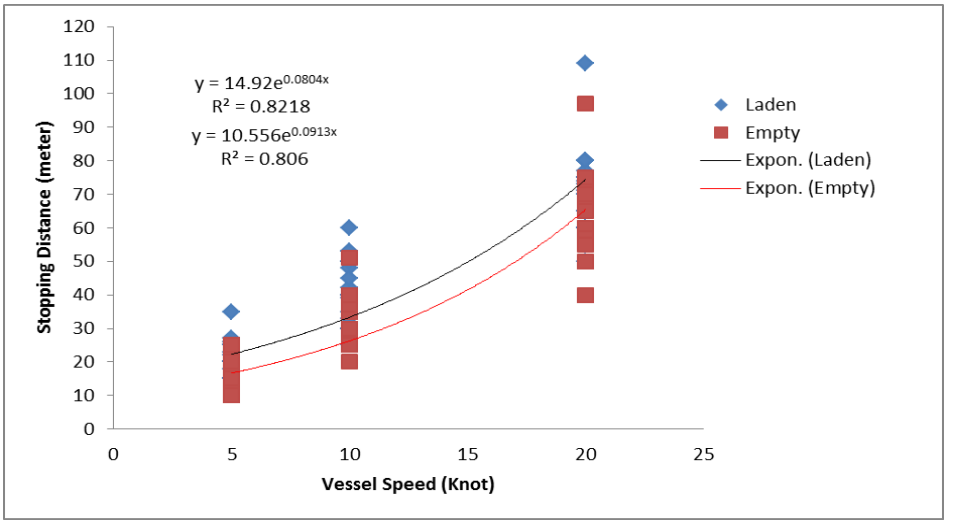

Figure 4 Regression Curve of Jukung Stopping Distance in Tidal Conditions

The survey result showed the successive vessels will sail faster when the distance between the two vessels are greater. Conversely, if the distance is closer to the vessel in front, then the vessel's speed will be reduced. This similar with the research regarding the highway traffic flow.

3.3. Fairway capacity

The traffic flow of rivers in Indonesia is small and consequently it is difficult to empirically determine the fairway capacity navigable by various types of vessels. In this research, traffic capacity was proposed to be applied to determine the capacity of the fairway navigable by one type of vessel.

The fairway capacity which is only sailed by barges and jukungs, both empty and laden, is presented in Figures 5 and 6 where the inflection point of the curve is defined as the capacity.

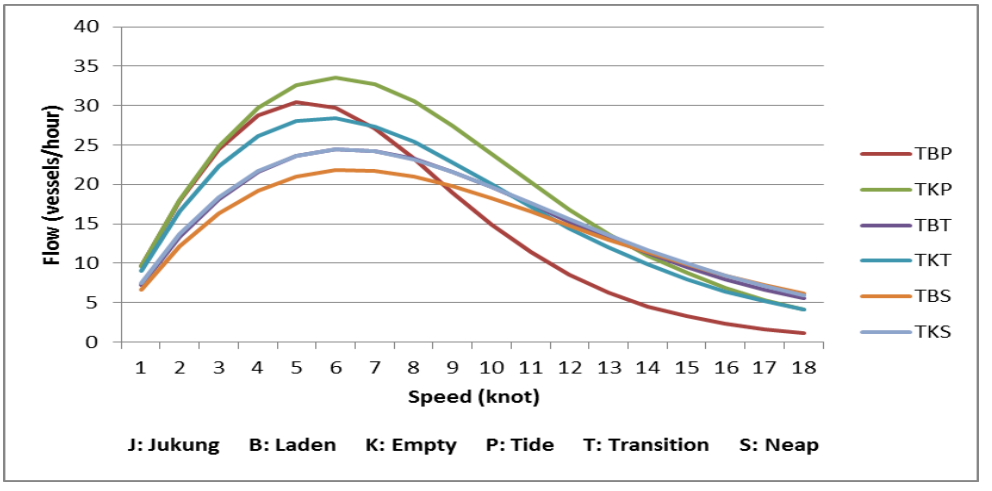

Figure 5 The Relationship between Barges Speed and Traffic Flow In Various Conditions

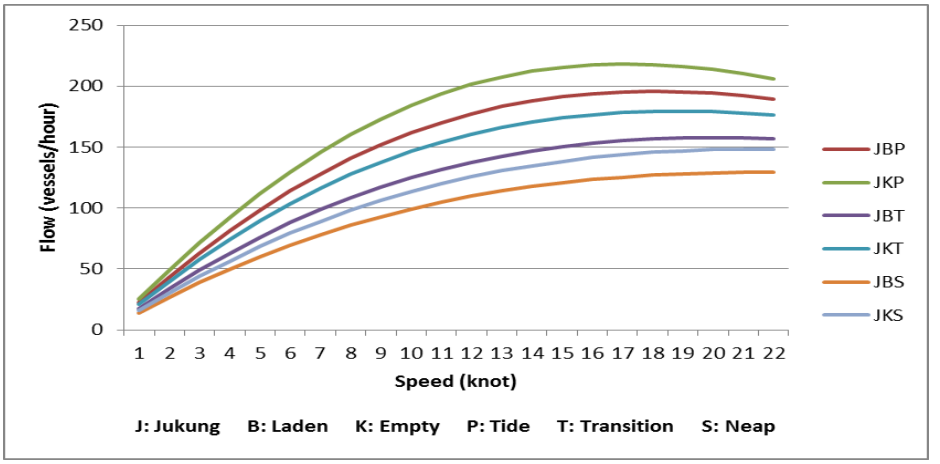

Figure 6 The Relationship between Jukungs Speed and Traffic Flow In Various Conditions

The fairway capacity that is sailed by one type of vessel in various tidal conditions can be seen in Table 4.

Table 4. Calculation Result of Fairway Capacity

Type of Vessel	Fairway Capacity (vessel/hour)		
	Tide	Transition	Neap
Laden Barge	30	24	22
Empty Barge	34	28	24
Laden Jukung	196	158	129
Empty Jukung	218	180	148

Source: calculation results

The fairway capacity is determined based on standard capacity. Standard capacity is the fairway capacity when it is sailed only by empty jukungs in the tide conditions. Fairway characteristics other than the standard conditions are determined by multiplying the influence factor and correction factor with a standard capacity, namely:

$$C_V^T = C_0 . f_V . f_T \quad (8)$$

Where:
C_V^T = fairway capacity, the capacity of the river being sailed by one type of vessels in certain river stream conditions
C_0 = basic capacity
f_V = influence factor of type of vessel
f_T = correction factor of river stream condition

After fairway capacity navigable by barges and jukungs in a variety of stream conditions has been obtained, the value of the influence factor can be determined. The influence factor of vessels during tidal conditions is determined by dividing fairway capacity sailed by one type of vessels during tide by the standard capacity, i.e.

f_v
- v_1 (Laden Barge) = 0.138
- v_2 (Empty Barge) = 0,156
- v_3 (Laden Jukung) = 0.899

Furthermore, correction factor for determining traffic capacity for a wide range of river stream conditions (tide, transitional and neap) is obtained by dividing the fairway capacity traversed only by jukungs in the transition condition or neap by standard capacity, namely:

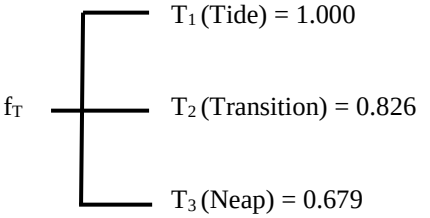

4 Discussion

The fairway capacity which is only navigable by barges, both laden and empty, is presented in Figure 5. Differences in fairway traffic capacity that are only sailed by laden barges and empty barges are relatively small. This shows both have the same efficiency when sailing in Musi Fairway. A laden barge sailing at high speed is easier to be controlled, but will find it hard to stop when the vessel's captain decelerates. On the contrary, an empty barge is more difficult to control, but it is easier to stop. The fairway capacity which is only navigable by jukung is shown in figure 6. The difference of traffic capacity between the fairway that is passed only by empty jukungs and that by laden is quite significant; it is also shown that empty jukungs sail more efficiently than the laden jukungs.

Table 4 shows the fairway capacity for vessel lane against the stream that tends to be larger than vessel lane in the direction of the stream. Barges and jukungs sailing against the stream are more easily controlled than the vessels sailing in the direction of the stream, and therefore can maneuver better.

The quality of the capacity value is determined according to the collected data. Two important parameters obtained from the survey are the minimum stopping distance and minimum spacing. Both of these parameters have been obtained from interviews with the vessels' captains based on their experiences driving the vessels in the fairway. The minimum stopping distance was determined at the time of data collection based on three categories of speed vessels, i.e. fast, moderate and slow. Speed categories must be set because at the time of the pilot survey, the vessels' captains had trouble in determining the minimum stopping distances for the vessel speeds, which are varied, i.e. 2, 5, 8, 10, 15, 20 knots; that is why the speed categories were used to resolve the problem. These categories were more easily understood by the vessels' captains at the time of the survey, but it has led to difficulty in determining a more accurate minimum stopping distance. Regression was used to determine the minimum stopping distance for a wide range of vessel speeds that are more varied.

5. Conclusions and suggestions

The results indicate that the method proposed in this study can be used to determine the fairway traffic capacity that navigable by one type of vessel. The method is quite accured if the data measurements are well conducted. But this method cannot be used to estimate fairway traffic capacity navigable by various types of vessel. In addition, this method cannot predict the performance of the system if the conditions or parameters of the system are changed or corrected, it must be done through data collection and recalculation. A more efficient method is a simulation model using computer software so that fairway traffic capacity navigable by more than one type of vessel can be known and the effect of changes in the conditions or parameters of the system capacity can be estimated more easily and quickly

References

[1] V. A. Tuan, Making Passenger Inland Waterways A Sustainable Transport Mode in Asia Current Situation and Challenges, in: Proceedings of the Eastern Asia Society for Transportation Studies, vol. 8, 2011.
[2] T. Rallis, Intercity Transport: Engineering and Planning, The Macmillan Press Ltd, London, 1977.
[3] Y. Fuji, K. Tanaka, Traffic Capacity, The Journal of Navigation 24, 543-552, 1971.

[4] Ming Huang, Gan Weidong, Liu Mingjun, Research on the Navigating Capacity of Ship in the Three Gorges Reservoir Waterway, in: ICTIS, ASCE 2011.
[5] A. Frima, Capacity Study for the Rio de la Plata Waterway in Argentina, Thesis, Civil Engineering Ports and Waterways, Technische Universiteit Delf, Belanda, 2004.
[6] N. Fisher, M. Treiber, B. Sohngen, Modelling and Simulating Traffic Flow on Inland Waterways, PIANC World Congress, San Fransisco, 2014
[7] Gi-Tae Yeo, M. Roe, Sang-Moon Soak, Evaluation of the Marine Traffic Congestion of North Harbour in Busan Port, Journal of Waterway, Port, Coastal and Ocean Engineering, 2007.
[8] Z. Guo, W. Wang, X. Song, G. Tang, A New Method to Measure the Passing Capacity of Coastal Waterway Considering Service Level by Simulation Computation, Journal of the Eastern Asia Society for Transportation Studies, Vol. 8, 2010.
[9] X. Qu, Q. Meng, Development and Application of a Simulation Model for Vessels in the Singapore Straits, Expert System Applications 39, 2012, 8430-8438
[10]Lin-ying Chen, Jun-min Mou, Simulating Traffic in Waterway Network Based on Gap Acceptance Theory, Wuhan University of Technology, China, 2011.
[11] D. Parikesit, R. Novitarini, K. Kushari, The Characteristics of Rural Water Transport: Case Studies of Threes Provinces in Indonesia, in: Proceedings of the Eastern Asia Society for Transportation Studies, Vol. 4, October, 2003
[12]Tim Jurnalistik Kompas, Jelajah Musi, Kompas, Jakarta, 2010.
[13]A.D. May, Traffic Flow Fundamentals, Prentice Hall, Englewood Cliffs, New Jersey, 2005.
[14]H. Sutomo, Appropriate Saturation Flow At Traffic Signals in Javanese Cities: A Modelling Approach, *Doctoral Dissertation*, Institute for Transportation Studies, The University of Leeds, 1992.
[16]Departemen Perhubungan, Laporan Akhir Studi Bentuk Desain Alat Angkutan Sungai Pedalaman (Inland Waterways) di Daerah Kalimantan, Sumatera dan Papua, 2007.

Available online at www.sciencedirect.com

ScienceDirect

Procedia Engineering 00 (2017) 000–000

Procedia Engineering

www.elsevier.com/locate/procedia

Sustainable Civil Engineering Structures and Construction Materials 2016, SCESCM 2016

Effect of car access and habit on students' behavior using a car

Rudy Setiawan[a,*], Wimpy Santosa[b], Ade Sjafruddin[c]

[a]*Civil Engineering Study Program, Petra Christian University, Siwalankerto 121-131, Surabaya 60236, Indonesia*
[b]*Civil Engineering Study Program, Parahyangan Catholic University, Ciumbuleuit 94, Bandung 40141, Indonesia*
[c]*Civil Engineering Study Program, Bandung Institute of Technology, Ganesha 10, Bandung 40132, Indonesia.*

Abstract

This study reports an analysis of psychological factors influencing student behavior to reduce using cars for the journey to campus from the perspective of the Norm-Activation Model, with the addition of students' car access, and car use habit for the journey to campus. Students from three different university campuses completed a survey on their car commuting behavior. Results indicated that car use habit, awareness of consequences, and ascription of responsibility explain 63% variance of personal norm. Personal norm explains 47% variance of the behavioral intention. In turn, behavioral intention, car use habit, and car access explain 54% of the variance of the actual car use. Car use habit and ascription of responsibility were the strongest factors that affect personal norm, and car use habit was the strongest factors that affect actual car use behavior, while car access significantly affect car use habit and actual car use behavior. Implications of these findings are that in order to reduce car use, the university should implement both structural and psychological intervention. To be effective interventions should be designed to removing opportunities for the enactment of car use habit, also to enhance the sense of responsibility towards the negative effect of car use.

Peer-review under responsibility of the organizing committee of SCESCM 2016.

Keywords: Students' car use; norm activation model; car access; car use habit.

* Corresponding author. Tel.: +62-8123-257-693; fax: +62-31-8436418.
E-mail address: rudy@petra.ac.id

Peer-review under responsibility of the organizing committee of SCESCM 2016.

1. Introductions

Private car, although it provides many societal functions as well, also contributes to various problems, such as traffic congestion and environmental pollution. About 70% urban air pollution generated from vehicle exhausts [1]. Despite attempts at diminishing the environmental impact of cars use by means of technological innovations (e.g. fuel cell technology, hybrid fuel systems, and more efficient engines), factors affect car use behavior and intentions to reduce it are crucial to examine when design the travel demand management policies to reduce car use. Because various trends tend to invalidate positive effect of car technological innovations, such as increased car ownership and increased the frequency of car use [2].

In 2012, there were 73,035 university students in Surabaya [3], and some of them are the private university, that intensity to use of private cars usually high, but has a limited resource to provide parking facilities, such as Petra Christian University [4]. Therefore, private university has to decide between providing a parking facilities or to preserve open green space to diminishing the impact of air pollution to the health of campus community, also to avert traffic congestion and social conflict with local residents.

University has an opportunity and important active role to achieve sustainable campus transportation, to reduce the environmental effect because of the use of motor vehicles, and to keep the quality of life of the campus community, as well people living around it [5]. University is the appropriate location to implement and to observation transport policy changes, as well as having administrative control over the management of campus transportation facilities inside the campus [6]. In addition, encouraging sustainable campus travel behaviors an essential concern. At least for promoting sustainability, the role model for society, deepen understanding of sustainability and increase campus community health through sustainable mode choices [7].

An effective solution to address the issues related to car usage requires a reduction in car traffic volume based on changes in car use behavior [8]. Because traveling is an expressive activity, there are an instrumental and emotional element in the behavior and travel options [9, 10]. Hence, policy to change individual car use behavior would be more effective when the measure is directed to motivational factors on car use [11, 12, and 13].

Currently, random utility theory is the most common model used to study how people make choices related to the selection of transportation mode; in general, consideration is focused on the evaluation of attributes associated with the options available [14]. Research in developing countries demonstrates that some social-psychological variables can contribute significantly to the utility model and support to increase conformity with the utility model [15]. Therefore, it is important to add the attitude and identity traits through inherent variables approach, since there is interaction between the attitudes, beliefs, emotions, personality traits, and values when individuals choose an alternative and to integrate attitudes and personality traits with the evaluation of mode choice model in order to recognize the effect of the variables underlying transport mode choice [16].

Behavior model is an approach to determine psychological factors that most influence students' behavior in using cars for university routes. Such knowledge is a useful input in planning various campus transport policies. There are different models of behavior that can be used to review the psychological factors that influence the individual mode choice, among others, Norm-Activation Model (NAM) [17].

NAM was suggested to explain the altruistic behavior that was initially developed to describe the behavior of the pro-social behavior. Thus, researchers use NAM in the conceptualization of behavior to reducing car usage as a behavior that is driven mainly by pro-social behavior. That view is reflected in the assumption that personal norm (PN) is the most important determinant of mode choice [2].

PN is an obligation that was felt by individuals to keep his personal behavior be in line with full and total comprehension of personal value that is considered important by these individuals. NAM assumes that the formation and activation of Personal Norm are the results of the interaction between a cognitive, emotional, and social factor. In NAM, PN is affected by the ascription of responsibility (AR) and awareness of the consequences (AC). When individuals feel a personal responsibility due to the consequences, such individual will perceive a moral obligation to protect the well-being of others, and value the well-being of other individual and believe that his behavior will give other individuals the consequences. Thus, AR and AC are important pre-condition cognitive for the establishment of PN.

Added habits into the NAM, significantly increased the explained variation in car use behavior [18], also improve both the moderating effect of habits on the connection between personal norms, behavioral intention, and actual

behavior and explained behavioral variation and a [19]. Habits are relatively stable behavioral patterns, which have been strengthened in the past [20]. Students' car use habit is essential for forecasting students' car use behavior for the journey to campus because students regularly travel to the campus about the same time every day with the same route and the same intention [13]. Habits behavior not necessarily prefaced by a behavioral intention; a strong habit may be able to help to predict actual behavior more precisely than a behavioral intention [15]. Therefore, the more often behavioral patterns are successfully performed in stable condition, the most crucial habits become as a predictor of actual behavior, and the insignificant become behavior intentions as a predictor of actual behavior [19].

Up to now, however, there has been limited analysis of the integration of NAM, students' car use habit and students' car access on student behavior model to reduce using cars for the journey to campus [13, 21]. Therefore, to understand the nature of the connections between the various psychological factors that affect the actual behavior of students' car use for the journey to campus, the main issues that will be explored through this research is to determine these relationships based on the integration of Norm Activation Model (NAM), students' car use habit, and students' car access. The psychological factors analyzed in this study are students' awareness of consequences of car use (AC), students' ascription of responsibility of car use (AR), students' personal norm of car use (PN), students' car use habit (H), and students' car access for the journey to campus (CA).

It is expected that the study findings can be beneficial for designing campus transportation policies to reducing students' car usage for university routes. Findings on the psychological factors that mostly affect students' actual car use behavior for the journey to campus can provide the recommendation in considering both psychological interventions and structural interventions, which needs to be implemented by the campus to affect students' actual behavior using cars for the journey to campus.

2. Methods

A convenience sample of the university student from three private universities in Surabaya, Indonesia: (1) Widya Mandala Catholic University (WMCU), (2) Surabaya University (SU), and (3) Petra Christian University (PCU) [22], were approached to participate in the study. 312 students (136 female, 176 male) completed the study. The breakdown of students was as follows: 53 WMCU, 124 SU, 135 PCU; 86 have one car, 125 have two cars, 72 have three cars, 29 have four or more cars, and 264 have access to at least one car for the journey to campus, 48 have access to two or more car for the journey to campus. The study used a self-report paper and pencil questionnaire. Each latent variable has three or more indicators, with the exception for students' car access and students' actual behavior using a car for the journey to campus (Table 1).

Table 1. Indicators used for the latent variables

Latent Variable	Number of Item	Cronbach's α	Construct Reliability	Variance Extracted
Actual car use behavior (AB)	1	n/a	n/a	n/a
Behavioral intention to use car (BI)	4	0.63	0.743	0.420
Personal norm to reduce using car (PN)	4	0.60	0.700	0.373
Ascription of responsibility to reduce using car (AR)	3	0.76	0.768	0.525
Awareness of consequences to reduce using car (AC)	3	0.69	0.767	0.525
Car access for the journey to campus (CA)	1	n/a	n/a	n/a
Car use habit for the journey to campus (H)	7	0.91	0.910	0.595

3. Results

Estimation of the model was conducted using AMOS [23] and Table 2 show the result that met the statistical portion of the suitability of the model. There are three invalid constructs with Variance Extracted (VE)<0.50, i.e. PN (0.373), and BI (0.420), but all invalid constructs are have qualified Construct Reliability (CR $\geqslant$ 0.70). The Model is assumed optimum because Modification Indices (MI) did not offer any addition of error covariance that can increase validity and reliability model construct significantly, and increase the model goodness of fit.

As can be seen from Figure 1, NAM Structural Model, all Standard Loading Factor (SLF) are significant ($p \leq$ .05). Construct AC and AR has had a significant positive effect to PN, construct PN has had a significant negative effect to BI and construct BI has had a significant positive effect to AB.

Table 2. Model goodness of fit

Goodness of Fit Indicators	NAM	NAM+CA	NAM+H	NAM+CA+H
Absolute-Fit Measures				
χ^2 (Chi-Square)	1,039.666	1,009.059	849.459	789.633
Significance of Probability	0.000	0.000	0.000	0.000
Degree of Freedom	215	214	212	210
CMIN/df	4.836	4.715	4.007	3.760
GFI	0.764	0.776	0.813	0.827
RMR	0.178	0.178	0.126	0.114
RMSEA	0.111	0.109	0.098	0.094
Incremental-Fit Measures				
TLI	0.693	0.702	0.759	0.779
NFI	0.695	0.704	0.751	0.769
AGFI	0.698	0.711	0.756	0.773
RFI	0.641	0.650	0.703	0.721
IFI	0.742	0.751	0.801	0.819
CFI	0.739	0.748	0.798	0.816

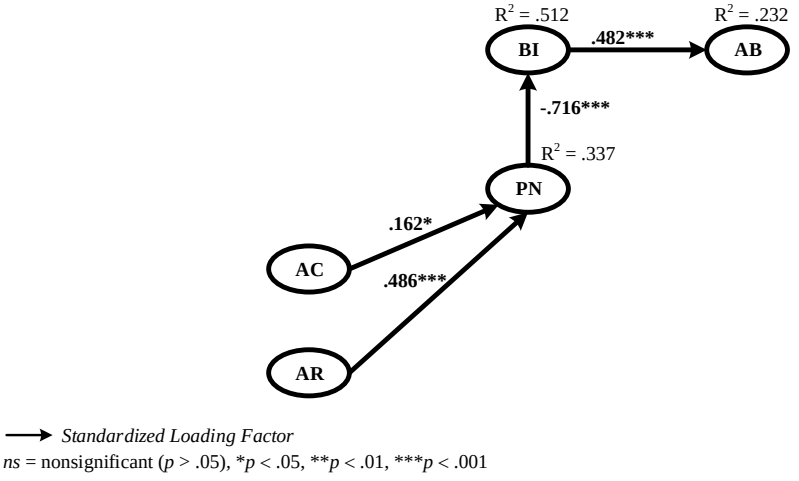

Figure 1. NAM structural model

Based on NAM structural model, increasing students' awareness of consequences to reduce using car (AC) and ascription of responsibility to reduce using car (AR) will increase students' personal norm (PN) to reduce using cars for the journey to campus, while increasing of PN will decrease or reduce students' behavioral intention to use car

(BI) for the journey to campus. Therefore, decreasing or reducing of BI will decreasing or reducing students' actual car use behavior (AB) for the journey to campus. AC and AR explained about 34% variance of PN, whereas construct PN can explain about 51% variance of BI, and about 23% variance of AB explained by BI. Construct PN is significantly affected both by construct AR and AC.

As can be seen from Figure 2, NAM+CA Structural Model, all standard loading factor (SLF) are significant ($p \leq .050$), except for the effect of AC to PN ($p = .057$). Construct AR has had a significant positive effect to PN, construct PN has had a significant negative effect to BI, while construct BI and CA has had a significant positive effect to AB.

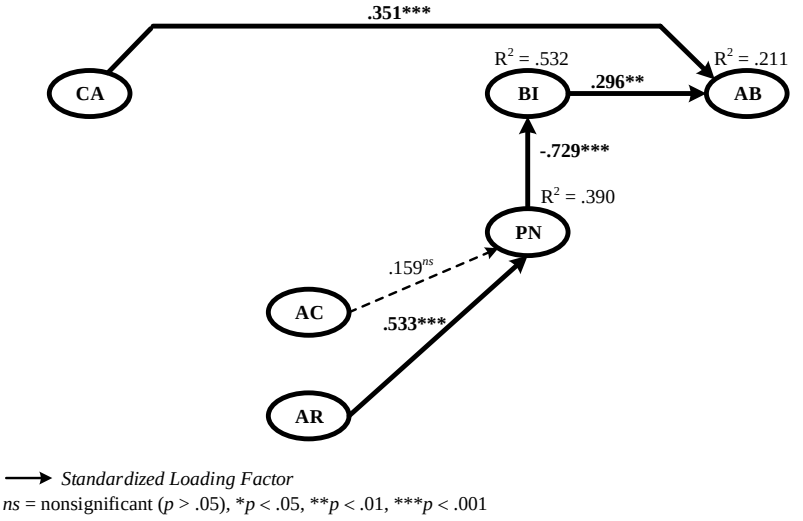

Figure 2. NAM+CA structural model

Based on NAM+CA structural model, increasing of AR will increase PN. Increasing of PN will decrease or reduce BI, while increasing students' car access for the journey to campus (CA) and BI, will increasing of AB. AC and AR explained about 39% variance of PN (increase about 16% compare with previous model, NAM), whereas construct PN can explain about 53% variance of BI (increase about 4% compare with NAM), and about 21% variance of AB explained by BI and CA (decrease about 9% compare with NAM). Construct PN is only affected by construct AR.

As can be seen from Figure 3, NAM+H Structural Model, all standard loading factor (SLF) are significant ($p \leq .050$), except for the effect of H to AC ($p = .528$) and H to AR ($p = .882$). Students' car use habit for the journey to campus has had a significant positive effect to AB, and a significant negative effect to PN. AC and AR have had a significant positive effect to PN, while PN has had a significant negative effect to BI, and BI has had a significant positive effect to AB.

Based on NAM+H structural model, although increasing AC and AR will increase PN, but increasing H will decrease PN. In this model, PN is affected both by positive and negative influence, while AB, more influence by H than by BI. H, AC and AR explained about 63% variance of PN (increase about 61% compare with previous model, NAM+CA), whereas construct PN can explain about 48% variance of BI (decrease about 11% compare with NAM+CA), and about 53% variance of AB explained by BI and H (increase about 153% compare with NAM+CA).

As can be seen from Figure 4, NAM+CA+H Structural Model, all standard loading factor (SLF) are significant ($p \leq .05$), except for the effect of H to AC ($p = .528$) and H to AR ($p = .890$). CA gives both significant positive effect to H ($p \leq .001$) and AB ($p = .039$). H has had a significant negative effect to PN ($p \leq .001$), and significant positive effect to AB ($p \leq .001$). Both AC and AR have had a significant positive effect to PN ($p = .040$ and $p \leq .001$), while PN has had a significant negative effect on students' intention-behavior of using cars, that intention has had a significant positive effect to AB ($p = .025$).

Based on NAM+CA+H structural model, increasing of students' car access for the journey to campus (CA) will increase students' car use habit for the journey to campus (H), and students' actual car use behavior (AB). Increasing of students' car use habit for the journey to campus (H) will decrease students' personal norm to reduce using a car (PN), but also increase students' actual car use behavior (AB). About 19% of the variance in H was explained by students' car access for the journey to campus (CA), whereas H, awareness of consequences to reduce using car (AC), and ascription of responsibility to reduce using car (AR) can explain about 63% variance of PN (almost the same as previous model, NAM+H). About 47% variance of BI explained by PN (decrease about 0.2% compare with NAM+H), and about 54% of the variance in AB was explained by H and CA (increase about 1.5% compare with NAM+H).

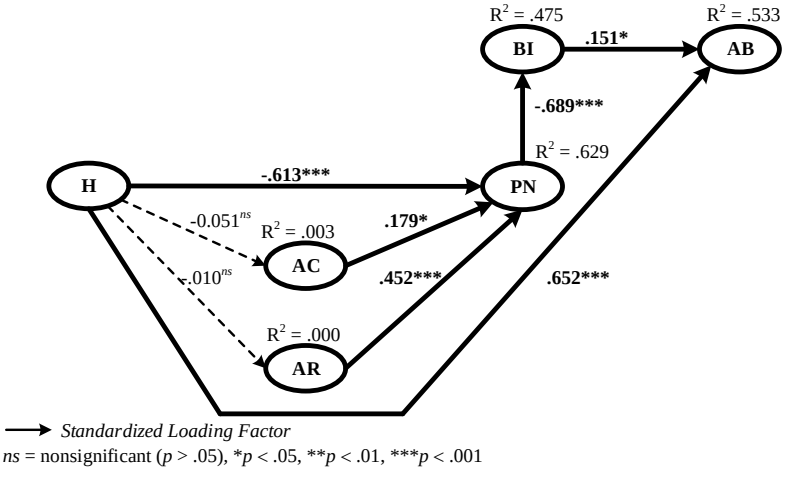

Figure 3. NAM +H structural model

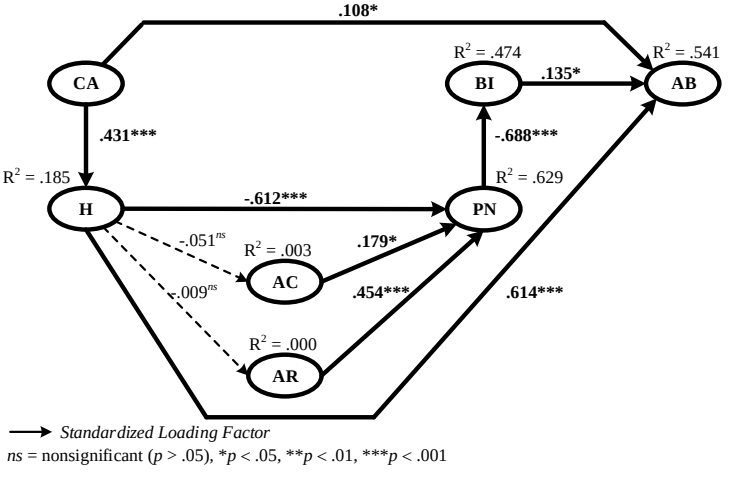

Figure 4. NAM+CA+H structural model

4. Discussion

Behavior model is an approach to find out the psychological factors that mostly affect students' behavior to reduce using cars for the journey to campus. Such information is a beneficial input in devising various campus transport strategies. Several conclusions can be acquire based on the connections between factors in NAM, NAM+CA, NAM+H, and NAM+ CA+H structural model. The goodness of fit of the model is getting better along

with the addition of CA and H (Table 2). Both AR and AC gives positive influence to PN, although the influence of AR to PN is always greater than the influence of AC to PN.

Added H to NAM and NAM+CA, has had a significant negative effect of H to PN. Thus, it can be said that the impact of H very strong against altruistic behavior (NAM). Therefore, add students' car use habits into the NAM not only significantly increased the explained variation in students' actual behavior, but also improve both the explained behavioral variation and a moderating effect of habits on the connection between personal norms, behavioral intention, and actual behavior.

Added CA and H in NAM (NAM+CA+H) have a good effect, although reduce the influence of BI to AB and decrease BI variance, AB variance increase significantly, and the SLF between PN-BI and BI-AB are still significant. Thereby, the more students perceive have access to a car for the journey to campus and the stronger their habit to use a car for the journey to campus, the insignificant become their behavior intentions affect their actual behavior to use a car for the journey to campus.

Thus, campus needs to develop strategies of intervention which is a combination of the hard transport measure (structural interventions) and the soft transport measure (psychological intervention), to affect students' motivation to reduce car use. Motivation to reduce car use is affected by individual and contextual factors. Such interventions should be aimed primarily to raise students' sense of responsibility with regard to the negative effect of using a car for the journey to campus.

Structural intervention can be either facility (such as student dormitories, restricted parking location inside campus area, preferential parking space for rideshare, and bike facilities). Other structural interventions can be either financial disincentives or incentives (e.g., the enforcement of the higher parking fee for solo driver on the contrary free parking for rideshare and vanpool member, guaranteed ride home for rideshare and vanpool member, the chance to try a vanpool service free of charge, ease of bike ownership installment). Meanwhile, the psychological intervention can be in the form of campaigns and educational programs (e.g., positive impact of using others mode choice for the journey to campus and travel awareness campaigns the negative effect of using a car). Another form of psychological interventions is such as car-sharing and public transport marketing information schemes, and personalized travel planning.

5. Conclusions

This study explored the relationship between the various psychological factors that affect the students' behavior to reduce using cars for the journey to campus based on Norm Activation Model, with the addition of students' car access and car use habit for the journey to campus. Overall, the results highlight that students' car use habit for the journey to campus and students' ascription of responsibility to reduce using car were the strongest factors that influence students' personal norm to reduce using a car, and students' car use habit was the strongest factors that influence students' actual car use behavior. While students' car access significantly affect students' car use habit and students' actual car use behavior. Finally, students' actual car use behavior are more affect by students' car use habit, than by students' intention-behavior of using cars, and by students' car access for the journey to campus.

Although, students' personal norm to reduce using car negatively influence students' behavior intention to use a car. Students' car use habit and car access for the journey to campus had a positive influence on students' actual car use behavior. Thus, if the student has developed strong car use habit in the previous semester and has easy access to use a car, they are very likely to use the car for the journey to campus. Furthermore, students' car use habit also influence by students' car access.

The results of the study have implications for university policy, that in order to affect the use of a car, the university should implement both psychological and structural intervention. To be effective interventions should be designed to removing opportunities for the enactment of car use habit, and specifically attempting to raise students' sense of responsibility towards the negative effect of using a car to campus.

References

[1] Kusminingrum, N. and Gunawan, G., Polusi Udara Akibat Aktivitas Kendaraan Bermotor di Jalan Perkotaan Pulau Jawa dan Bali, Retrieved on 2016-04-07 http://pu.go.id/uploads/services/infopublik20130926120104.pdf

[2] Abrahamse, W., Steg, L., Gifford, R., and Vlek, C., Factors Influencing Car Use for Commuting and the Intention to Reduce It: A Question of Self-interest or Morality?, Transportation Research Part F: Traffic Psychology and Behaviour, 12(4), 2009, pp. 317–324.

[3] Higher Education Database, Retrieved on 2012-09-01 http://forlap.dikti.go.id/mahasiswa/homerekap/RDgxNDdGMzQtMzQ4Ri00MTlELUFFNUItOThBMDdBRUUzQjUy/1

[4] Setiawan, R. Student Behavior Model Using Cars for Traveling to Campus, Doctoral Dissertation, Parahyangan Catholic University, 2014, unpublished.

[5] Poinsatte, F. and Toor, W., Finding a New Way: Campus Transportation for the 21st Century, University of Colorado Environmental Center, 1999. Retrieved on 2012-09-23 http://www.colorado.edu/ecenter/sites/default/files/attached-files/e5506f80de570bfa902419c8584179bfbae0f8 7f.pdf

[6] Bond, A. and Steiner, R. L., Sustainable Campus Transportation through Transit Partnership and Transportation Demand Management: A Case Study from the University of Florida, Berkeley Planning Journal, 19(1), 2006, pp. 125–142.

[7] Zhou, J. Sustainable commute in a car-dominant city: Factors affecting alternative mode choices among university students, Transportation Research Part A: Policy and Practice, 46(7), 2012, pp. 1013–1029.

[8] Steg, L. and Gifford, R., Sustainable Transportation and Quality of Life, Journal of Transport Geography, 13(1), 2005, pp. 59–69.

[9] Steg, L., Vlek, C., and Slotegraaf, G., Instrumental-reasoned and Symbolic-affective Motives for using a Motor Car, Transportation Research Part F: Traffic Psychology and Behaviour, 4(3), 2001, pp. 151–169.

[10] Stradling, S. G., Handbook of Traffic Psychology, First edition, Chapter 34 Travel Mode Choice, Academic Press, UK, 2011.

[11] Steg, L., Affective Motives for Car Use, European Transport Conference, 1999, pp. 13–28.

[12] Garling, T., Changes of Private Car Use in Response to Travel Demand Management, 3rd International Conference on Traffic & Transport, Nottingham, UK, 2004, Retrieved on 2012-05-07 http://129.125.2.51/psy/onderwijs/firststep/content/papers/4.2.pdf

[13] Klöckner, C. A. and Matthies, E., Structural Modeling of Car Use on the Way to the University in Different Settings: Interplay of Norms, Habits, Situational Restraints, and Perceived Behavioral Control, Journal of Applied Social Psychology, 39(8), 2009, pp. 1807–1834.

[14] Ortuzar, J. and Willumsen, L., Modelling Transport, Third edition, John Wiley & Sons, UK, 2001.

[15] Domarchi, C., Tudela, A., and González, A., Effect of Attitudes, Habit and Affective Appraisal on Mode Choice: An Application to University Workers, Transportation, 2008, 35(5), 585–599.

[16] Vredin Johansson, M., Heldt, T. and Johansson, P., the Effects of Attitudes and Personality Traits on Mode Choice, Transportation Research Part A: Policy and Practice, 40(6), 2006, pp. 507–525.

[17] Anable, J., Lane, B., and Kelay, T., an Evidence Base Review of Public Attitudes to Climate Change and Transport Behaviour, 2006. Retrieved on 2012-05-07 http://assets.dft.gov.uk/publications/pgr-sustainable-eviewtransportbehaviourclimatechange-pdf /iewofpublicattitudestocl573 0.pdf

[18] Klöckner, Matthies, E., and Hunecke, M., Problems of Operationalizing Habits and Integrating Habits in Normative Decision-Making Models, Journal of Applied Social Psychology, 33(2), 2003, 396–417.

[19] Klöckner, C. A., and Matthies, E., Two Pieces of the Same Puzzle? Script-Based Car Choice Habits between the Influence of Socialization and Past Behavior, Journal of Applied Social Psychology, 42(4), 2012, 793–821.

[20] Verplanken, B., Aarts, H., Knippenberg, A., and Knippenberg, C. (1994), Attitude versus General Habit: Antecedents of Travel Mode Choice, Journal of Applied Social Psychology, 24(4), 1994, 285–300.

[21] Bamberg, S. and Schmidt, P., Incentives, Morality, or Habit?: Predicting Students' Car Use for University Routes with the Models of Ajzen, Schwartz, and Triandis, Environment & Behavior, 35(2), 2003, pp. 264–285.

[22] Setiawan, R., Santosa, W., and Sjafruddin, A., Integration of Theory of Planned Behavior and Norm Activation Model on Student Behavior Model Using Cars for Traveling to Campus, Civil Engineering Dimension, 16(2), 2014, 117-122.

[23] Arbuckle, J. L., AMOS 21 User's Guide, Retrieved on 2012-05-07 ftp://public.dhe.ibm.com/software/analytics/spss/documentation/amos/21.0 /en/Manuals/IBM_SPSS_Amos_Users_Guide.pdf

Available online at www.sciencedirect.com

ScienceDirect

Procedia Engineering00 (2017) 000–000

Procedia Engineering

www.elsevier.com/locate/procedia

Sustainable Civil Engineering Structures and Construction Materials, SCESCM 2016

The application of road lighting standard towards sustainable transportation in large cities in Indonesia

A.Caroline Sutandi[a], Rory Daywin Anggano Pinem[a] *

[a]*Civil Engineering Department, Faculty of Engineering, Parahyangan Catholic University, Ciumbuleuit 94, Bandung 40141, Indonesia*

Abstract

Road lighting is an important road-furniture to improve road user's visibility during dark condition. The aim of this study is to evaluate and then recommend the application of road lighting standard towards sustainable transportation. Case study is carried out on a road with 2.3 km length and 51 light poles in a large city Bandung in Indonesia. Indonesia National Standard (SNI-7391:2008) and international standard CIE (Commission International de I'Echairage) are used to evaluate the road lighting. Lux meter, laser distance meter, and GPS application used to measure the field data. Result study indicated there are good average-luminance (cd/m^2), good overall light-uniformity (U_0), poor longitudinal light-uniformity (U_1), and fair threshold-increment value (TI) of the road lighting. Recommended solution toward sustainable transportation are implementation of uniform distance and height of light poles, uniform kind of LED, periodic maintenance of light function and using solar cell panel as an electric energy source.

Peer-review under responsibility of the organizing committee of SCESCM 2016.

Keywords: road lighting, national and international standard, sustainable transportation, large cities, Indonesia

1. Introduction

Sustainable transportation including good road infrastructure provides positive contribution to sustainable city [1, 2, 3]. Sustainable city is a global sustainable development agenda [4, 1, 5] regarding many components to be fulfilled for example innovation and green city, green and sustainable transportation with low level of travel time and pollution emission, efficient in the use of resources, resulting in cost and energy savings, and quality of life, using advanced technology including information and communication technology (ICT).

* Corresponding author. Tel.: +62 22 2033691; fax: +62 22 2033692.
E-mail address: caroline@unpar.ac.id

Peer-review under responsibility ofthe organizing committee of SCESCM 2016.

City with good road infrastructure including road geometric, road traffic, and traffic furniture will lead to improve the quality of life of the society. Besides traffic signs and traffic marking, one of traffic furniture is road lighting. The aim of this study is to evaluate and then recommend the application of road lighting standard towards sustainable transportation in large cities in Indonesia. Case study is carried out on a road with 2.3 km along in a large city Bandung in Indonesia. Results of this study are beneficial to fulfill road lighting standard towards sustainable transportation in large cities, not only in Indonesia but also in other developing countries with similar conditions.

2. Road lighting

Good road lighting provides benefits both for the motorist and to the community in general. The benefits to the community accrue through improved security of property, lower crime rates, enhancement of commercial / business areas, pedestrian safety, and the significant reduction in other night time road accident [6, 7, 8, 9].

Road lighting is measured by luminance, the different brightness of a sheet, in candelas/sq and Illuminance, the amount of light falling on each sheet in lux. Pavement brightness is achieved by locating the road lighting luminaires in such positions relation to each other and to the layout of the road that the road pavement is lighted by a series of “T” shape light patterns [10, 11, 9, 12].

The principal objectives in the lighting of traffic roads are to reveal objects on the carriageway and its verges and to indicate the course of the route ahead. In Australia and New Zealand, design criteria of traffic road lighting are designed to satisfy certain criteria:

- Level of luminance of road pavement against which objects are expected to be seen in silhouette must be sufficiently high to provide the contrast necessary for visibility.
- Uniformity of luminance is desirable to ensure that dark area of size sufficient to conceal an object of significant dimensions (0.3 m height) does not occur.
- Direct illumination: in the common situation where objects are seen on or against a background of the road verges, footpaths and fences etc., it is necessary to consider the direct illumination of these features.
- Control of glare: at the levels of lighting applicable to traffic routes, glare from luminaires is accentually by the relatively low level of average brightness behind luminaires and may cause both visual discomfort and disability.

Warrants for the provision of lighting to the levels specified for the categories may be determined by taking into account such factors as:

- the nature of the road terms of its hierarchical importance and its geometric standard.
- the nature and extent of abutting development and access control.
- the volume of traffic during the hour of darkness.
- the operating speed of traffic and/or the prevailing speed limit.
- the volume of pedestrian and bicycle traffic and its interaction with motor vehicle traffic.
- the frequency and nature of intersection.
- the historical or expected night accident rate.
- the level of lighting proposed and its cost.
- the location and nature of overhead power distribution.
- the location and form of any local area traffic management devices.

Moreover, traffic road lighting layout, include items as follow:

- geometry: the major task in preparing a lighting design for a section of road is the determination of the basic geometry of the installation. This involves the selection of the luminaire, the arrangement of luminaire, the mounting height, and the spacing of luminaire.
- Route Guidance: the ability of the lighting layout, as seen in perspective, to enhance drivers’ appreciation of both the alignment of the road and the location and nature of points of discontinuity in an important attribute of a road lighting scheme.

Road Safety Aspects: in general, the lighting layout is desirable to minimise the number of fixed hazards beside the roadway [9].

2.1. National road lighting standard

The standard of road lighting has been developed in terms of various light technical parameters which form quantitative measures of an installation. There are national standard specific in each country and also international standard. In Indonesia, there are 2 standards regarding road lighting. They are light specification for road lighting in the city [13] and road lighting specification for urban roads SNI 7391:2008 [14].

Road lighting planning should considers traffic volume, road cross sections, intersection condition, road geometric including horizontal and vertical alignment, kind and texture of road surface pavement that influence reflection of light, selection of kind and quality of light, power supply, number and position of light poles (necessity), operational cost, maintenance cost, road and city long range planning, accident rate, and crime rate. Position of road lighting in urban area is presented in Figure 1, kind of light for road lighting is presented in Table 1, and SNI standard regarding lighting distribution rate, lighting uniformity rate (overall uniformity U_0, longitudinal uniformity U_1), and threshold increment value is presented in Table 2 [14].

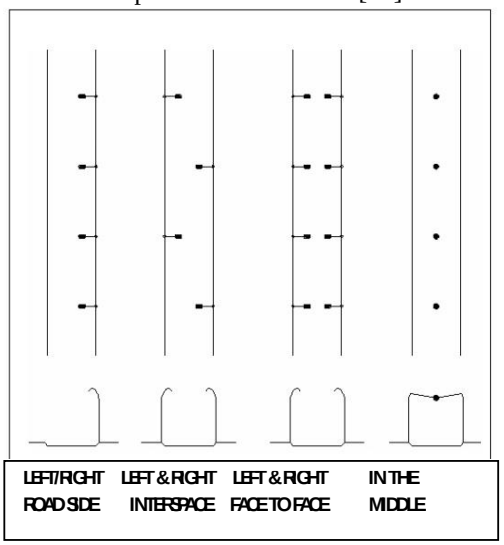

Fig 1. Position of road lighting in urban area [14]

2.2. International road lighting standard

International standard CIE [16] regarding classification system of the international of illumination, are also used to evaluate lighting distribution rate (cd/m^2), lighting uniformity rate (overall uniformity U_0, longitudinal uniformity U_1), and threshold increment value (%).

Lighting quality standard on the road is measured by lighting distribution rate (cd/m^2), lighting uniformity rate (overall uniformity U_0, longitudinal uniformity U_1), and threshold increment value (%). The equations of illumination value and threshold increment are presented in equation 1 and equation 2 respectively while CIE quality standard is presented in Table 3.

$$L_V = \frac{k \,.\, E_{gl}}{\Theta^n} \quad (1)$$

with:

L_V = veiling luminance

E_{gl} = illumination value at the center of light (lux)

n = 2,3-0,07*log(Θ) for 0,2°< Θ≤2°

n = 2 if Θ> 2°

$$k = 9.05(1 + (\frac{age}{66.4})^4)$$

k = constant to age with

Θ = angle between visibility line and light line as presented in Figure 2

$$TI = 65\frac{Lv}{Lavg^{0.8}} \quad (2)$$

with:

TI = threshold increment value (%)

L_v = lumination value with parallel straight vision to the road (cd/m^2)

L_{avg} = average lumination (cd/m^2)

Table 1. Kind of light for road lighting [14]

Kind of lamp	Average efficiency (lumen/watt)	Average life plan (hour)	Energy (watt)	Influence to color of object	Explanation
Fluorescent tube with low pressure	60 - 70	8,000 – 10,000	18 - 20; 36 - 40	moderate	- local and collector road; - good efficiency with short life; - limited implementation;
Mercury gas with high pressure (MBF/U)	50 - 55	16,000 – 24,000	125; 250; 400; 700	moderate	- local road, collector road, and intersection; - low efficiency with long life and small light size; - limited implementation
Sodium gas with low pressure (SOX)	100 - 200	8,000 – 10,000	90; 180	Very poor	- local road, collector road, intersection, crossroad, tunnel, rest area; - very high efficiency with long life and large light size, poor light with yellow color; - recommended implementation due to high efficiency;
Sodium gas with high pressure (SON)	110	12,000 – 20,000	150; 250; 400	Poor	- collector road, arterial road, toll road, large intersection, and interchange; - high efficiency with very long life and small light size, good light; - very recommended implementation;

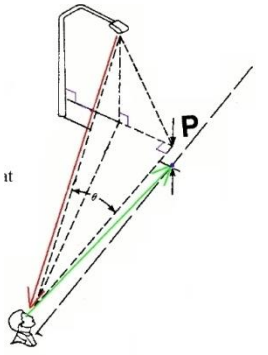

Fig 2. Veiling luminance [11]

Table 2. SNI standard regarding lighting distribution rate, lighting uniformity rate (overall uniformity U_0, longitudinal uniformity U_1), and threshold increment value [14]

Road hierarchy	Illumination			Lumination			Threshold increment
	E_{avg} (lux)	Uniformity $g_1=E_{min}/E_{max}$	L_{avg} (cd/m^2)	Uniformity $U_0=L_{min}/L_{max}$	Uniformity $U_1=L_{min}/L_{avg}$	Glare	Threshold increment value TI (%)
Crosswalk	1 - 4	0.10	0.10	0.40	0.50	4	20
Local road							
- Primary	2 - 5	0.10	0.50	0.40	0.50	4	20
- Secondary	2 - 5	0.10	0.50	0.40	0.50	4	20
Collector road							
- Primary	3 - 7	0.14	1.00	0.40	0.50	4 - 5	20
- Secondary	3 - 7	0.14	1.00	0.40	0.50	4 - 5	20

Road hierarchy	Illumination			Lumination			Threshold increment
	E_{avg} (lux)	Uniformity $g_1=E_{min}/E_{max}$	L_{avg} (cd/m^2)	Uniformity $U_0=L_{min}/L_{max}$	Uniformity $U_1=L_{min}/L_{avg}$	Glare	Threshold increment value TI (%)
Arterial road							
- Primary	11 - 20	0.14 – 0.20	1.50	0.40	0.50 - 0.70	5 - 6	10 - 20
- Secondary	11 - 20	0.14 – 0.20	1.50	0,40	0.50 - 0.70	5 - 6	10 - 20
Arterial road with control and toll road	15 - 20	0.14 – 0.20	1.50	0.40	0.50 - 0.70	5 - 6	10 - 20
Elevated road, interchange, and tunnel	20 - 25	0.20	2.00	0.40	0.70	6	10

Table 3. CIE standard regarding lighting distribution rate, lighting uniformity rate (overall uniformity U_0, longitudinal uniformity U_1), and threshold increment value [12]

Standard	Lighting distribution rate (cd/m^2)	Uniformity rate		Threshold increment value (%)
CIE	L_{avg}	U_0	U_1	TI
	(0.5 – 2.0)	0.4	0.5 – 0.7	(10 – 20) %

3. Case study and field data

Case study is carried out in arterial road in a large city Bandung in Indonesia (presented in Figure 3). There are 51 light poles on the road with 2.3 km along. Secondary data regarding kind (sodium yellow light), power (350

watt), lumen (30,000) and angle (45º) of the road light and also road width (1/3UD with 14 meter road width) was obtained from Bandung public work department.

While primary data is coordinate (latitude, longitude) on left or right road side, height (m), distance (m), illumination value (E_{gl}) in lux of all road lighting. Illumination of each road light is measured six times in order to get minimum and maximum values. Then, E_{gl} is used to count veiling luminance L_V. Lux meter, laser distance meter, and GPS application are used as tools to obtain the primary data. Primary data of each light pole is presented in Table 4 [17].

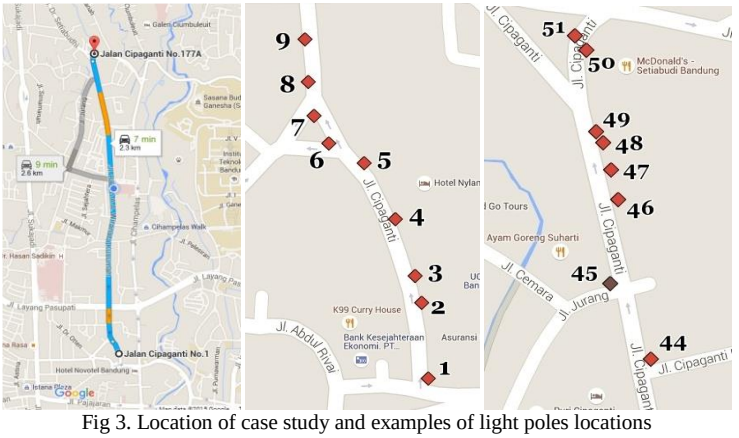

Fig 3. Location of case study and examples of light poles locations on the road side in a large city Bandung in Indonesia [15]

4. Analysis and result study

Furthermore, using primary and secondary data, road lighting parameter i.e. lighting distribution rate (cd/m^2), lighting uniformity rate (overall uniformity U_0, longitudinal uniformity U_1), and threshold increment value (%) were counted using equation 1, equation 2, and standards for each light pole, and the results is presented in Table 5. Results of comparison between road lighting parameter in Table 5 and national standard (SNI) and international standards (CIE) are presented in Table 6. In more detail, based on existing road lighting conditions, road lighting parameter in Table 5 and those fulfillment to national and international standards in Table 6, it is indicated that:

- lighting distribution rate L_{avg} (cd/m^2) of one road light to another is different because of difference of each height light pole, difference distance between poles, and difference of position of each light pole along the road side. 33 of 51 road lights (65 %) fulfill CIE standard and only 4 road lights (8 %) fulfill SNI standard. The condition can occur because L_{avg} value in CIE standard is in range (0.5 cd/m^2 – 2 cd/m^2) but L_{avg} value in SNI standard is fix (1.5 cd/m^2).
- 45 of 51 road lights (88 %) fulfill lighting overall uniformity rate (U_0) and 10 of 51 road lights (20 %) fulfill lighting longitudinal uniformity rate (U_1) of both standards because U_0 value (0.4) and U_1 value (0.5 – 0.7) in both standards is the same.
- 6 of 51 road lights are broken. Therefore, it can be said that all good condition road lights (45 road lights) fulfill overall uniformity rate U_0. Whereas, only 10 road lights fulfill longitudinal uniformity rate U_1 because there are many branches cover the light from the road lights.
- 28 of 51 road lights (55 %) fulfill threshold increment value TI (%) of both standards because TI value (10% - 20%) in both standards is the same.

There are national and international standards regarding road lighting. Nevertheless, road lighting in large cities in Indonesia is implemented before the issue of the standards because the large cities have been developed hundreds years ago. Therefore, not all of the road lights, position and uniform height of light poles fulfill all parameters in the standards.

Table 4. Road lighting primary data [17]

Light pole	Coordinate		Height (m)	Distance between poles (m)	E_{gl} (lux)	Light pole	Coordinate		Height (m)	Distance between poles (m)	E_{gl} (lux)
	Latitude	Longitude					Latitude	Longitude			
1	54.2532	36.1878	5.832	0	27	27	53.6070	36.1506	6.531	52	10
2	54,2226	36.1854	5.749	57	0	28	53.5692	36.1482	6.521	70	21
3	54.2118	36.1824	5.732	21	0	29	53.5284	36.1464	6.586	77	17
4	54.1890	36.1746	5.721	45	0	30	53.5140	36.1458	6.583	26	23
5	54.1662	36.1626	5.742	48	0	31	53.4888	36.1506	6.681	47	12
6	54.1584	36.1488	6.352	30	19	32	53.4630	36.1422	6.523	50	32
7	54.1470	36.1428	6.348	24	77	33	53.4348	36.1488	6.423	54	4
8	54.1332	36.1410	5.765	26	69	34	53.4192	36.1488	6.613	29	30
9	54.1158	36.1398	5.741	32	0	35	53.3958	36.1482	6.431	43	35
10	54.0810	36.1338	5.752	65	0	36	53.3718	36.1464	6.512	45	21
11	54.0492	36.1362	5.746	58	25	37	53.3292	36.1452	6.542	80	25
12	54.0342	36.1350	5.863	28	40	38	53.2908	36.1380	6.498	72	20
13	54.0072	36.1356	6.163	50	19	39	53.2734	36.1374	6.653	32	25
14	53.9646	36.1338	6.253	79	50	40	53.2212	36.1272	6.467	99	19
15	53.9250	36.1302	6.315	76	22	41	53.2020	36.1248	6.475	36	28
16	53.8824	36.1314	6.324	78	14	42	53.1540	36.1122	6.485	92	21
17	53.8434	36.1308	6.265	71	20	43	53.1450	36.1098	6.421	17	45
18	53.7990	36.1314	6.065	82	68	44	53.0988	36.1014	6.462	86	24
19	53.7792	36.1308	6.261	36	8	45	53.0706	36.0870	6.478	60	30
20	53.7510	36.1332	6.326	52	10	46	53.0394	36.0894	6.496	59	21
21	53.7300	36.1374	6.475	40	16	47	53.0280	36.0870	6.512	22	48
22	53.7240	36.1386	6.519	10	108	48	53.0178	36.0840	6.437	20	25
23	53.6994	36.1428	6.431	47	23	49	53.0136	36.0816	6.485	10	30
24	53.6730	36.1572	6.523	55	10	50	52.9830	36.0780	6.413	57	14
25	53.6520	36.1524	6.521	39	23	51	52.9770	36.0738	6.512	13	16
26	53.6346	36.1536	6.583	32	32						

Table 5. Lighting distribution rate (L_{avg}), lighting uniformity rate (overall uniformity U_0, longitudinal uniformity U_1), and threshold increment value (TI)

Light pole	L_{avg} (cd/m^2)	U_l	U_0	Lv	TI (%)	Light pole	L_{avg} (cd/m^2)	U_l	U_0	Lv	TI (%)
1	0.733	0.818	0.920	0.123	10.219	27	0.217	0.538	0.808	0.045	10.038
2	0.000	0.000	0.000	0.000	0.000	28	0.554	0.704	0.857	0.095	9.945
3	0.000	0.000	0.000	0.000	0.000	29	0.521	0.833	0.960	0.077	8.460
4	0.000	0.000	0.000	0.000	0.000	30	0.533	0.692	0.844	0.104	11.231
5	0.000	0.000	0.000	0.000	0.000	31	0.217	0.583	0.808	0.055	12.045
6	0.500	0.640	0.800	0.086	9.769	32	0.817	0.838	0.949	0.145	11.112
7	1.983	0.905	0.958	0.350	13.148	33	0.071	0.400	0.706	0.018	9.821
8	1.746	0.905	0.959	0.313	13.047	34	0.796	0.833	0.942	0.136	10.635
9	0.000	0.000	0.000	0.000	0.000	35	0.975	0.881	0.949	0.159	10.547
10	0.000	0.000	0.000	0.000	0.000	36	0.588	0.815	0.936	0.095	9.491
11	0.558	0.643	0.806	0.114	11.768	37	0.608	0.786	0.904	0.114	10.988
12	1.029	0.867	0.947	0.182	11.544	38	0.542	0.800	0.923	0.091	9.645
13	0.496	0.818	0.908	0.086	9.835	39	0.608	0.786	0.904	0.114	10.988
14	1.292	0.828	0.929	0.227	12.032	40	0.438	0.800	0.914	0.086	10.870
15	0.525	0.731	0.905	0.100	10.879	41	0.708	0.844	0.953	0.127	10.895
16	0.296	0.556	0.845	0.064	10.954	42	0.579	0.846	0.950	0.095	9.600
17	0.542	0.769	0.923	0.091	9.645	43	1.238	0.906	0.970	0.204	11.206
18	1.733	0.919	0.981	0.309	12.932	44	0.675	0.833	0.926	0.109	9.706
19	0.196	0.500	0.766	0.036	8.707	45	0.813	0.861	0.954	0.136	10.460
20	0.242	0.667	0.828	0.045	9.198	46	0.567	0.808	0.926	0.095	9.769
21	0.463	0.773	0.919	0.073	8.756	47	1.250	0.804	0.900	0.218	11.857
22	2.850	0.974	0.991	0.491	13.798	48	0.579	0.714	0.863	0.114	11.428
23	0.654	0.862	0.955	0.104	9.538	49	0.846	0.865	0.946	0.136	10.129
24	0.279	0.667	0.716	0.045	8.196	50	0.325	0.750	0.923	0.064	10.160
25	0.600	0.852	0.958	0.104	10.221	51	0.429	0.944	0.990	0.073	9.296
26	0.842	0.865	0.950	0.145	10.847						

Table 6. Number of light poles that fulfilled and unfulfilled the road lighting parameter based on CIE and SNI Standards

Road lighting parameter	CIE Standard		SNI Standard	
	Fulfilled	Unfulfilled	Fulfilled	Unfulfilled
L_{avg}	33	18	4	47
U_0	45	6	45	6
U_1	10	41	10	41
TI	28	23	28	23

5. Recommendations

Based on existing condition, analysis and result study, recommended solution that can be implemented toward sustainable transportation are uniform distance between light poles, uniform height of each pole, uniform kind of light using light emitting diode (LED), position of light poles are on left side and right side (not only on left side or right side) because the road has wide road width (14 meter), periodic maintenance of light function and branches that cover road lighting by public work authority, and regarding Indonesia is a country that has a long dry season, using solar cell panel as an electric energy source is suitable. Results of this study are beneficial and can be implemented to fulfill road lighting standard towards sustainable transportation in large cities in Indonesia and also in other developing countries with similar conditions.

6. Conclusions

Road lighting is a part of road furniture that has to fulfill the standards towards sustainable transportation and sustainable city as a nowadays necessity living place. Not all of the road lights and light poles in the large city fulfill all parameters in the standards. Therefore, a number of recommended solutions need to be implemented soon with high effort and high wish by road authority. They begin with evaluation of existing road lights and light poles condition based on standards and then fix it if there is any part of road lighting that unfulfilled the standards. Furthermore, doing periodic maintenance and regular road lighting audit in order to ensure that road lighting in the city is fulfill the standards. Results of this study are beneficial to fulfill road lighting standard towards sustainable transportation in large cities, not only in Indonesia but also in other developing countries with similar conditions.

References

[1] Sutandi, A. Caroline, 'The Significant Importance to Measure Road Safety', *Applied Mechanics and Materials Vol 776 (2015)* pp 66-73 © (2015) Trans Tech Publications, Switzerland, ISSN: 1662-7482, doi:10.4028/www.scientific.net/AMM.776.66.
[2] Black, William R., *'Sustainable Transportation – Problems and Solutions'*, The Guiford Press, A Division of Guiford Publication Inc., 72 Spring Street, New York, NY 10012, www.guiford.com, 2010, pp 3-12.
[3] Schafer, A., 'The global demand for motorized mobility', *Transportation Research A*32(6), 455-477, 1998.
[4] World Bank, *Transforming Transportation (2015) Smart Cites for Shared Prosperity*, January 15-16, 2015, World Bank Headquarters, Preston Auditorium, available at http://www.worldbank.org/en/events/2014/12/18/transforming-transportation-2015-smart-cities-for-shared-prosperity**,** acceded February 2015.
[5] Sutandi, A. Caroline, 'Pentingnya Transportasi Umum Untuk Kepentingan Publik', *Public Administration Journal*, Volume 12 Nomor 1, April 2015 ISSN 1412-7040 pp 19-34Social and Political Sciences Faculty, Parahyangan Catholic University, Bandung, Indonesia.
[6] Patel, M., Parmar, A., Patel, V., and Patel, D.M., '*Road Lighting as an Accident Counter Measure',* 296-304, 2014.
[7] Clark, R.V., '*Improving Street Lighting to Reduce Crime in Residential Area',* Problem-Oriented Guides for Police, Washington, DC, 2008.
[8] Assum, T., Bjørnskau, T., Fosser, S., Sagberg, F., '*Risk compensation – the case of road lighting',* Accident Analysis and Prevention 31, 1999, pp 545-553.
[9] Ogden, K.W. and Taylor S.Y., '*Traffic Engineering and Management'*, Institute of Transport studies, Department of Civil Engineering, Monash University, Clayton, Vic 3168, Australia, 1999.
[10] Gibbons, R.B., '*Glare Modeling Formulae',* Virginia Tech Transportation Institute, 2012.
[11] Thayer, T. and Calais, K., '*Illumination Design for Transportation Applications',* 2006.
[12] Van Bommel, W.J.M. and De Boer, J.B., '*Road Lighting'*, Philip Technical Library, New York, NY, 1980.
[13] Directorate General of Public Work, '*Spesifikasi Lampu Penerangan Jalan Kota*', Bina Marga, NO.12/S/BNKT/1991, 1991.
[14] National Standard Board in Indonesia, '*Spesifikasi Penerangan Jalan di Jalan Perkotaan*', SNI 7391:2008, 2008.
[15] Google map, accessed April 2016, 2016
[16] Commission International de l'Éclairage, '*Road Lighting Calculations'.* CIE No. 140. Vienna, Austria: Commission Internationale de l'Éclairage, 2000.
[17] Pinem, Rory Daywin Anggano, '*Road Lighting on Cipaganti Street Bandung*', thesis, Civil Engineering Department, Faculty of Engineering, Parahyangan Catholic University, Bandung, Indonesia, 2015.

Available online at www.sciencedirect.com

ScienceDirect

Procedia Engineering00 (2017) 000–000

Procedia Engineering

www.elsevier.com/locate/procedia

Sustainable Civil Engineering Structures and Construction Materials, SCESCM 2016

Analysis of demand responsive pelican crossing in mixed traffic conditions

Budi Yulianto[a,*], Setiono[a]

a Department of Civil Engineering, Sebelas Maret University, Jl. Ir Sutami 36A, Surakarta 57126,Indonesia

Abstract

Demand responsive Pelican Crossing has been used widely at midblock pedestrian crossing. However this controller has not been tested in mixed traffic conditions, where the traffic streams are heterogeneous, lack of lane discipline and high proportion of motorcycles. This paper describes an evaluation of the performance of demand responsive Pelican Crossing using Extension Principle (PC VAC-EP) under mixed traffic conditions. An investigation was carried out to find the most appropriate extension time for the PC VAC-EP that was suitable for mixed traffic. The best performance of the PC VAC-EP was, then, compared with the Pelican Crossing Conventional (PC C) on validated simulated pedestrian crossing. The effectiveness of the proposed PC VAC-EP and PC C were evaluated by the simulation program VISSIM.

Peer-review under responsibility of the organizing committee of SCESCM 2016.

Keywords: actuated control; mixed traffic; pelican crossing.

1. Introduction

Pelican Crossing is a signal control that applied at the crosswalk facilities to regulate traffic movement, both vehicles and pedestrians from each direction of travel to prevent accidents, minimize delay of vehicles and pedestrians. Pelican Crossing Conventional (PC C) used in Indonesia works based on pedestrian demand only. The length of green time of vehicle and pedestrian stages are constant.

Vehicle Actuated Control (VAC) is one of signal control type that responsive to traffic demand as registered by the vehicle actuation detectors on the approaches. The main feature of VAC is its ability to adjust the length of green

* Corresponding author. Tel.: +62-811-126-33-314; fax: +62-271-634-524.
*E-mail address:*budi.yulianto@ft.uns.ac.id

Peer-review under responsibility ofthe organizing committee of SCESCM 2016.

time based on traffic conditions on the ground. The most common method of VAC is an Extension Principle [1]. VAC Extension Principle (VAC-EP) has been used widely in most of midblock pedestrian crossing, especially in develop countries to regulate pedestrians crossing certain roads safely and comfortably.

The VAC-EP was developed based on non-mixed traffic conditions (in developed countries), where vehicles move in clearly defined lanes and very low proportion of motorcycles in the traffic. This type of control has not been tested and used at midblock pedestrian crossing in Indonesia where the traffic streams are heterogeneous consisting of different type of vehicles and with a particularly high proportion (30% - 70%) of motorcycles. Also due to lack of lane discipline, queues at approach are built up based on the optimum road space utilization which means vehicles can occupy any position across the road based on the available space [2].

This paper describes the evaluation of the performance of Pelican Crossing using VAC-EP (PC VAC-EP) under mixed traffic conditions with particularly high proportion of motorcycles. As the extension time is one of the most critical parameters to affect the overall performance of PC VAC-EP [3], therefore, an investigation was carried out to find the most appropriate extension time for the PC VAC-EP that was suitable for mixed traffic. The best performance of the PC VAC-EP was, then, compared with the PC C on validated simulated pedestrian crossing. The effectiveness of the proposed PC VAC-EP and PC C were evaluated by the simulation program VISSIM [3].

2. Overview of pedestrian signal control

2.1. Pelican Crossing Conventional (PC C)

PCC has been used widely in midblock pedestrian crossing in Indonesia. Under PC C, the length of green time of vehicle and pedestrian stages are constant. It works based on pedestrian demand only. When pedestrian activated the system, the vehicle stage will change to pedestrian stage after vehicle stage has reached the total length of green time. Logic of the PC C can be seen on Fig. 1.

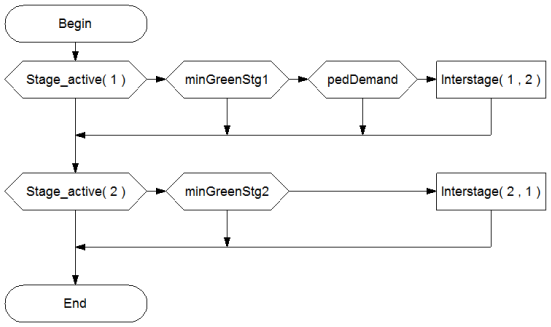

Fig. 1. Logic of PC C

2.2. Pelican Crossing using Vehicle Actuated Control Extension Principle (PC VAC-EP)

The VAC-EP has been used widely at intersection and midblock pedestrian crossing in many countries. Under this control, the green time of stage is adjusted based on the extension time and time gap between vehicles crossing the point detector a certain distance from the stop line [1]. There are three parameters required by the VAC-EP, namely the minimum green time, the extension time and the maximum green time. A green signal is activated for at least the minimum green time to provide sufficient time for all vehicles potentially stored between the detector and the stop line to enter the intersection. The green interval is extended by resetting the extension time every time an actuation vehicle is recorded after the minimum green time expires. If the detectors record another vehicle within this extension time, the green will be extended again from the time of this actuation, by the length of the extension time. If the time gap (headway) between vehicles becomes greater than this extension time, then this green interval will be terminated before it reaches its maximum green value. In such circumstances, where there are no vehicles detected on a particular approach, the controller can skip over that stage and move directly to the next stage in the

sequence. Fig. 2 shows typical detector configuration of PC VAC-EP at midblock pedestrian crossing. Logic of the PC VAC-EP can be seen on Fig. 3.

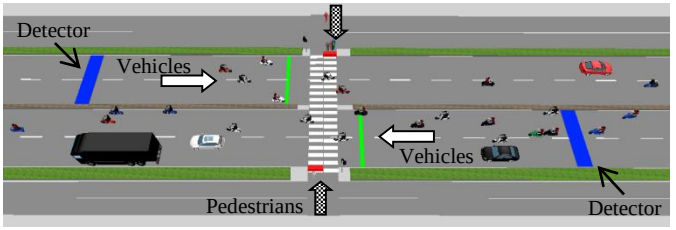

Fig. 2. Typical detector configuration of PC VAC-EP at midblock pedestrian crossing

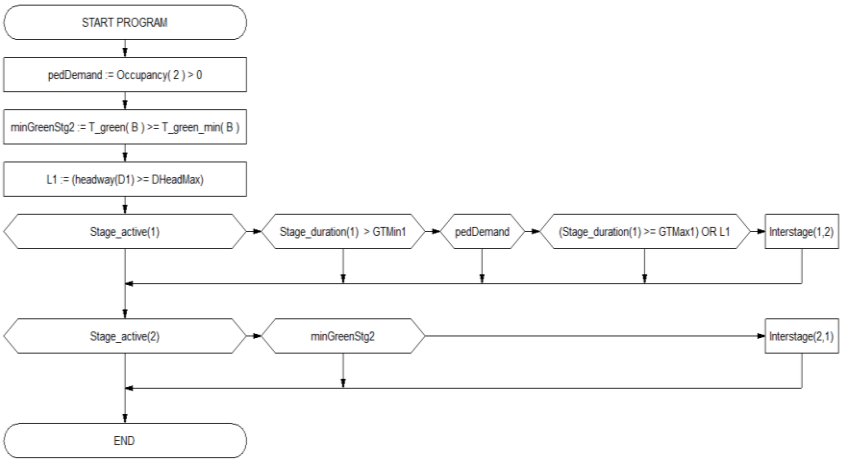

Fig. 3. Logic of PC VAC-EP

3. Simulation studies

In this simulation studies, VISSIM 7.10 was used to analyze the performance of the PC C and PC VAC-EP. In order to simulate mixed traffic condition, all vehicle types were modeled individually. The vehicle can occupy any position across the available lane space depend on the safe lateral clearance among vehicles. Motorcycles use inter-vehicular spaces to come to the front of the queue, and fill any lane space available between two vehicles. A motorcycle can squeeze between two vehicles moving side-by-side, or two successive vehicles moving in the same lane. Validated VISSIM simulated pedestrian crossing of the previous study was used in this study [4]. The signal controller program of the PC C and PC VAC-EP was developed using Vehicle Actuated Program language in VISSIM. This way, the signal controller program could interact directly with VISSIM via internal signal state generator [2].

3.1. Case study

In this research, the evaluation of the performance of PC C and PC VAC-EP was done on pedestrian crossing at Jalan Kolonel Sutarto Surakarta City, see Fig. 2. Traffic flow used is based on real data on pedestrian crossing during peak hour. Traffic compositions on the road network are presented in Table 1. Set of vehicle and pedestrian volume for all cases is presented in Table 2.

Table 1. Traffic composition (%) used in the simulation

Direction	Motorcycle	Light Vehicle	Heavy Vehicle	Bus
East	85,0	12,9	0,5	1,6
West	84,4	12,4	0,8	2,4

Table 2. Traffic volume used in the simulation

Case	Traffic	Case	Traffic	Case	Traffic	Pedestrian
1a	2000	2a	2500	3a	3000	25
1b	2000	2b	2500	3b	3000	50
1c	2000	2c	2500	3c	3000	75
1d	2000	2d	2500	3d	3000	100
1e	2000	2e	2500	3e	3000	125
1f	2000	2f	2500	3f	3000	150

3.2. Parameter controllers

In the case of the PC C, minimum green time of vehicle stage was 60 seconds, green time of pedestrian stage was 18 seconds, amber was 3 seconds, intergreen vehicle and pedestrian were 5 seconds and 15 seconds respectively.

One of the most critical parameters that affect the overall performance of VAC-EP is the extension time. The extension time is a function of detector position [5]. The detector locations used in this study based on the results of the simulation studies carried out by Yulianto [6]. His simulation studies showed that the VAC-EP with detector position of 30 metres gave the best controller performance (in term of average delay) in mixed traffic conditions. In order to obtain a good performance of the PC VAC-EP, therefore, the extension time of 2.0, 2.5, 3.0, 3.5 and 4.0 were tested for comparison. The minimum and maximum green time vehicle was 7.0 seconds and 60 seconds, respectively. Amber and intergreen similar to that used in the PC C.

3.3. Simulation results

Identical simulations were run for approximately one-hour periods on the PC VAC-EP and PC C to produce the output value (i.e. delay) of vehicle and pedestrian, for all case studies. The output value of the PC VAC-EP with different extension time is compared with each other. The best performance of the PC VAC-EP is, then, compared with the PC C on validated simulated pedestrian crossing.

The average vehicle and pedestrian delay at pedestrian crossing in one-hour simulation time for the PC VAC-EP with different extension time for all cases can be seen in Fig. 4. The simulation results show that the PC VAC-EP with an extension time of 2.0 seconds produced the highest average vehicle delay and lowest average pedestrian delay.

Controller with longer extension time (3.0-4.0) tends to use the maximum green time. This made the vehicle stage has priority than pedestrian stage. As consequence, the pedestrian have to wait longer for their right of way to cross the road. Thus caused pedestrian delay is longer.

As the aim of the pedestrian crossing controller to produce the lowest pedestrian delay, therefore, PC VAC-EP with an extension time of 2.0 seconds is the best controller than controller with other extension times. Apart from that, in terms of safety, pedestrian tends to non-compliance to the signal if they wait longer than 30 seconds. Comparison of the average vehicle and pedestrian delay at pedestrian crossing in one-hour simulation time between the PC C and PC VAC-EP for all cases can be seen in Fig. 5.

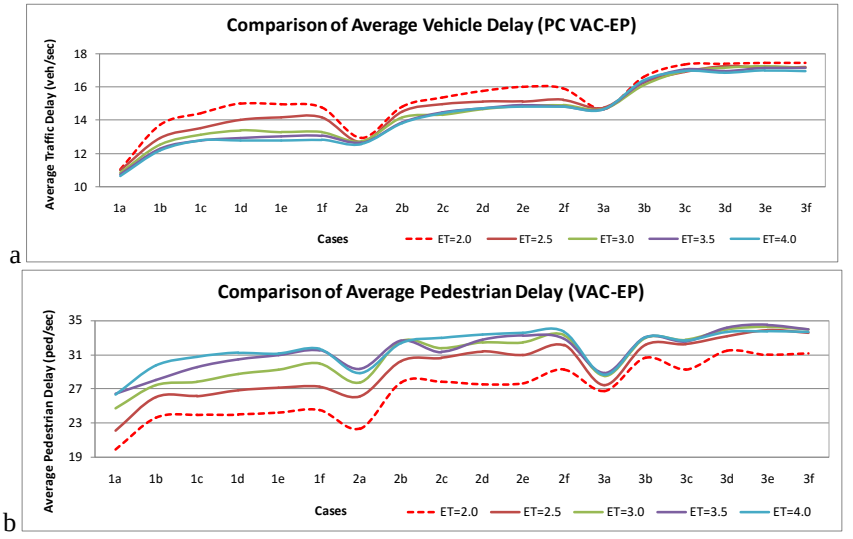

Fig. 4. Comparison of average traffic and pedestrian delay of PC VAC-EP with different extension time

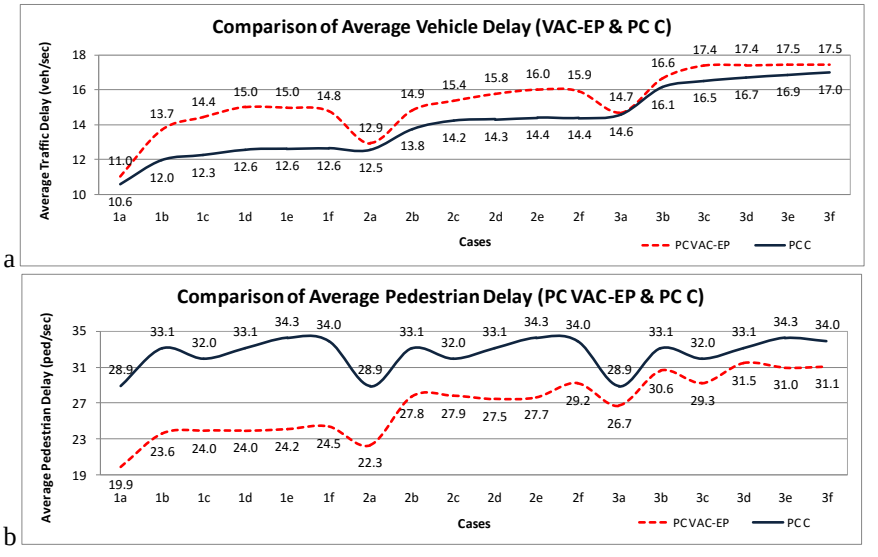

Fig. 5. Comparison of average traffic and pedestrian delay of PC C and PC VAC-EP

The simulation results indicate that the PC VAC-EP performs much better than the PC C in terms of average pedestrian delay for all different set traffic volumes. The PC VAC-EP yields an improvement of 8.1%-45.2% on the average pedestrian delay, see Fig. 6. In terms of vehicle delay, the performance of PC VAC-EP decreases between 0.5%-16.2%.

Overall, the performance of the PC VAC-EP better than PCC due to it has ability to adjust the length of green time in response to real traffic flows variations.

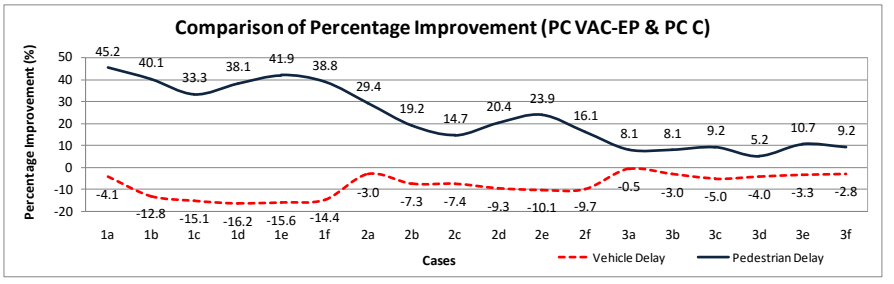

Fig. 6. Comparison of percentage improvement of PC VAC-EP in terms of traffic and pedestrian delay

4. Conclusions

Demand responsive Pelican Crossing, namely PC VAC-EP has been tested on different set of traffic with different extension time in mixed traffic conditions. The simulation results show that controller with extension time 2.0 seconds produces the lowest pedestrian delay. The effectiveness of the PC VAC-EP was compared to the PC C. The simulation results indicate that the performance of the PC VAC-EP better than the PC C in terms of average pedestrian delay. The performance of the PC VAC-EP can be improved by applying artificial intelligence e.g. fuzzy logic on the controller logic depend on the objective of the pedestrian crossing [6−8].

Acknowledgment

This research was funded by grant of the mandatory research group of Sebelas Maret University Surakarta.

References

[1] Kell, J.H and Fullerton, I J., Manual of Traffic Signal Design – Chapter 7: Detectors, Institute of Transportation Engineers, Prentice Hall, Englewood Cliffs, New Jersey, 1991.
[2] Yulianto, B., Application of Fuzzy Logic to Traffic Signal Control Under Mixed Traffic Conditions. Traffic Engineering and Control, International Journal of Traffic Management and Transportation Planning, Vol. 44, No. 9, November, 2003, pp. 332-336.
[3] Fellendorf, M., VISSIM: A microscopic Tool to evaluate Actuated Signal Control including Bus Priority, Technical paper, Session 32, 64th ITE Annual Meeting, Dallas, October 1994.
[4] Al'Alimi, F., Analisis Kinerja Pedestrian Crossing Pada Kondisi Mixed Traffic. Skripsi S1 2015. Universitas Sebelas Maret Surakarta Indonesia.
[5] Bullen, A.G.R., Effects of Actuated Signal Settings and Detector Placement on Vehicle Delay, Transportation Research Record 1244, 1989, pp. 32-38.
[6]Yulianto, B., Application of Fuzzy Logic to Traffic Signal Control Under Mixed Traffic Conditions. PhD Thesis 2007. University Newcastle upon Tyne UK.
[7]Sayers, T.M., Bell, M.G.H., Meiden, T., and Buch, F. Traffic Responsive Signal Control Using Fuzzy Logic – A Practical Modular Approach, Proceedings EUFIT 1996, Aachen, Germany, September 2-4, pp. 2159-2163.
[8]Sayers, T.M., Anderson, J., and Clement, S. The Multi-objective Optimisation of a Traffic Control System. Abbreviated Presentation Sessions of the 14th International Symposium on Transportation and Traffic Theory. Jerusalem, Israel, 20-23 July 1999, pp. 153-176.